

## Review

# The Role of Organic Aerosol in Atmospheric Ice Nucleation – A Review

Daniel Alexander Knopf, Peter Alpert, and Bingbing Wang

ACS *Earth Space Chem.*, Just Accepted Manuscript • DOI: 10.1021/acsearthspacechem.7b00120 • Publication Date (Web): 19 Jan 2018

Downloaded from <http://pubs.acs.org> on January 24, 2018

### Just Accepted

“Just Accepted” manuscripts have been peer-reviewed and accepted for publication. They are posted online prior to technical editing, formatting for publication and author proofing. The American Chemical Society provides “Just Accepted” as a free service to the research community to expedite the dissemination of scientific material as soon as possible after acceptance. “Just Accepted” manuscripts appear in full in PDF format accompanied by an HTML abstract. “Just Accepted” manuscripts have been fully peer reviewed, but should not be considered the official version of record. They are accessible to all readers and citable by the Digital Object Identifier (DOI®). “Just Accepted” is an optional service offered to authors. Therefore, the “Just Accepted” Web site may not include all articles that will be published in the journal. After a manuscript is technically edited and formatted, it will be removed from the “Just Accepted” Web site and published as an ASAP article. Note that technical editing may introduce minor changes to the manuscript text and/or graphics which could affect content, and all legal disclaimers and ethical guidelines that apply to the journal pertain. ACS cannot be held responsible for errors or consequences arising from the use of information contained in these “Just Accepted” manuscripts.



ACS Publications

ACS Earth and Space Chemistry is published by the American Chemical Society. 1155 Sixteenth Street N.W., Washington, DC 20036

Published by American Chemical Society. Copyright © American Chemical Society. However, no copyright claim is made to original U.S. Government works, or works produced by employees of any Commonwealth realm Crown government in the course of their duties.

# 1      The Role of Organic Aerosol in Atmospheric Ice Nucleation – A Review

10     2    Daniel A. Knopf<sup>1\*</sup>, Peter A. Alpert<sup>2</sup>, Bingbing Wang<sup>3</sup>

11     3    <sup>1</sup> Institute for Terrestrial and Planetary Atmospheres / School of Marine and Atmospheric Sciences, Stony Brook University,  
12     4    Stony Brook, NY 11794-5000, USA.

13     5    <sup>2</sup> Laboratory of Environmental Chemistry, Paul Scherrer Institute, 5232 Villigen, Switzerland.

14     6    <sup>3</sup> State Key Laboratory of Marine Environmental Science, College of Ocean and Earth Sciences, Xiamen University, Xia-  
15     7    men, 361102, China.

## 23     8    KEYWORDS

24     9    *ORGANIC AEROSOL, ICE NUCLEATION, ORGANIC MATTER, AMORPHOUS PHASE STATE, MOLECULAR  
25     10   DYNAMICS SIMULATION, LABORATORY EXPERIMENTS, FIELD MEASUREMENTS, ORGANIC COATING*

26     11  
27     12  
28     13  
29     14   **ABSTRACT:** Predicting the formation of ice in the atmosphere presents one of the great challenges in  
30     15   physical sciences with important implications for the chemistry and composition of the Earth's atmos-  
31     16   phere, the hydrological cycle, and climate. Among atmospheric ice formation processes, heterogeneous  
32     17   ice nucleation proceeds on aerosol particles ranging from a few nanometers to micrometers in size,  
33     18   commonly referred to as ice nucleating particles (INPs). Research over the last two decades has demon-  
34     19   strated that organic matter (OM) is ubiquitous in the atmosphere, present as organic aerosol (OA) parti-  
35     20   cles or as coatings on other particle types. The physicochemical properties of OM make predicting how  
36     21   OM can contribute to the INP population challenging. This review focuses on the role of OM in INPs,

1       22 summarizing and highlighting recent advances in our understanding of the ice nucleation process gained  
2       23 from theoretical, laboratory, and field studies. Examination of ice residuals and INPs with analytical  
3       24 techniques demonstrates that OM participates in atmospheric ice crystal formation. Molecular dynamic  
4       25 simulations provide insight into the microscopic processes that initiate ice nucleation. The amorphous  
5       26 phase state of OM in the supercooled and metastable regime is identified as a key factor in assessing the  
6       27 particles' nucleation pathways and rates. A theoretical model is advanced, based on particle water ac-  
7       28 tivity, to holistically predict amorphous phase changes and ice nucleation rates of particles coated by  
8       29 OM. The goal of this review is to synthesize our current understanding and propose future research di-  
9       30 rections needed to fully evaluate how OA particles contribute to INPs in the atmosphere.  
10  
11  
12  
13  
14  
15  
16  
17  
18  
19  
20  
21  
22  
23  
24      32 INTRODUCTION  
25  
26  
27      33 Water and its solid crystalline form, ice, are ubiquitous on land and in the air. Ice has not only been  
28  
29      34 observed on Earth but also on planets<sup>1-2</sup> and moons<sup>3-5</sup> throughout the solar system, making it a particu-  
30  
31      35 larly interesting subject since its melted form can provide the means for life<sup>6</sup>. The formation of ice in the  
32  
33      36 Earth's atmosphere changes the radiative properties of clouds by modulating their interaction with in-  
34  
35      37 coming shortwave and outgoing longwave radiation thereby impacting the radiative balance and thus,  
36  
37  
38      38 climate<sup>7-12</sup>. Greater than 50% of Earth's precipitation originates via the ice phase<sup>13</sup> and hence atmos-  
39  
40      39 pheric ice nucleation plays a key role in the global hydrological cycle<sup>14</sup>. Ice crystals formed in the upper  
41  
42      40 troposphere and lower stratosphere (UT/LS) can sediment, resulting in water removal and causing de-  
43  
44      41 hydration of the UT/LS<sup>15-16</sup>. This has consequences for the water vapor distribution and thus the radia-  
45  
46      42 tion budget considering that water vapor is the strongest greenhouse gas<sup>17-18</sup>. Ice particles at the tropo-  
47  
48      43 pause control the water transport into the LS affecting stratospheric chemical composition. Surfaces of  
49  
50      44 ice crystals can serve as heterogeneous sites for reactions resulting in ozone destruction and act as a sink  
51  
52      45 of HNO<sub>3</sub><sup>19-21</sup>. Despite recognition of the importance of atmospheric ice formation, our predictive under-  
53  
54      46 standing is still insufficient for its representation in climate models<sup>7,22</sup>.  
55  
56  
57  
58  
59  
59  
60

47 Cloud droplet and primary ice crystal nucleation proceed on aerosol particles which are suspensions  
1 of liquid or solid matter having sizes of a few nanometers to hundreds of micrometers. Ice multiplication  
2 mechanisms may proceed after some initial ice is present<sup>23-26</sup>. Whereas mineral dust particles and  
3 sea spray aerosol (SSA) account for the greatest aerosol mass concentrations, organic aerosol (OA)  
4 makes up a significant fraction of the ambient global tropospheric aerosol<sup>7, 27-35</sup>. OA can contribute 20–  
5 90% by mass to the submicron aerosol<sup>27</sup>. OA can be directly emitted from sources such as fossil fuel  
6 combustion and biomass burning, termed primary OA (POA) whereas secondary organic aerosol (SOA)  
7 stems from the oxidation of volatile organic compounds (VOCs), the latter contributing significantly to  
8 the global OA burden<sup>28, 36-39</sup>. The impact of organic matter (OM) generally on atmospheric ice nuclea-  
9 tion is not well understood since its widespread atmospheric presence has been only thoroughly estab-  
10 lished with advancements of novel aerosol particle analytical techniques<sup>27-29, 31, 33</sup>. In contrast, biological  
11 particles (excluded from our definition of OM) and insoluble inorganic material such as mineral dust  
12 have been studied for their ice forming propensity for a much longer time<sup>40-47</sup>. The focus of this article  
13 is on the role of OM in atmospheric ice nucleation, concentrating on the last one to two decades of re-  
14 search that have linked OA particles with ice nucleation. It builds upon previous reviews that provide  
15 excellent overviews of various ice nucleation data sets including inorganic (e.g., mineral dust) and bio-  
16 logical particle types and associated theoretical data representations<sup>10, 48-57</sup>.

39  
40 This review is organized as follows. The presence of OA in the atmosphere is first briefly surveyed,  
41 followed by a discussion of the unique physicochemical properties of OM and OA and their effects on  
42 atmospherically relevant ice formation pathways. Then the current microscopic understanding of homo-  
43 geneous and heterogeneous ice nucleation is summarized. This is followed by a description of selected  
44 field measurements that include chemical speciation of the ice nucleating particles (INPs) and ice resid-  
45 uals (IRs). An INP represents a material or object that is assumed to be the agent responsible for ob-  
46 served heterogeneous nucleation<sup>58</sup> and an IR represents the particle left over after the ice is sublimated.  
47  
48 We further discuss recent laboratory studies examining atmospheric OA and OM surrogates for ice nu-  
49 cleation. Then the current theoretical descriptions of ice nucleation data are summarized and a new ice  
50  
51  
52  
53  
54  
55  
56  
57  
58  
59  
60

1        73 nucleation model is suggested to predict ice nucleation by inorganic particles coated by amorphous OM.  
2        74 Finally, a summary and suggestions for future research directions responding to open questions on the  
3        75 contributions of OM and OA to atmospheric INPs are presented.  
4  
5  
6  
7        76 *Composition of Organic Aerosols*  
8  
9  
10      77 OA particles are ubiquitous and have been observed in natural remote and anthropogenically impact-  
11      78 ed regions as displayed in Fig. 1<sup>29</sup>. Sulfate compounds in significant amounts can be associated with OA  
12      79 particles (Fig. 1)<sup>59</sup>. The condensed-phase OM is typically discriminated as hydrocarbon-like OA (HOA),  
13      80 semi-volatile (SV-) and low-volatile oxygenated OA (LV-OOA), and extremely LV-OOA (ELV-OOA).  
14  
15  
16  
17  
18  
19      81 Volatility decreases as species' oxidation level increases (O:C)<sup>60-62</sup>. For example, POA from fossil fuel  
20      82 combustion and other urban sources falls typically in the class of HOA<sup>31</sup>. SOA forms as the oxidation  
21      83 products of anthropogenically or biogenically emitted volatile organic compounds (VOCs) partition to  
22      84 the condensed phase<sup>60, 63</sup>. OA can also form via aqueous-phase chemical reactions between dissolved  
23      85 OM and soluble trace gases within cloud droplets and subsequent evaporation of the droplets<sup>64-68</sup>.  
24  
25  
26  
27  
28  
29  
30  
31      86 Atmospheric aerosol particles resemble a complex chemical mixture of compounds<sup>69-79</sup>. Gas-  
32      87 particle interactions and coagulation of different particle types yield aerosol particles that can be multi-  
33      88 compositional and multiphase. Inorganic species such as sulfates and nitrates can condense on particles,  
34      89 leading to chemical modification, changes in hygroscopicity, and changes in ice nucleation propensity<sup>53,</sup>  
35      90 <sup>80-88</sup>. The mixing state of a particle population is a quantitative measure of the number of particles com-  
36      91 posed of one or any mixture of components. It therefore describes the particles' heterogeneous composi-  
37      92 tion and has important effects on the radiative scattering and absorption cross sections<sup>89-92</sup>. The particle  
38      93 mixing state is also a crucial parameter for ice nucleation, yielding information about the specific chem-  
39      94 ical species on the particle surface which will interact with a supercooled aqueous solution or water va-  
40      95 por that is supersaturated with respect to ice. Chemical analysis of IRs has shown the physicochemical  
41      96 complexity of INPs<sup>54, 93-94</sup>. The recent advances in single particle micro-spectroscopic analyses of aero-  
42      97 sol particle populations further demonstrate the complex morphology and composition of ambient aero-  
43  
44  
45  
46  
47  
48  
49  
50  
51  
52  
53  
54  
55  
56  
57  
58  
59  
60

1        98      sol<sup>70</sup>. In photochemically active environments where oxidation of VOCs can occur or after long-range  
2        99      transport, aerosol particles have been observed to be dominated or coated by OM<sup>69-74, 79, 95-102</sup>. In such  
3        100     dynamic processes, it is expected that atmospheric aging could continuously alter the chemical com-  
4        101     plexity of OM and its ice nucleation propensity.  
5  
6  
7  
8  
9  
10      102     *Phase State of OM in the Atmosphere*

11  
12      103     It is commonly assumed that INPs contain insoluble and/or solid substrates which facilitate ice nu-  
13  
14      104     cleation<sup>40</sup>. However, it has been shown that OM with varying phases, macromolecules, and organic  
15  
16      105     monolayers can initiate ice nucleation<sup>103-112</sup>. A unique feature of OA particles is that they can be amor-  
17  
18      106     phous and can exist in different phases, including liquid, semisolid, and solid (or glassy) states, in re-  
19  
20      107     sponse to changes of temperature (T) and relative humidity (RH)<sup>113-116</sup>. This is in contrast to particles  
21  
22      108     comprised of inorganic salts which have a thermodynamically defined phase transition from crystalline  
23  
24      109     solid to liquid (deliquescence)<sup>117</sup>, for instance. Phases of OA reflect different particle viscosities and  
25  
26      110     thus different substrate hardness, all of which potentially impact ice nucleation<sup>105, 118-119</sup>. A characteristic  
27  
28      111     parameter is the glass transition temperature, T<sub>g</sub>, that describes the viscosity of a liquid on the order of  
29  
30      112     10<sup>12</sup> Pa s, where the molecular motion is so slow that it can be considered a solid<sup>113, 120-121</sup>. Species with  
31  
32      113     very low T<sub>g</sub>, such as sulfuric acid or water, can act as a plasticizer that significantly decreases T<sub>g</sub> of a  
33  
34      114     particle if present among other components<sup>113-114</sup>. At low temperatures, e.g., in the UT/LS where the at-  
35  
36      115     mospheric temperature can be as low as 180 K, it is conceivable that the majority of OM can be present  
37  
38      116     in a solid state<sup>113</sup>. This has been evaluated by a recent global modelling study of the SOA phase state<sup>122</sup>.  
39  
40  
41  
42  
43  
44  
45      117     Fig. 2a displays global simulations of the annual average of T<sub>g</sub>/T that is taken as representative of the  
46  
47      118     SOA phase state for different altitudes<sup>122</sup>. Although there are regions where SOA can be solid in the sur-  
48  
49      119     face boundary layer, the model results suggest that most of the SOA particles are solid above 500 hPa  
50  
51      120     (~5 km), where middle (440-700 hPa) and high (<440 hPa) clouds can contain ice crystals and are pre-  
52  
53      121     sent 18% and 33% of the time globally, respectively<sup>123-124</sup>. In the cold polar regions, mixed-phase clouds  
54  
55      122     that contain supercooled water droplets and ice crystals can exist at much lower altitudes<sup>125-128</sup>.  
56  
57  
58  
59  
60

123        The organic phase state impacts water diffusivity and typical condensed-phase mixing time scales  
124        (Fig. 2b) that ultimately govern the time that solid OM needs to transition to a more liquid state and  
125        come into equilibrium with water vapor<sup>119, 129</sup>. This organic solid-to-liquid transition is termed humidity-  
126        induced amorphous deliquescence<sup>130</sup>. Fig. 2b shows that mixing timescales,  $\tau_{cd}$ , of OA particles with  
127        water can range from several minutes to days at temperatures low enough for ice formation. Thus,  $\tau_{cd}$   
128        can be longer than typical cloud activation time periods (governed by the updraft velocity), potentially  
129        inhibiting full deliquescence and allowing the OA to serve as a substrate for ice nucleation.  
130

### 130 *Ice Nucleation Pathways*

131        Fig. 3 introduces the basic ice nucleation modes<sup>40, 58, 131-132</sup> for exemplary values of RH and supersat-  
132        uration with respect to ice ( $RH_{ice}$  and  $S_{ice}$ , respectively), where the temperature and humidity trajectories  
133        not necessarily depict all atmospheric conditions that allow for ice formation. The purpose of Fig. 3 is to  
134        provide a differentiation between the nucleation modes and to introduce which ice nucleation pathways  
135        are discussed in this review. These definitions are based on a macroscopic viewpoint and may not reflect  
136        the actual microscopic or molecular processes at the particle interface<sup>40, 58</sup>. A supercooled water or  
137        aqueous solution droplet can freeze by homogeneous ice nucleation (Fig. 3A). The presence of an insol-  
138        uble particle such as a mineral dust can act as INP when immersed in a supercooled droplet (Fig. 3B).  
139        Deliquescence of salts<sup>117</sup> and water uptake can precede immersion freezing (Fig. 3C). Water condensa-  
140        tion immediately prior to ice nucleation, termed condensation freezing, is assumed to resemble the situa-  
141        tion of immersion freezing<sup>55, 133</sup>. Immersion freezing is suggested to be the dominant ice nucleation  
142        pathway in the atmosphere<sup>134-137</sup>. Pathways B and C can also occur at supercooled temperatures. Path-  
143        way D displays deposition ice nucleation where ice forms on an INP from the supersaturated gas phase.  
144        Processes not discussed here that can also take place in the atmosphere are contact ice nucleation<sup>53, 131</sup>  
145        (Fig. 3E), inside-out evaporation freezing<sup>132, 138</sup> (Fig. 3F), and ice multiplication<sup>23-24</sup>. Contact ice nuclea-  
146        tion occurs when an INP collides or comes into contact with a supercooled water or aqueous solution  
147        droplet<sup>139</sup>. Inside-out freezing occurs when an INP is in contact with the liquid-air interface, establishing

1        148 three interfaces (i.e., gas, solid, liquid), at supercooled conditions. Ice multiplication refers to the gener-  
2        149 ation of ice crystals via fracturing processes during droplet freezing or riming of ice by supercooled  
3        150 droplets, or from ice-ice collisions.  
4  
5  
6  
7        151 Impact of Organic Matter on Ice Nucleation Pathway  
8  
9  
10      152 When amorphous OA or OM are involved in ice nucleation, the condensed-phase diffusion processes  
11  
12      153 within OA particles will ultimately govern the ice nucleation pathway<sup>105, 113, 118-119, 121, 140-141</sup>. Since  
13  
14      154 amorphous OM does not display a sharp deliquescence point, a layer of complexity to above described  
15  
16      155 nucleation modes is added when predicting the thermodynamic conditions under which ice nucleation  
17  
18      156 proceeds. A demonstration of this is given by Berkemeier et al. (2014)<sup>119</sup>, who applied a numerical ki-  
19      157 netic molecular flux model to quantify the relationship between the ice nucleation pathway and OA vis-  
20  
21      158 cosity governed by diffusivity of both the organic species and water. Fig. 4 illustrates the different stages  
22  
23      159 during deliquescence of an amorphous OA particle as full deliquescence relative humidity (FDRH) is  
24  
25      160 approached<sup>119</sup>. The water activity,  $a_w$ , of the aqueous solution surrounding the solid organic particle core  
26  
27      161 at FDRH is in equilibrium with water partial pressure. The formation of ice depends on the propensity  
28  
29      162 of the solid organic core to initiate ice nucleation in the supercooled aqueous solution as depicted in Fig.  
30  
31      163 4. The existence of a glass transition and FDRH leads to the following potential scenarios of atmospher-  
32  
33      164 ic ice nucleation that are uniquely attributable to the presence of amorphous OM<sup>112, 119</sup>: (1) Ice formation  
34  
35      165 in the glassy region may be due to ice nucleation on the solid organic particle, i.e., deposition ice nu-  
36  
37      166 cleation. (2) During partial deliquescence (PD), a residual solid core is coated by an aqueous shell and  
38  
39      167 immersion freezing may proceed. (3) At FDRH only homogeneous freezing will occur at temperatures  
40  
41      168 below ~238 K. (4) The presence of a glassy phase in disequilibrium with surrounding water vapor (e.g.,  
42  
43      169 cloud activation at fast updrafts as discussed below), may suppress or initiate ice nucleation beyond the  
44  
45      170 homogeneous ice nucleation limit.

52  
53      171 Fig. 5 presents atmospheric ice nucleation pathways considering the ice nucleation modes dis-  
54  
55      172 cussed and the presence of inorganic and amorphous organic aerosol particles. It shows in a more com-  
56  
57      173 plete manner compared to Fig. 3, how particle composition impacts the formation of ice as a response to  
58  
59  
60

1      changes in thermodynamic conditions expressed as T, RH, and  $\text{RH}_{\text{ice}}$ . Fig. 5 displays the thermodynamic  
2      conditions of the condensed-phase. In other words, if the condensed-phase is in disequilibrium with the  
3      gas-phase, ice nucleation may proceed at different T and RH. Immersion freezing is depicted in path-  
4      ways a-e (Fig. 5). This nucleation pathway can occur at condensed-phase water subsaturated (Fig. 5,  
5      pathway c-e) or saturated conditions (Fig. 5, pathways a-b) where particle water activity,  $a_w < 1$  or  $a_w =$   
6      1, respectively. Deposition ice nucleation can proceed at ice-supersaturated gas phase and water-  
7      subsaturated conditions (Fig. 5, pathway g).

8  
9  
10  
11  
12  
13  
14  
15  
16  
17      Three cloud phase regimes can be discriminated in the atmosphere as indicated in Fig. 3. At tempera-  
18      tures warmer than the ice melting line of 273.15 K only liquid clouds exist. At temperatures cooler than  
19  
20  
21      the ice melting line and warmer than the homogeneous freezing temperature of supercooled water,  
22  
23      mixed-phase clouds may form with supercooled droplets and ice crystals coexisting. Only ice crystals  
24  
25      are present at temperatures colder than the homogeneous freezing of pure water, which is typical of cir-  
26  
27      rus clouds. This review highlights observations from laboratory and field studies of ice nucleation by  
28  
29  
30      OA/OM under conditions of RH and T similar to cirrus and mixed phase clouds, while emphasizing the  
31  
32      challenges in predicting OA acting as INPs.

33  
34  
35  
36  
37  
38  
39  
40  
41  
42  
43  
44  
45  
46  
47  
48  
49  
50  
51  
52  
53  
54  
55  
56  
57  
58  
59  
60  
The physicochemical characteristics of the INPs in these cloud regimes will govern the ice nu-  
cleation pathways. Fig. 5 displays the equilibrium T and RH under which immersion freezing or deposi-  
tion ice nucleation proceed but also exemplifies how initial chemical composition of the particle can  
affect ice formation routes. The composition of liquid droplets is constrained by the water saturation line  
where  $a_w = 1$  by definition, which represents pure water. Cloud droplet solute concentration is typically  
low, on the order of  $10^2 \mu\text{M}^{142}$ , for which  $a_w \approx 1$  is a reasonable assumption. An increase in humidity  
beyond liquid saturation leaves droplet  $a_w = 1$  unchanged. For colder temperatures, the homogeneous  
freezing limit defines the humidity region above which only ice exists (any solution droplet present will  
freeze). The Kelvin effect leading to increased water vapor pressure<sup>143</sup> is important to consider for parti-

1       198      cles smaller than 0.2  $\mu\text{m}$ , but can be neglected in this discussion because ambient INPs are typically  
2       199      larger<sup>40, 53</sup>.  
3  
4

5       200      Mineral dust is a common particle type in the atmosphere and serves as a large source of INPs<sup>49-</sup>  
6  
7       201      <sup>50</sup>. Dust particles may take up water under subsaturated conditions and act also as cloud condensation  
8  
9       202      nuclei (CCN)<sup>144-155</sup>, in particular, when coated with hygroscopic material due to aging processes<sup>156-157</sup>.  
10  
11      Dust particles may initiate immersion freezing under subsaturated<sup>158-159</sup> and saturated conditions<sup>49</sup> (Fig.  
12  
13      14, 204     5, pathways a-c). Dissolvable inorganic species present as coatings or as a particle, deliquesce promptly  
15  
16      17, 205     upon increases in RH<sup>117</sup> followed by water uptake (see Fig. 5, pathways d and f). However, amorphous  
18  
19      19, 206     OM can exhibit humidity-induced amorphous deliquescence<sup>130</sup> above the  $T_g$  or corresponding  $\text{RH}_{\text{ice}}$   
20  
21      21, 207     (e.g., the red, green, or golden lines in Fig. 5, pathway e) until full deliquescence (FD) occurs (Fig. 5,  
22  
23      24, 208     dashed green line). Also note how the presence of sulfates in SOA (Fig. 5, red line) decreases  $T_g$  as  
25  
26      26, 209     shown for the case of  $\alpha$ -pinene SOA (Fig 5, green line)<sup>112</sup>. These phase state changes present a challenge  
27  
28      28, 210     for predictions of ice nucleation kinetics because of the competition and relationship between the ice  
29  
30      30, 211     nucleation rate and changes in organic phase state. When a single organic species deliquesces, the solid  
31  
32      32, 212     OM surface area decreases as the surrounding  $a_w$  of the aqueous solution increases, both affecting the  
33  
34      34, 213     ice nucleation rate as discussed in the next section.  
35  
36  
37      37, 214     *Specific Effects of Organic Matter on Ice Nucleation*  
38

39      39, 215     Cooling and humidification rates of air masses complicate the predictions of ice formation from  
40  
41      40, 216     amorphous OA particles. These rates can change  $T_g$  and FDRH which depend on particle viscosity or  
42  
43      42, 217     diffusivity and thus are kinetic parameters. This contrasts with typical thermodynamic parameters, e.g.,  
44  
45      44, 218     the melting temperature of a solid. Therefore, the atmospheric conditions under which phase transitions  
46  
47      46, 218     occur depend also on the updraft velocity, which directly impacts cooling and humidification rates. A  
48  
49      48, 219     slower updraft velocity allows for more time for deliquescence to proceed, potentially resulting in full  
50  
51      50, 220     deliquescence of the OA particle at warmer and drier conditions compared to when a faster updraft is  
52  
53      53, 221     active. Therefore, the same OM can be present in different phase states under the same atmospheric  
54  
55      55, 222     thermodynamic conditions (i.e., T and  $\text{RH}_{\text{ice}}$ ) resulting in different ice nucleation pathways and corre-  
56  
57  
58      58, 223     9  
59  
60

1 224 sponding ice nucleation rates. OA particle size or coating thickness can also impact the rate and atmos-  
2 225 pheric altitude of the organic phase change, as larger particles or thicker coatings require more time to  
3 226 reach full deliquescence.  
4  
5

6 227 Another peculiarity of amorphous OM concerns the potential change in particle morphology upon  
7 228 nucleation of ice from an aqueous organic solution droplet. As water crystallizes, a freeze-induced phase  
8 229 separation into pure ice and a freeze-concentrated solution can occur<sup>140, 160-164</sup>. Hence, ice nucleation  
9 230 may not necessarily result in a pure ice crystal but an ice crystal with inclusions or one which is partially  
10 231 or fully coated by the freeze-concentrated solution. This can have implications for water vapor pressure,  
11 232 multiphase chemical kinetics when the frozen particles act as reactive substrates, and the particles' ra-  
12 233 diative properties. The remaining highly concentrated aqueous organic solution can also form a glass<sup>140,</sup>  
13 234 <sup>165</sup>. Subsequent ice sublimation can leave a highly porous solid organic particle behind with implications  
14 235 for particle radiative properties and cloud formation<sup>165-166</sup>. In addition, these cloud cycling processes  
15 236 may allow for pre-activation of the OA particles, thereby enhancing the particle's ice nucleation rate in  
16 237 subsequent ice activation cycles<sup>167-169</sup>.  
17  
18

19 238 Upon solidification and crystallization, OM can display different polymorphisms<sup>170-172</sup> when under-  
20 239 going temperature changes<sup>173-174</sup>. The expected interfacial changes upon transition from one to another  
21 240 polymorphic phase have not yet been examined with regard to water interaction, e.g., via interfacial hy-  
22 241 drogen bonding. Temperature can influence organic mixtures where, e.g., mixtures of fatty acids<sup>175-176</sup>  
23 242 can be miscible at ambient conditions but are immiscible at lower temperature resulting in demixing<sup>177</sup>.  
24 243 However, as pointed out by Marcolli et al. (2004)<sup>178</sup>, in the presence of a sufficiently high number of  
25 244 miscible organic and inorganic components, a liquid (or an amorphous solid) is the thermodynamically  
26 245 stable phase. The authors observed a decrease of the deliquescence RH with an increasing number of  
27 246 components present in the solution. This in turn would decrease the particle's ability to act as an INP.  
28 247 However, it has also been observed that in complex inorganic/organic particles, efflorescence (liquid-to-  
29  
30  
31  
32  
33  
34  
35  
36  
37  
38  
39  
40  
41  
42  
43  
44  
45  
46  
47  
48  
49  
50  
51  
52  
53  
54  
55  
56  
57  
58  
59  
60

1 248 solid transition) can occur upon increasing humidity<sup>179</sup>. How these phase transitions proceed at super-  
2 249 cooled temperatures or in the metastable regime is not known.  
3  
4

5 250 Lastly, the occurrence of liquid-liquid phase separation (LLPS) in inorganic-organic particles<sup>180-183</sup>  
6  
7 251 and OM<sup>184-186</sup> upon increases in humidity has been observed. LLPS can impact droplet surface tension  
8  
9 252 and as such potentially cloud droplet activation<sup>187</sup>. However, occurrence of LLPS at temperatures rele-  
10  
11 253 vant for ice nucleation has not been investigated, except for a study by You et al. (2015)<sup>181</sup>, and its im-  
12  
13 254 pact on ice nucleation in aerosol particles or cloud droplets in terms of organic phase, interfacial tension  
14  
15 255 and water activity has not yet been examined.  
16  
17  
18  
19 256  
20  
21 257 MICROSCOPIC DESCRIPTIONS OF ICE NUCLEATION  
22  
23  
24 258 *Homogeneous Ice Nucleation*  
25  
26  
27 259 Homogeneous ice nucleation in aqueous solution is considered to be a stochastic process which de-  
28  
29 260 pends on the volume of the solution and the time that it remains supercooled as well as  $S_{ice} > 1^{40}$ . The  
30  
31 261 presence of inorganic and/or organic solutes depresses the freezing point from the one of pure water,  
32  
33 262 resulting in freezing temperatures lower than  $\sim 238$  K<sup>188-190</sup>. The homogeneous ice nucleation rate coeffi-  
34  
35 263 cient,  $J_{hom}$ , of pure water as a function of temperature is still under investigation with a recent study  
36  
37 264 suggesting a maximum value of  $J_{hom}^{\max} \approx (2 \times 10^{12} \pm 10^2)$  cm<sup>-3</sup> s<sup>-1</sup> at about 229 K<sup>191</sup>. A change in the  
38  
39 265 ice nucleation rate may impact the evolution of clouds for temperatures as warm as 243 K<sup>192</sup>. Recently,  
40  
41 266 Lupi et al. (2017)<sup>193</sup>, showed that the ice nucleation rate can depend strongly on the prevalent ice poly-  
42  
43 267 morph, i.e., hexagonal ice, cubic ice<sup>194</sup>, or a mixture of the two referred to as stacking disordered ice<sup>195</sup>.  
44  
45 268 They found that stacking-disordered critical crystallites at 230 K are more stable than hexagonal ones by  
46  
47 269 about 14 kJ mol<sup>-1</sup> of crystallite, which corresponds to nucleation rates more than 3 orders of magnitude  
48  
49 270 larger than those predicted by classical nucleation theory (CNT) assuming only hexagonal ice. When  
50  
51 271 analyzing experimental ice nucleation rates, assuming the presence of hexagonal critical crystallites in-

1 272 stead of stacking-disordered critical crystallites will result in the underestimation of the ice-liquid inter-  
2 273 facial free energy.

4  
5 274 It has been shown experimentally that  $J_{hom}$  and median freezing temperature,  $T_f$ , can be predicted us-  
6 ing solution  $a_w$  as the ice nucleation determinant, independent of the solute's nature<sup>140, 190, 196-199</sup>. Theo-  
7 275 retical studies have corroborated the applicability of  $a_w$  to describe homogeneous ice nucleation<sup>200-202</sup>.  
8 276  
9 277 The temperature dependence of  $a_w$  in aqueous inorganic or organic solutions is only established for few  
10 278 solutes and remains a matter of current research<sup>140, 190, 196, 198, 203-211</sup>. An additional unanswered question  
11 279 concerns the role of the vapor-liquid interface in initiating homogeneous ice nucleation based on argu-  
12 280 ments of partial wettability following Young's equation<sup>212-215</sup>. Initial molecular dynamics (MD) simula-  
13 281 tions indicated that nucleation does not actually occur at the vapor-liquid interface but close to it (i.e.,  
14 282 the subsurface)<sup>216-217</sup>. A recent computational study using a nanofilm found that ice nucleation initiates  
15 283 away from the air-water interface, in a region that is more favorable to the formation of cubic ice<sup>218</sup>.  
16 284  
17 285 *Heterogeneous Ice Nucleation*

18 286 The basic requirements for a particle to initiate ice nucleation heterogeneously are that<sup>40, 58</sup>: i) it must  
19 287 be insoluble; ii) it must be larger than the critical ice nucleus germ, estimated to be  $> 0.1 \mu\text{m}$ ; iii) its sur-  
20 288 face must have chemical bonds that can interact with and arrange water molecules, iv) it must have a  
21 289 crystallographic match representing geometrical arrangement of bonds, or v) there must be active sites  
22 290 representing localized phenomena on the substrate surface of varying quality. Despite advances in in-  
23 291 strumentation that allow for visualization of substrate locations at which ice forms<sup>219-220</sup>, in situ observa-  
24 292 tions of ice nucleation on the nanometer and subnanometer scale have not yet been achieved. Recall that  
25 293 the ice nucleation pathways<sup>40, 58</sup> are macroscopically defined, and the underlying microscopic processes  
26 294 are not well understood. For example, it has been suggested that deposition ice nucleation is the result of  
27 295 homogeneous ice nucleation of water residing in nano-size pores; the latter causing a strong "negative"  
28 296 Kelvin effect thereby reducing the water vapor pressure and impacting  $S_{ice}$ <sup>221</sup>. This is in line with a so-  
297  
298  
299  
300  
301  
302  
303  
304  
305  
306  
307  
308  
309  
310  
311  
312  
313  
314  
315  
316  
317  
318  
319  
320  
321  
322  
323  
324  
325  
326  
327  
328  
329  
330  
331  
332  
333  
334  
335  
336  
337  
338  
339  
340  
341  
342  
343  
344  
345  
346  
347  
348  
349  
350  
351  
352  
353  
354  
355  
356  
357  
358  
359  
360  
361  
362  
363  
364  
365  
366  
367  
368  
369  
370  
371  
372  
373  
374  
375  
376  
377  
378  
379  
380  
381  
382  
383  
384  
385  
386  
387  
388  
389  
390  
391  
392  
393  
394  
395  
396  
397  
398  
399  
400  
401  
402  
403  
404  
405  
406  
407  
408  
409  
410  
411  
412  
413  
414  
415  
416  
417  
418  
419  
420  
421  
422  
423  
424  
425  
426  
427  
428  
429  
430  
431  
432  
433  
434  
435  
436  
437  
438  
439  
440  
441  
442  
443  
444  
445  
446  
447  
448  
449  
450  
451  
452  
453  
454  
455  
456  
457  
458  
459  
460  
461  
462  
463  
464  
465  
466  
467  
468  
469  
470  
471  
472  
473  
474  
475  
476  
477  
478  
479  
480  
481  
482  
483  
484  
485  
486  
487  
488  
489  
490  
491  
492  
493  
494  
495  
496  
497  
498  
499  
500  
501  
502  
503  
504  
505  
506  
507  
508  
509  
510  
511  
512  
513  
514  
515  
516  
517  
518  
519  
520  
521  
522  
523  
524  
525  
526  
527  
528  
529  
530  
531  
532  
533  
534  
535  
536  
537  
538  
539  
540  
541  
542  
543  
544  
545  
546  
547  
548  
549  
550  
551  
552  
553  
554  
555  
556  
557  
558  
559  
5510  
5511  
5512  
5513  
5514  
5515  
5516  
5517  
5518  
5519  
5520  
5521  
5522  
5523  
5524  
5525  
5526  
5527  
5528  
5529  
5530  
5531  
5532  
5533  
5534  
5535  
5536  
5537  
5538  
5539  
5540  
5541  
5542  
5543  
5544  
5545  
5546  
5547  
5548  
5549  
5550  
5551  
5552  
5553  
5554  
5555  
5556  
5557  
5558  
5559  
55510  
55511  
55512  
55513  
55514  
55515  
55516  
55517  
55518  
55519  
55520  
55521  
55522  
55523  
55524  
55525  
55526  
55527  
55528  
55529  
55530  
55531  
55532  
55533  
55534  
55535  
55536  
55537  
55538  
55539  
55540  
55541  
55542  
55543  
55544  
55545  
55546  
55547  
55548  
55549  
55550  
55551  
55552  
55553  
55554  
55555  
55556  
55557  
55558  
55559  
55560  
55561  
55562  
55563  
55564  
55565  
55566  
55567  
55568  
55569  
55570  
55571  
55572  
55573  
55574  
55575  
55576  
55577  
55578  
55579  
55580  
55581  
55582  
55583  
55584  
55585  
55586  
55587  
55588  
55589  
55590  
55591  
55592  
55593  
55594  
55595  
55596  
55597  
55598  
55599  
555100  
555101  
555102  
555103  
555104  
555105  
555106  
555107  
555108  
555109  
555110  
555111  
555112  
555113  
555114  
555115  
555116  
555117  
555118  
555119  
555120  
555121  
555122  
555123  
555124  
555125  
555126  
555127  
555128  
555129  
555130  
555131  
555132  
555133  
555134  
555135  
555136  
555137  
555138  
555139  
555140  
555141  
555142  
555143  
555144  
555145  
555146  
555147  
555148  
555149  
555150  
555151  
555152  
555153  
555154  
555155  
555156  
555157  
555158  
555159  
555160  
555161  
555162  
555163  
555164  
555165  
555166  
555167  
555168  
555169  
555170  
555171  
555172  
555173  
555174  
555175  
555176  
555177  
555178  
555179  
555180  
555181  
555182  
555183  
555184  
555185  
555186  
555187  
555188  
555189  
555190  
555191  
555192  
555193  
555194  
555195  
555196  
555197  
555198  
555199  
555200  
555201  
555202  
555203  
555204  
555205  
555206  
555207  
555208  
555209  
555210  
555211  
555212  
555213  
555214  
555215  
555216  
555217  
555218  
555219  
555220  
555221  
555222  
555223  
555224  
555225  
555226  
555227  
555228  
555229  
555230  
555231  
555232  
555233  
555234  
555235  
555236  
555237  
555238  
555239  
555240  
555241  
555242  
555243  
555244  
555245  
555246  
555247  
555248  
555249  
555250  
555251  
555252  
555253  
555254  
555255  
555256  
555257  
555258  
555259  
555260  
555261  
555262  
555263  
555264  
555265  
555266  
555267  
555268  
555269  
555270  
555271  
555272  
555273  
555274  
555275  
555276  
555277  
555278  
555279  
555280  
555281  
555282  
555283  
555284  
555285  
555286  
555287  
555288  
555289  
555290  
555291  
555292  
555293  
555294  
555295  
555296  
555297  
555298  
555299  
555300  
555301  
555302  
555303  
555304  
555305  
555306  
555307  
555308  
555309  
555310  
555311  
555312  
555313  
555314  
555315  
555316  
555317  
555318  
555319  
555320  
555321  
555322  
555323  
555324  
555325  
555326  
555327  
555328  
555329  
555330  
555331  
555332  
555333  
555334  
555335  
555336  
555337  
555338  
555339  
555340  
555341  
555342  
555343  
555344  
555345  
555346  
555347  
555348  
555349  
555350  
555351  
555352  
555353  
555354  
555355  
555356  
555357  
555358  
555359  
555360  
555361  
555362  
555363  
555364  
555365  
555366  
555367  
555368  
555369  
555370  
555371  
555372  
555373  
555374  
555375  
555376  
555377  
555378  
555379  
555380  
555381  
555382  
555383  
555384  
555385  
555386  
555387  
555388  
555389  
555390  
555391  
555392  
555393  
555394  
555395  
555396  
555397  
555398  
555399  
555400  
555401  
555402  
555403  
555404  
555405  
555406  
555407  
555408  
555409  
555410  
555411  
555412  
555413  
555414  
555415  
555416  
555417  
555418  
555419  
555420  
555421  
555422  
555423  
555424  
555425  
555426  
555427  
555428  
555429  
555430  
555431  
555432  
555433  
555434  
555435  
555436  
555437  
555438  
555439  
555440  
555441  
555442  
555443  
555444  
555445  
555446  
555447  
555448  
555449  
555450  
555451  
555452  
555453  
555454  
555455  
555456  
555457  
555458  
555459  
555460  
555461  
555462  
555463  
555464  
555465  
555466  
555467  
555468  
555469  
555470  
555471  
555472  
555473  
555474  
555475  
555476  
555477  
555478  
555479  
555480  
555481  
555482  
555483  
555484  
555485  
555486  
555487  
555488  
555489  
555490  
555491  
555492  
555493  
555494  
555495  
555496  
555497  
555498  
555499  
555500  
555501  
555502  
555503  
555504  
555505  
555506  
555507  
555508  
555509  
555510  
555511  
555512  
555513  
555514  
555515  
555516  
555517  
555518  
555519  
555520  
555521  
555522  
555523  
555524  
555525  
555526  
555527  
555528  
555529  
555530  
555531  
555532  
555533  
555534  
555535  
555536  
555537  
555538  
555539  
555540  
555541  
555542  
555543  
555544  
555545  
555546  
555547  
555548  
555549  
555550  
555551  
555552  
555553  
555554  
555555  
555556  
555557  
555558  
555559  
555560  
555561  
555562  
555563  
555564  
555565  
555566  
555567  
555568  
555569  
555570  
555571  
555572  
555573  
555574  
555575  
555576  
555577  
555578  
555579  
555580  
555581  
555582  
555583  
555584  
555585  
555586  
555587  
555588  
555589  
555590  
555591  
555592  
555593  
555594  
555595  
555596  
555597  
555598  
555599  
5555100  
5555101  
5555102  
5555103  
5555104  
5555105  
5555106  
5555107  
5555108  
5555109  
5555110  
5555111  
5555112  
5555113  
5555114  
5555115  
5555116  
5555117  
5555118  
5555119  
5555120  
5555121  
5555122  
5555123  
5555124  
5555125  
5555126  
5555127  
5555128  
5555129  
5555130  
5555131  
5555132  
5555133  
5555134  
5555135  
5555136  
5555137  
5555138  
5555139  
5555140  
5555141  
5555142  
5555143  
5555144  
5555145  
5555146  
5555147  
5555148  
5555149  
5555150  
5555151  
5555152  
5555153  
5555154  
5555155  
5555156  
5555157  
5555158  
5555159  
5555160  
5555161  
5555162  
5555163  
5555164  
5555165  
5555166  
5555167  
5555168  
5555169  
5555170  
5555171  
5555172  
5555173  
5555174  
5555175  
5555176  
5555177  
5555178  
5555179  
5555180  
5555181  
5555182  
5555183  
5555184  
5555185  
5555186  
5555187  
5555188  
5555189  
5555190  
5555191  
5555192  
5555193  
5555194  
5555195  
5555196  
5555197  
5555198  
5555199  
5555200  
5555201  
5555202  
5555203  
5555204  
5555205  
5555206  
5555207  
5555208  
5555209  
5555210  
5555211  
5555212  
5555213  
5555214  
5555215  
5555216  
5555217  
5555218  
5555219  
5555220  
5555221  
5555222  
5555223  
5555224  
5555225  
5555226  
5555227  
5555228  
5555229  
5555230  
5555231  
5555232  
5555233  
5555234  
5555235  
5555236  
5555237  
5555238  
5555239  
5555240  
5555241  
5555242  
5555243  
5555244  
5555245  
5555246  
5555247  
5555248  
5555249  
5555250  
5555251  
5555252  
5555253  
5555254  
5555255  
5555256  
5555257  
5555258  
5555259  
5555260  
5555261  
5555262  
5555263  
5555264  
5555265  
5555266  
5555267  
5555268  
5555269  
5555270  
5555271  
5555272  
5555273  
5555274  
5555275  
5555276  
5555277  
5555278  
5555279  
5555280  
5555281  
5555282  
5555283  
5555284  
5555285  
5555286  
5555287  
5555288  
5555289  
5555290  
5555291  
5555292  
5555293  
5555294  
5555295  
5555296  
5555297  
5555298  
5555299  
5555300  
5555301  
5555302  
5555303  
5555304  
5555305  
5555306  
5555307  
5555308  
5555309  
5555310  
5555311  
5555312  
5555313  
5555314  
5555315  
5555316  
5555317  
5555318  
5555319  
5555320  
5555321  
5555322  
5555323  
5555324  
5555325  
5555326  
5555327  
5555328  
5555329  
5555330  
5555331  
5555332  
5555333  
5555334  
5555335  
5555336  
5555337  
5555338  
5555339  
55553310  
55553311  
55553312  
55553313  
55553314  
55553315  
55553316  
55553317  
55553318  
55553319  
55553320  
55553321  
55553322  
55553323  
55553324  
55553325  
55553326  
55553327  
55553328  
55553329  
55553330  
55553331  
55553332  
55553333  
55553334  
55553335  
55553336  
55553337  
55553338  
55553339  
555533310  
555533311  
555533312  
555533313  
555533314  
555533315  
555533316  
555533317  
555533318  
555533319  
555533320  
555533321  
555533322  
555533323  
555533324  
555533325  
555533326  
555533327  
555533328  
555533329  
555533330  
555533331  
555533332  
555533333  
555533334  
555533335  
555533336  
555533337  
555533338  
555533339  
555533340  
555533341  
555533342  
555533343  
555533344  
555533345  
555533346  
555533347  
555533348  
555533349  
555533350  
555533351  
555533352  
555533353  
555533354  
555533355  
555533356  
555533357  
555533358  
555533359  
555533360  
555533361  
555533362  
555533363  
555533364  
555533365  
555533366  
555533367  
555533368  
555533369  
555533370  
555533371  
555533372  
555533373  
555533374  
555533375  
555533376  
555533377  
555533378  
555533379  
555533380  
555533381  
555533382  
555533383  
555533384  
555533385  
555533386  
555533387  
555533388  
555533389  
555533390  
555533391  
555533392  
555533393  
555533394  
555533395  
555533396  
555533397  
555533398  
555533399  
5555333100  
5555333101  
5555333102  
5555333103  
5555333104  
5555333105  
5555333106  
5555333107  
5555333108  
5555333109  
5555333110  
5555333111  
5555333112  
5555333113  
5555333114  
5555333115  
5555333116  
5555333117  
5555333118  
5555333119  
5555333120  
5555333121  
5555333122  
5555333123  
5555333124  
5555333125  
5555333126  
5555333127  
5555333128  
5555333129  
5555333130  
5555333131  
5555333132  
5555333133  
5555333134  
5555333135  
5555333136  
5555333137  
5555333138  
5555333139  
5555333140  
5555333141  
5555333142  
5555333143  
5555333144  
5555333145  
5555333146  
5555333147  
5555333148  
5555333149  
5555333150  
5555333151  
5555333152  
5555333153  
5555333154  
5555333155  
55553331

1        296      called two-step nucleation mechanism<sup>222</sup> where a liquid condensate forms prior to nucleation which can  
2        297      explain nucleation of a solid phase initiated by pockets and at wedges on substrate surfaces<sup>223-226</sup>.  
3  
4  
5        298      When interpreting heterogeneous ice nucleation on the molecular scale, one should keep in mind that  
6  
7        299      substrate surfaces can be readily covered by organic gases. For example, after about 1 s exposure to SV-  
8  
9        300      VOCs at concentrations in the range of ~1 ppb, an organic layer can form on a substrate which is direct-  
10  
11      301      ly proportional to the uptake coefficient of the adsorbing gas<sup>227</sup>, termed adventitious carbon in surface  
12  
13      302      science<sup>228</sup>. Surface tension studies on levitated single droplets demonstrate surface contamination in  
14  
15      303      minutes, even when purging with high purity N<sub>2</sub> gas<sup>229</sup>. Under very careful experimental conditions,  
16  
17      304      VOCs, ammonia, or amines can still be present and partition to the condensed-phase<sup>230-232</sup>. The use of  
18  
19      305      cold traps for carrier gases to generate humidified gas flows can minimize contamination by trace gas  
20  
21      306      species<sup>233</sup>. The choice of water source may also impact cleanliness of INP surfaces, where the most  
22  
23      307      commonly applied water is Millipore water (resistivity of > 18.3MΩ cm) throughout various studies,  
24  
25      308      but also triple-distilled water<sup>234</sup>, or a combination of Millipore water with ion exchange column<sup>231</sup> are  
26  
27      309      used. How carbon contamination of surfaces present as a monolayer or several monolayers affects ice  
28  
29      310      nucleation has not yet been systematically assessed. Hence, microscopic interpretation of ice nucleation  
30  
31      311      experiments should be done with caution.  
32  
33  
34  
35  
36

37        312      Currently, computer experiments such as MD simulations<sup>235</sup> and Monte Carlo calculations provide  
38  
39      313      the best means to improve our molecular understanding of heterogeneous ice nucleation on a scale not  
40  
41      314      yet feasible to examine in laboratory experiments. Focus in these simulations has been placed on the  
42  
43      315      role of inorganic substrates such as mineral dusts or AgI acting as INPs<sup>236-246</sup>. In addition, how the pres-  
44  
45      316      ence of an electric field and different surface geometries impact ice nucleation has been examined<sup>247-250</sup>.  
46  
47      317      Despite these and other studies<sup>242-243, 251-252</sup>, a clear picture of which substrate features represent key  
48  
49      318      physicochemical parameters for description of heterogeneous ice nucleation has not yet emerged. For  
50  
51      319      example, a good ice lattice match with the substrate seems not to be required<sup>251-253</sup> while the degree of  
52  
53      320      hydrophobicity and surface morphology may play important roles<sup>243, 252</sup>. The ice nucleation propensity  
54  
55  
56  
57  
58  
59  
60

321 can be lost if adsorption of water is too great<sup>243</sup>. The formation of an ice embryo may be favored away  
322 from the liquid-solid interface, i.e., in the second overlayer of water from the substrate and not on the  
323 substrate itself<sup>244, 252</sup>. Potentially, a combination of all these factors could define the ice nucleation pro-  
324 pensity of any particular substrate, but the lack of defining parameters makes developing theoretical de-  
325 scriptions of heterogeneous ice nucleation challenging.

12326 Fitzner et al. (2017)<sup>254</sup> recently investigated precritical water cluster formation from two substrates,  
13 either rough or smooth, having the same ice nucleation rate. The rough surface yielded pure hexagonal  
14 ice and, additionally, precritical cluster formation mimicked homogeneous freezing. This can be under-  
15 stood given that if hetero- and homogeneous ice nucleation yield the same ice polymorph (hexagonal  
16 ice), then condensation and evaporation of precritical clusters should proceed similarly. In contrast, pre-  
17 critical clusters formed within 5 Å of the smooth surface prior to ice nucleation lead to stacking disor-  
18 dered ice (cubic and hexagonal ice) and polymorphism. This implies when assessing the enhancement  
19 of heterogeneous ice nucleation compared to homogeneous freezing, knowledge of the formed poly-  
20 morph is crucial. In other words, the crystal face unique to a respective polymorph templated by the  
21 substrate may be more important than the actual substrate structure itself in understanding what does or  
22 does not make an ice nucleator<sup>254</sup>.

36  
37 Computer simulations of ice nucleation initiated by carbonaceous or organic substrates have just be-  
38 gun to gain attention. Molinero and coworkers<sup>255-258</sup> and Cabriolu<sup>259</sup> have used MD simulations to study  
39 heterogeneous ice nucleation on graphene or graphite substrates. These studies found that ice nucleation  
40 follows classical nucleation theory (CNT)<sup>259</sup> and that the transition from liquid to crystal occurs in a  
41 single activated step mainly controlled by the size of the ice nucleus<sup>255</sup>. In addition, they observed that  
42 the hydrophilicity of the graphitic surface is not a good predictor of ice nucleation ability, but that order-  
43 ing of liquid water in contact with the substrate plays an important role in the heterogeneous ice nuclea-  
44 tion mechanism<sup>257</sup>. This could help explain the experimentally observed insignificant increase in ice nu-  
45 cleation by O<sub>3</sub> oxidized Lamp Black 101 soot, a reference material for soot<sup>260</sup>. Hydrophobic and hydro-  
46 phobic surfaces have been shown to inhibit ice nucleation on some substrates<sup>261</sup>, but not others<sup>262</sup>.  
47  
48  
49  
50  
51  
52  
53  
54  
55  
56  
57  
58  
59  
60

1       346      philic atomically rough surfaces do not induce layering and thus do not promote heterogeneous nu-  
2       347      cleation of ice<sup>258</sup>. Fig. 6 shows the structure of interfacial water on a graphitic surface that has been  
3       348      modified by adding OH groups every 1 nm, thereby enhancing surface hydrophilicity determined from a  
4       349      MD simulation<sup>258</sup>. Hexagonal patches can be identified in the first and second layer of water molecules.  
5       350      The authors suggest that the rare formation of bilayer patches of hexagons (i.e., the fluctuations in the  
6       351      second layer) may be associated with the nucleation of ice. However, the water does not show a specific  
7       352      alignment or structure associated with given OH surface features (Fig. 6). This finding is similar to re-  
8       353      cent simulations showing for different hydroxylated substrates that neither the symmetry of the OH pat-  
9       354      terns nor the similarity between a substrate and ice correlate well with the ice nucleation ability<sup>261</sup>.  
10  
11  
12  
13  
14  
15  
16  
17  
18  
19  
20  
21  
22  
23  
24  
25  
26  
27  
28  
29  
30  
31  
32  
33  
34  
35  
36  
37  
38  
39  
40  
41  
42  
43  
44  
45  
46  
47  
48  
49  
50  
51  
52  
53  
54  
55  
56  
57  
58  
59  
60

355      It is well known from experimental studies that organic monolayers with alcohol head groups act as  
356      ice nucleating surfaces, being more efficient at nucleating ice than monolayers with the same chain  
357      length but with carboxyl headgroups<sup>106-109, 111, 262-263</sup>. A recent MD simulation study captured these ob-  
358      served freezing trends and attributed the variation in ice nucleation temperatures to spatial fluctuations  
359      in the monolayer and lattice mismatch<sup>264</sup>.  
360  
361

362      Another microscopic model of ice nucleation by a solid in contact with a liquid and surrounding gas  
363      phase is the three-phase contact line concept<sup>132, 138, 265-274</sup>. Under partial wetting, the gas, solid, and liq-  
364      uid phase exist in contact with each other establishing a contact line in three dimensions. CNT can ex-  
365      plain why ice nucleation is preferred and faster at the contact line compared to nucleation in the bulk<sup>266</sup>.  
366      The free energy cost of creating the interface around the nucleus is lowest at the point of the three pre-  
367      existing interfaces compared to, e.g., creating an interface within the liquid phase<sup>266, 268</sup>. The contact line  
368      concept was applied to help explain inside-out freezing<sup>132, 138</sup> and the superior ability of proteins from  
369      the bacterium *Pseudomonas syringae* to freeze water<sup>271</sup>. Interface-specific sum frequency generation  
370      (SFG) spectroscopy coupled with MD simulation indicated that the protein features a hydrophilic-  
371      hydrophobic-hydrophilic pattern<sup>271</sup>. This pattern imposes structural changes in the adjacent water, alter-  
372  
373  
374  
375  
376  
377  
378  
379  
380  
381  
382  
383  
384  
385  
386  
387  
388  
389  
390  
391  
392  
393  
394  
395  
396  
397  
398  
399  
400  
401  
402  
403  
404  
405  
406  
407  
408  
409  
410  
411  
412  
413  
414  
415  
416  
417  
418  
419  
420  
421  
422  
423  
424  
425  
426  
427  
428  
429  
430  
431  
432  
433  
434  
435  
436  
437  
438  
439  
440  
441  
442  
443  
444  
445  
446  
447  
448  
449  
450  
451  
452  
453  
454  
455  
456  
457  
458  
459  
460  
461  
462  
463  
464  
465  
466  
467  
468  
469  
470  
471  
472  
473  
474  
475  
476  
477  
478  
479  
480  
481  
482  
483  
484  
485  
486  
487  
488  
489  
490  
491  
492  
493  
494  
495  
496  
497  
498  
499  
500  
501  
502  
503  
504  
505  
506  
507  
508  
509  
510  
511  
512  
513  
514  
515  
516  
517  
518  
519  
520  
521  
522  
523  
524  
525  
526  
527  
528  
529  
530  
531  
532  
533  
534  
535  
536  
537  
538  
539  
540  
541  
542  
543  
544  
545  
546  
547  
548  
549  
550  
551  
552  
553  
554  
555  
556  
557  
558  
559  
5510  
5511  
5512  
5513  
5514  
5515  
5516  
5517  
5518  
5519  
5520  
5521  
5522  
5523  
5524  
5525  
5526  
5527  
5528  
5529  
5530  
5531  
5532  
5533  
5534  
5535  
5536  
5537  
5538  
5539  
5540  
5541  
5542  
5543  
5544  
5545  
5546  
5547  
5548  
5549  
5550  
5551  
5552  
5553  
5554  
5555  
5556  
5557  
5558  
5559  
55510  
55511  
55512  
55513  
55514  
55515  
55516  
55517  
55518  
55519  
55520  
55521  
55522  
55523  
55524  
55525  
55526  
55527  
55528  
55529  
55530  
55531  
55532  
55533  
55534  
55535  
55536  
55537  
55538  
55539  
55540  
55541  
55542  
55543  
55544  
55545  
55546  
55547  
55548  
55549  
55550  
55551  
55552  
55553  
55554  
55555  
55556  
55557  
55558  
55559  
55560  
55561  
55562  
55563  
55564  
55565  
55566  
55567  
55568  
55569  
55570  
55571  
55572  
55573  
55574  
55575  
55576  
55577  
55578  
55579  
55580  
55581  
55582  
55583  
55584  
55585  
55586  
55587  
55588  
55589  
55590  
55591  
55592  
55593  
55594  
55595  
55596  
55597  
55598  
55599  
555100  
555101  
555102  
555103  
555104  
555105  
555106  
555107  
555108  
555109  
555110  
555111  
555112  
555113  
555114  
555115  
555116  
555117  
555118  
555119  
555120  
555121  
555122  
555123  
555124  
555125  
555126  
555127  
555128  
555129  
555130  
555131  
555132  
555133  
555134  
555135  
555136  
555137  
555138  
555139  
555140  
555141  
555142  
555143  
555144  
555145  
555146  
555147  
555148  
555149  
555150  
555151  
555152  
555153  
555154  
555155  
555156  
555157  
555158  
555159  
555160  
555161  
555162  
555163  
555164  
555165  
555166  
555167  
555168  
555169  
555170  
555171  
555172  
555173  
555174  
555175  
555176  
555177  
555178  
555179  
555180  
555181  
555182  
555183  
555184  
555185  
555186  
555187  
555188  
555189  
555190  
555191  
555192  
555193  
555194  
555195  
555196  
555197  
555198  
555199  
555200  
555201  
555202  
555203  
555204  
555205  
555206  
555207  
555208  
555209  
555210  
555211  
555212  
555213  
555214  
555215  
555216  
555217  
555218  
555219  
555220  
555221  
555222  
555223  
555224  
555225  
555226  
555227  
555228  
555229  
555230  
555231  
555232  
555233  
555234  
555235  
555236  
555237  
555238  
555239  
555240  
555241  
555242  
555243  
555244  
555245  
555246  
555247  
555248  
555249  
555250  
555251  
555252  
555253  
555254  
555255  
555256  
555257  
555258  
555259  
555260  
555261  
555262  
555263  
555264  
555265  
555266  
555267  
555268  
555269  
555270  
555271  
555272  
555273  
555274  
555275  
555276  
555277  
555278  
555279  
555280  
555281  
555282  
555283  
555284  
555285  
555286  
555287  
555288  
555289  
555290  
555291  
555292  
555293  
555294  
555295  
555296  
555297  
555298  
555299  
555300  
555301  
555302  
555303  
555304  
555305  
555306  
555307  
555308  
555309  
555310  
555311  
555312  
555313  
555314  
555315  
555316  
555317  
555318  
555319  
555320  
555321  
555322  
555323  
555324  
555325  
555326  
555327  
555328  
555329  
555330  
555331  
555332  
555333  
555334  
555335  
555336  
555337  
555338  
555339  
555340  
555341  
555342  
555343  
555344  
555345  
555346  
555347  
555348  
555349  
555350  
555351  
555352  
555353  
555354  
555355  
555356  
555357  
555358  
555359  
555360  
555361  
555362  
555363  
555364  
555365  
555366  
555367  
555368  
555369  
555370  
555371  
555372  
555373  
555374  
555375  
555376  
555377  
555378  
555379  
555380  
555381  
555382  
555383  
555384  
555385  
555386  
555387  
555388  
555389  
555390  
555391  
555392  
555393  
555394  
555395  
555396  
555397  
555398  
555399  
555400  
555401  
555402  
555403  
555404  
555405  
555406  
555407  
555408  
555409  
555410  
555411  
555412  
555413  
555414  
555415  
555416  
555417  
555418  
555419  
555420  
555421  
555422  
555423  
555424  
555425  
555426  
555427  
555428  
555429  
555430  
555431  
555432  
555433  
555434  
555435  
555436  
555437  
555438  
555439  
555440  
555441  
555442  
555443  
555444  
555445  
555446  
555447  
555448  
555449  
555450  
555451  
555452  
555453  
555454  
555455  
555456  
555457  
555458  
555459  
555460  
555461  
555462  
555463  
555464  
555465  
555466  
555467  
555468  
555469  
555470  
555471  
555472  
555473  
555474  
555475  
555476  
555477  
555478  
555479  
555480  
555481  
555482  
555483  
555484  
555485  
555486  
555487  
555488  
555489  
555490  
555491  
555492  
555493  
555494  
555495  
555496  
555497  
555498  
555499  
555500  
555501  
555502  
555503  
555504  
555505  
555506  
555507  
555508  
555509  
555510  
555511  
555512  
555513  
555514  
555515  
555516  
555517  
555518  
555519  
555520  
555521  
555522  
555523  
555524  
555525  
555526  
555527  
555528  
555529  
555530  
555531  
555532  
555533  
555534  
555535  
555536  
555537  
555538  
555539  
555540  
555541  
555542  
555543  
555544  
555545  
555546  
555547  
555548  
555549  
555550  
555551  
555552  
555553  
555554  
555555  
555556  
555557  
555558  
555559  
555560  
555561  
555562  
555563  
555564  
555565  
555566  
555567  
555568  
555569  
555570  
555571  
555572  
555573  
555574  
555575  
555576  
555577  
555578  
555579  
555580  
555581  
555582  
555583  
555584  
555585  
555586  
555587  
555588  
555589  
555590  
555591  
555592  
555593  
555594  
555595  
555596  
555597  
555598  
555599  
5555100  
5555101  
5555102  
5555103  
5555104  
5555105  
5555106  
5555107  
5555108  
5555109  
5555110  
5555111  
5555112  
5555113  
5555114  
5555115  
5555116  
5555117  
5555118  
5555119  
5555120  
5555121  
5555122  
5555123  
5555124  
5555125  
5555126  
5555127  
5555128  
5555129  
5555130  
5555131  
5555132  
5555133  
5555134  
5555135  
5555136  
5555137  
5555138  
5555139  
5555140  
5555141  
5555142  
5555143  
5555144  
5555145  
5555146  
5555147  
5555148  
5555149  
5555150  
5555151  
5555152  
5555153  
5555154  
5555155  
5555156  
5555157  
5555158  
5555159  
5555160  
5555161  
5555162  
5555163  
5555164  
5555165  
5555166  
5555167  
5555168  
5555169  
5555170  
5555171  
5555172  
5555173  
5555174  
5555175  
5555176  
5555177  
5555178  
5555179  
5555180  
5555181  
5555182  
5555183  
5555184  
5555185  
5555186  
5555187  
5555188  
5555189  
5555190  
5555191  
5555192  
5555193  
5555194  
5555195  
5555196  
5555197  
5555198  
5555199  
5555200  
5555201  
5555202  
5555203  
5555204  
5555205  
5555206  
5555207  
5555208  
5555209  
5555210  
5555211  
5555212  
5555213  
5555214  
5555215  
5555216  
5555217  
5555218  
5555219  
5555220  
5555221  
5555222  
5555223  
5555224  
5555225  
5555226  
5555227  
5555228  
5555229  
5555230  
5555231  
5555232  
5555233  
5555234  
5555235  
5555236  
5555237  
5555238  
5555239  
5555240  
5555241  
5555242  
5555243  
5555244  
5555245  
5555246  
5555247  
5555248  
5555249  
5555250  
5555251  
5555252  
5555253  
5555254  
5555255  
5555256  
5555257  
5555258  
5555259  
5555260  
5555261  
5555262  
5555263  
5555264  
5555265  
5555266  
5555267  
5555268  
5555269  
5555270  
5555271  
5555272  
5555273  
5555274  
5555275  
5555276  
5555277  
5555278  
5555279  
5555280  
5555281  
5555282  
5555283  
5555284  
5555285  
5555286  
5555287  
5555288  
5555289  
5555290  
5555291  
5555292  
5555293  
5555294  
5555295  
5555296  
5555297  
5555298  
5555299  
5555300  
5555301  
5555302  
5555303  
5555304  
5555305  
5555306  
5555307  
5555308  
5555309  
5555310  
5555311  
5555312  
5555313  
5555314  
5555315  
5555316  
5555317  
5555318  
5555319  
5555320  
5555321  
5555322  
5555323  
5555324  
5555325  
5555326  
5555327  
5555328  
5555329  
5555330  
5555331  
5555332  
5555333  
5555334  
5555335  
5555336  
5555337  
5555338  
5555339  
5555340  
5555341  
5555342  
5555343  
5555344  
5555345  
5555346  
5555347  
5555348  
5555349  
5555350  
5555351  
5555352  
5555353  
5555354  
5555355  
5555356  
5555357  
5555358  
5555359  
5555360  
5555361  
5555362  
5555363  
5555364  
5555365  
5555366  
5555367  
5555368  
5555369  
5555370  
5555371  
5555372  
5555373  
5555374  
5555375  
5555376  
5555377  
5555378  
5555379  
5555380  
5555381  
5555382  
5555383  
5555384  
5555385  
5555386  
5555387  
5555388  
5555389  
5555390  
5555391  
5555392  
5555393  
5555394  
5555395  
5555396  
5555397  
5555398  
5555399  
5555400  
5555401  
5555402  
5555403  
5555404  
5555405  
5555406  
5555407  
5555408  
5555409  
5555410  
5555411  
5555412  
5555413  
5555414  
5555415  
5555416  
5555417  
5555418  
5555419  
5555420  
5555421  
5555422  
5555423  
5555424  
5555425  
5555426  
5555427  
5555428  
5555429  
5555430  
5555431  
5555432  
5555433  
5555434  
5555435  
5555436  
5555437  
5555438  
5555439  
5555440  
5555441  
5555442  
5555443  
5555444  
5555445  
5555446  
5555447  
5555448  
5555449  
5555450  
5555451  
5555452  
5555453  
5555454  
5555455  
5555456  
5555457  
5555458  
5555459  
5555460  
5555461  
5555462  
5555463  
5555464  
5555465  
5555466  
5555467  
5555468  
5555469  
5555470  
5555471  
5555472  
5555473  
5555474  
5555475  
5555476  
5555477  
5555478  
5555479  
5555480  
5555481  
5555482  
5555483  
5555484  
5555485  
5555486  
5555487  
5555488  
5555489  
5555490  
5555491  
5555492  
5555493  
5555494  
5555495  
5555496  
5555497  
5555498  
5555499  
5555500  
5555501  
5555502  
5555503  
5555504  
5555505  
5555506  
5555507  
5555508  
5555509  
5555510  
5555511  
5555512  
5555513  
5555514  
5555515  
5555516  
5555517  
5555518  
5555519  
5555520  
5555521  
5555522  
5555523  
5555524  
5555525  
5555526  
5555527  
5555528  
5555529  
5555530  
5555531  
5555532  
5555533  
5555534  
5555535  
5555536  
5555537  
5555538  
5555539  
5555540  
5555541  
5555542  
5555543  
5555544  
5555545  
5555546  
5555547  
5555548  
5555549  
5555550  
5555551  
5555552  
5555553  
5555554  
5555555  
5555556  
5555557  
5555558  
5555559  
55555510  
55555511  
55555512  
55555513  
55555514  
55555515  
55555516  
55555517  
55555518  
55555519  
55555520  
55555521  
55555522  
55555523  
55555524  
55555525  
55555526  
55

1 370 nating between liquid- and vapor-like water interfaces in contact with the protein, thereby resembling a  
2 371 contact line.  
3  
4

5 372 Computer simulations on the order of nanometers and nanoseconds will benefit our fundamental un-  
6 373 derstanding of ice nucleation but have yet to be validated by experimental observations, which are typi-  
7 374 cally on larger scales and proceed over longer time periods. Relevant physicochemical parameters and  
8 375 constraints to predict ice formation in clouds that spread kilometers in size and take minutes to hours to  
9 376 evolve, must be acquired from ice nucleation studies performed in the field and laboratory. Interface-  
10 377 specific experimental techniques such as SFG and second-harmonic generation (SHG) spectroscopy can  
11 378 yield information on water structure at supercooled temperatures<sup>271, 275-276</sup>. Experimental observations of  
12 379 changes in interfacial water structure as ice nucleation is approached allows for comparison and inter-  
13 380 pretation by MD simulation<sup>271, 276</sup>.  
14  
15  
16  
17  
18  
19  
20  
21  
22  
23  
24  
25  
26  
27  
28  
29  
30  
31  
32  
33  
34  
35  
36  
37  
38  
39  
40  
41  
42  
43  
44  
45  
46  
47  
48  
49  
50  
51  
52  
53  
54  
55  
56  
57  
58  
59  
60

## FIELD MEASUREMENTS OF ICE RESIDUALS AND ICE NUCLEATING PARTICLES

383 Field measurements in the past decades have resulted in a wealth of determined INP number concen-  
384 trations and examination of IRs<sup>40, 53-54, 277-285</sup>. In this article, we focus on recent field measurements that  
385 were accompanied by techniques allowing for chemical speciation of INPs and IRs. Furthermore, those  
386 of which that demonstrated any potential or lack thereof of OA, carbonaceous particles, or OM to act as  
387 INPs are included<sup>93-94, 96, 98, 101-102, 219, 278, 286-303</sup>. In the following we will discuss selected studies in more  
388 detail.

389 Cziczo et al. (2013) examined IRs from cirrus clouds using a Counterflow-Virtual-Impactor (CVI)  
390 coupled to Particle Ablation by Laser Mass Spectrometry (PALMS) and found a dominance of dust par-  
391 ticles and a smaller portion of organic containing particles, particularly organics associated with sul-  
392 fates, making up IRs<sup>93</sup>. These findings corroborate earlier observations by DeMott et al. (2003) also in-  
393 dicating that IRs consisted of organics and sulfates<sup>278</sup>. Froyd et al. (2010)<sup>290</sup> examined the composition  
394 of IRs in subvisible cirrus clouds as displayed in Fig. 7. They found that internal mixtures of neutralized

1 sulfate with OM dominated the IRs and were similar in size and chemically indistinguishable from their  
2 unfrozen sulfate-organic aerosol counterparts. Mineral dust particles were not enhanced in these subvi-  
3 sible cirrus IRs and biomass burning particles were depleted in the IRs (Fig. 7a). These organosulfate  
4 compounds, present in the free troposphere, have been identified as the sulfate ester of IEPOX (2,3-  
5 epoxy-2-methyl-1,4-butanediol, C<sub>5</sub>H<sub>10</sub>O<sub>3</sub>)<sup>304</sup>, a second generation oxidation product of isoprene<sup>305-307</sup>  
6 corroborating the role of SOA in cloud ice formation.  
7  
8  
9  
10  
11  
12  
13

14 During the Megacity Initiative: Local And Global Research Observations (MILAGRO) field cam-  
15 paign<sup>308</sup>, air masses were tracked and sampled at various sites downwind from Mexico City. From anal-  
16 ysis of individual particles with scanning transmission X-ray microscopy (STXM) coupled with near  
17 edge X-ray absorption fine structure spectroscopy (NEXAFS) and computer controlled scanning elec-  
18 tron microscopy with an energy dispersive X-ray analyzer (CCSEM/EDX), Moffet et al. (2010)<sup>74</sup>  
19 showed that as the aerosol plume evolved from the city center, the organic mass per particle increased,  
20 the fraction of carbon-carbon double bonds decreased, and organic functional groups were enhanced  
21 indicative of photochemical aging<sup>29, 61</sup>. These anthropogenic dominated OA and SOA particles initiated  
22 immersion freezing and deposition ice nucleation, however, at different particle temperature and humid-  
23 ity conditions than most particles studied in laboratory experiments<sup>101</sup>. These findings highlighted the  
24 potential of chemically complex, anthropogenically impacted OA and SOA particles to participate in ice  
25 cloud formation. An improved sampling procedure was used during the California Research at the Nex-  
26 us of Air Quality and Climate Change (CalNex) campaign<sup>309</sup> where ice nucleation experiments and sin-  
27 gle particle analyses by STXM/NEXAFS and CCSEM/EDX were conducted on concurrent particle  
28 samples<sup>98</sup>. In this photochemically active region, all examined particles possessed OM and the INPs  
29 were among those, determined at a statistically significant level and further corroborating the role of  
30 OM in ice nucleation.  
31  
32  
33  
34  
35  
36  
37  
38  
39  
40  
41  
42  
43  
44  
45  
46  
47  
48  
49  
50  
51  
52  
53  
54  
55  
56  
57  
58  
59  
60

At the Storm Peak Laboratory (Steamboat Springs, Colorado, elevation of 3210 m), Baustian et al. (2012) sampled ambient aerosol in the fine and coarse mode for particles acting as INPs using PALMS

420 and Raman spectroscopy<sup>287</sup>. In the fine mode, the INPs were dominated by mineral dust, though a frac-  
1  
2  
3  
4  
5  
6  
7  
8  
9  
10  
11  
12  
13  
14  
15  
16  
17  
18  
19  
20  
21  
22  
23  
24  
25  
26  
27  
28  
29  
30  
31  
32  
33  
34  
35  
36  
37  
38  
39  
40  
41  
42  
43  
44  
45  
46  
47  
48  
49  
50  
51  
52  
53  
54  
55  
56  
57  
58  
59  
60  
tion of organic particles acted as INPs as well (Fig. 8). In contrast, INPs in the coarse mode were domi-  
nated by OM. This difference in INP composition emphasizes the importance of assessing the physico-  
chemical properties of the entire aerosol population, encompassing both accumulation and coarse mode  
particles. Furthermore, the organic INPs of the coarse mode showed exceptional ice nucleation propen-  
sity for temperatures below 230 K, activating at significant rates close to RH<sub>ice</sub> of 100%.

McCluskey et al. (2014)<sup>292</sup> sampled laboratory prescribed burns and wildfires, showing that biomass  
burning leads to the release of particles that are active as immersion freezing INPs at temperatures from  
241 to 261 K using the Continuous Flow Diffusion Chamber (CFDC) technique<sup>310</sup>. The authors applied  
transmission electron microscopy/energy dispersive X-ray (TEM/EDX) to examine morphology and  
composition of IRs, observing that INPs from wildfires consisted largely of carbonaceous particles such  
as tar balls or minerals rather than soot particles. The authors hypothesized that either secondary pro-  
cesses resulting in carbonaceous particles or uplifting of soil matter could explain why these two parti-  
cle types made up the majority of INPs. Although a decrease in INP numbers was observed in some ex-  
periments when removing refractory black carbon (rBC) using laser ablation<sup>311-312</sup> during prescribed  
burns of some fuels, that does not explain why during wildfires BC was a deficient INP type.

During the Indirect and Semi-Direct Aerosol Campaign (ISDAC) field campaign<sup>313</sup> conducted over  
Alaska near Barrow, aerosol particles were examined for composition and cloud formation including ice  
nucleation using CCSEM/EDX, STXM/NEXAFS, and CFDC by means of a CVI<sup>288</sup> (Fig. 9A). In gen-  
eral, the authors found, in agreement with other studies<sup>96, 98, 101-102</sup>, that all ambient particles and cloud  
residuals contain some OM<sup>288</sup>. The analyzed IRs possessed an inorganic or soot core and were coated by  
OM dominated by carboxylic groups indicative of chemical aging. This study suggests that particle size,  
composition, and chemical processing impact the particles' cloud nucleating ability. Worringen and  
coworkers sampled IRs and INPs using three different techniques at the High Alpine Research Station  
Jungfraujoch (Switzerland)<sup>301</sup>. Their measurements indicated that Ca-rich particles, carbonaceous mate-

rial and metal oxides made up the major fraction of INPs and IRs (Fig. 9B). This study emphasizes that carbonaceous particles play a role in mixed-phase cloud formation and that different sampling techniques such as the ice selective inlet (ISI) and ice-CVI yield different particle type contributions to ambient INPs and IRs. The application of SEM with high-resolution instruments was found to be particularly suited for investigation of INPs and IRs. At the same site, Kupiszewski et al. (2017)<sup>302</sup> observed that larger (up to 1  $\mu\text{m}$  in diameter) BC-containing IRs increased the activated frozen fraction of particles. Furthermore, BC-containing IR were found to have a thick coating, emphasizing the importance of atmospheric particle aging for ice nucleation.

Knopf et al. (2014)<sup>96</sup> examined particles for their physicochemical properties and ice nucleation propensity during the Carbonaceous Aerosols and Radiative Effects Study (CARES) campaign located in Central California<sup>314</sup>. A novel experimental procedure allowed identification of individual INPs among hundreds or thousands of collected particles not acting as INPs. Furthermore, the identified INPs were chemically imaged and compared with the compositional signature of the non-INPs present in same air mass (Fig. 10A, B). This study found that all analyzed particles contained OM though different particle type classes were identified. The identified INPs belonging to a certain particle type class were indistinguishable from the particles of the same class that did not act as INPs. The authors suggested that this may be due to the underlying stochastic nature of nucleation processes necessitating knowledge about the entire particle population to predict ice nucleation. This finding is similar to observations by Froyd et al. (2010)<sup>290</sup> and Wang et al. (2012)<sup>98</sup>. The same technique was applied to examine free tropospheric particles as potential INPs, sampled in the Azores (Fig. 10B)<sup>102</sup>. At this remote location, all particles possessed OM as partial or full coating and initiated heterogeneous ice nucleation in the immersion mode at saturated and subsaturated conditions for temperatures between 235 and 246 and in the deposition mode at about 120%  $\text{RH}_{\text{ice}}$  and 222 K. These long range transported and chemically aged free tropospheric particles showed very similar ice nucleation propensity among the different samples collected

469 at the Pico Mountain Observatory. It was hypothesized that this is due to the similar nature of the organ-  
1  
2  
3  
4  
5  
6  
7  
8  
9  
10  
11  
12  
13  
14  
15  
16  
17  
18  
19  
20  
21  
22  
23  
24  
25  
26  
27  
28  
29  
30  
31  
32  
33  
34  
35  
36  
37  
38  
39  
40  
41  
42  
43  
44  
45  
46  
47  
48  
49  
50  
51  
52  
53  
54  
55  
56  
57  
58  
59  
60  
ic coating acquired by these particles.

471 These recent studies indicate that particle size and associated particle composition are crucial parame-  
7  
8  
9  
10  
11  
12  
13  
14  
15  
16  
17  
18  
19  
20  
21  
22  
23  
24  
25  
26  
27  
28  
29  
30  
31  
32  
33  
34  
35  
36  
37  
38  
39  
40  
41  
42  
43  
44  
45  
46  
47  
48  
49  
50  
51  
52  
53  
54  
55  
56  
57  
58  
59  
60  
ters governing ice nucleation. For example, limiting the sampled particle size range may skew the iden-  
tified numbers of ambient INPs. Though chemical speciation was not achieved on individual INPs, Ma-  
son and coworkers examined ambient aerosol particles, collected on substrates using an impactor, for  
immersion freezing in a size-segregated fashion spanning particle sizes from 180 nm to 10  $\mu\text{m}$  (deter-  
mined by the cut-points of the 10 impactor stages) and probed freezing temperatures between 243 and  
258 K<sup>315-317</sup>. Correlations between the INP concentration and measurements of total particles, fluores-  
cent bioparticles, BC, sodium, methanesulfonic acid, and wind speed were performed. Employing this  
technique at a marine coastal site, the greatest INP concentrations were found in the supermicron size  
range between 1.8 and 5.6  $\mu\text{m}$  in diameter with less than half of the INPs numbers at lower and larger  
particle sizes<sup>315</sup>. Key findings were that primary biological aerosol particles were likely the major  
source of INPs at 248 to 258 K, mineral dust may have also had an important contribution to INPs ac-  
tive at 243 K, and BC and marine particles were negligible contributors. A complementary study by the-  
se authors including sites in North America and Europe indicated a similar trend where supermicron  
particles yielded the highest INP numbers<sup>317</sup>. In fact, it was concluded that if either supermicron parti-  
cles or coarse-mode particles were not sampled at those ground sites, ~78 and 53% of immersion-mode  
INPs may have been missed<sup>317</sup>. Similar findings of higher correlation of INP numbers with supermi-  
crometer sized particles were observed during mountain-site INP measurements<sup>318-320</sup>.

## 51490 LABORATORY MEASUREMENTS OF ORGANIC ICE NUCLEATING PARTICLES

52  
53  
54  
55  
56  
57  
58  
59  
60  
Laboratory studies have tremendously aided in our understanding of ice nucleation by allowing ice  
formation to be observed under controlled conditions of T and RH<sub>ice</sub>, identifying previously unknown

493 and atmospherically relevant INPs, and relating particle chemical composition and mixing state to ice  
1 nucleation propensity<sup>49-50, 53</sup>. Experiments have linked amorphous OA particle phase states with ice nu-  
2 cleation ability<sup>105, 112, 321-327</sup>. Other studies have emphasized a reduction in the uncertainties of relevant  
3 physical parameters including T, S<sub>ice</sub>, INP surface area and nucleation time to improve ice nucleation  
4 descriptions<sup>328-333</sup>. Novel technical approaches have been applied to quantify the molecular interplay  
5 and water structure at an ice nucleating interface<sup>271, 276, 334</sup> and monitor ice nucleation at submicrometer  
6 resolution<sup>219-220, 335-336</sup>. Despite current progress, there still exists a knowledge gap to explain ice nuclea-  
7 tion on a fundamental and molecular level, when considering amorphous OM.  
8

19501      Organic particle types that have recently gained more attention for their ice nucleation ability are ma-  
20 rine derived particles<sup>279, 337</sup>, ice nucleating macromolecules (INMs)<sup>104, 110, 338-344</sup>, soil OM<sup>345-349</sup>, plant  
21 derived OM<sup>350-352</sup>, dissolved organic species<sup>140, 198-199, 353-356</sup>, OA<sup>103, 162, 168, 233, 312, 322-324, 357-366</sup>, and SOA  
22 particles<sup>105, 112, 167, 325-327, 367</sup>.

### 28505      *Ice Nucleation by SOA Particles*

30506      Previous studies have observed ice nucleation on laboratory generated SOA particles<sup>105, 167, 321,</sup>  
31           <sup>325-327, 367</sup>. To illustrate the challenging task of predicting ice nucleation from SOA, Fig. 11 shows a  
32 compilation of experimentally obtained frozen fraction values ( $f_{ice}$  = number of nucleated ice crys-  
33 tals/aerosol particle number) for ice nucleating SOA particles derived from  $\alpha$ -pinene as a precursor gas  
34 as a function of S<sub>ice</sub>. The homogeneous freezing regime is included as dotted lines for each dataset de-  
35 pendent on T and RH. We note that these studies all utilized particles with diameters on the order of 10<sup>2-</sup>  
36 43 10<sup>3</sup> nm. Ice formation by  $\alpha$ -pinene SOA particles from ozonolysis was investigated by Möhler et al.  
44512 (2008)<sup>321</sup> in a cloud chamber over activation time scales of ~90 s, representing cooling rates of about 1.5  
45           <sup>46</sup> K min<sup>-1</sup>. They observed that only a few ice nucleation events occurred in the heterogeneous freezing re-  
47513 gime while most were observed at homogeneous freezing conditions. Cloud chamber data over a wider  
48           <sup>49</sup> temperature range of 205-235 K for the same particle system are presented in Wagner et al. (2017)<sup>368</sup>,  
50           <sup>51</sup> revealing that ice nucleation occurred at or above homogeneous freezing conditions. Similarly, Ladino  
52           <sup>53</sup> 56517 revealed that ice nucleation occurred at or above homogeneous freezing conditions. Similarly, Ladino  
54           <sup>55</sup> 56517 revealed that ice nucleation occurred at or above homogeneous freezing conditions. Similarly, Ladino  
56           <sup>57</sup> 56517 revealed that ice nucleation occurred at or above homogeneous freezing conditions. Similarly, Ladino  
57           <sup>58</sup> 56517 revealed that ice nucleation occurred at or above homogeneous freezing conditions. Similarly, Ladino  
58           <sup>59</sup> 56517 revealed that ice nucleation occurred at or above homogeneous freezing conditions. Similarly, Ladino  
59           <sup>60</sup> 56517 revealed that ice nucleation occurred at or above homogeneous freezing conditions. Similarly, Ladino

et al. (2014)<sup>326</sup> found  $\alpha$ -pinene SOA particles with different O:C generated at room temperature to form ice in the homogeneous freezing regime when using a CFDC having a 12 s residence time, resulting in very short activation times (i.e., a cooling rate of  $300 \text{ K min}^{-1}$ ). However, when precooling the SOA particles, an increased ice nucleation propensity was observed attributed to the transitioning of the particles into a more viscous phase state. When using OH as the main oxidant for  $\alpha$ -pinene, Charnawskas et al. (2017)<sup>112</sup> demonstrated that biogenic SOA from OH reaction with isoprene,  $\alpha$ -pinene and longifolene formed ice only at the homogeneous freezing limit, i.e.,  $S_{\text{ice}}$  of 1.45-1.65 for temperatures between 210 and 235 K. This study applied typical cloud activation time scales on the order of ~20 min (or cooling rates of  $0.1 \text{ K min}^{-1}$ ) and observed the least favorable conditions for ice formation as seen in Fig. 11. The cooling rate applied to SOA particles is likely a significant parameter that affects observation of freezing and allows for accessing lower frozen fractions<sup>102, 112</sup>. Application of slower rates, enhances the likelihood that particles reach thermodynamic equilibrium resulting in PD or FD, both of which may reduce SOA ice nucleation efficiency leading to observed lower frozen fractions. Ignatius et al.<sup>327</sup> generated SOA particles by exposure of  $\alpha$ -pinene to  $O_3$  and OH radicals, at various temperatures between 235 and 268 K. In contrast to previous studies, exceptional heterogeneous ice nucleation efficiency was observed, where all freezing events took place below homogeneous freezing conditions. A possible explanation is that the SOA particles changed into a highly viscous glassy phase state prior to CFDC sampling as they were transported through tubing at a warmer T than the particles' formation temperature<sup>327</sup>, potentially leading to drying of the particles. The residence time in the CFDC was 10 s, likely probing the ice nucleation ability of solid SOA particles since time for reaching FD was too short<sup>112, 119</sup>. This case illustrates that if SOA in a glassy state are exposed to thermodynamic conditions in which they should be liquid, too short residence times may result in those particles maintaining their glass-like state and initiating deposition or immersion freezing. On the other hand, particles which are liquid and are too quickly exposed to conditions favoring a glassy phase (e.g., from room temperature to a lower temperature with too short residence time), may not have sufficient time to equilibrate and solidify. In this latter case, no ice nucleation or homogeneous ice nucleation would be expected to occur. Although the  $\alpha$ -

544 pinene SOA particles summarized in Fig. 11 may have different chemical composition, the most signifi-  
1  
545 cant parameter that changes the ice nucleation propensity expressed as  $f_{ice}$  is hypothesized to be the par-  
2  
546 ticle phase state prior to ice nucleation. When starting the ice nucleation experiment with liquid  $\alpha$ -  
3  
547 pinene SOA particles, the particles do not show significant ice nucleation propensity. However, if the  
4  
548 SOA particles are highly viscous or solid when entering an ice nucleation experiment, higher  $f_{ice}$  values  
5  
549 may be observed. In summary, unless the experimental T and RH trajectories or history are well known  
6  
12549 and compare close to atmospherically relevant cloud activation conditions, it will be difficult to ascer-  
7  
14550 tain the role of biogenically or anthropogenically derived SOA in atmospheric ice formation processes.  
8  
15  
16551  
17  
18  
19552  
20  
21553 Evaluation of the effect of different updraft velocities, which will govern the particles' RH and T  
22  
23  
24554 trajectories, on SOA particle phase state was conducted by Charnawskas et al. (2017)<sup>112</sup>. The authors  
25  
26555 modelled SOA particle phase and water uptake for different updraft velocities resulting in different hu-  
27  
28556 midification rates for the purposes of constraining heterogeneous ice nucleation regimes in the RH and  
29  
30557 T parameter space as shown in Fig. 12. These results were derived using a numerical diffusion model  
31  
32  
33558 that includes kinetics of gas-phase diffusion, reversible adsorption, surface-to-bulk transfer, and bulk  
34  
35559 diffusion of water through particles constrained by observations of particle hygroscopicity and viscosity  
36  
37560 as a function of RH and T<sup>119</sup>. Fig. 12 shows the thermodynamic conditions at which lofted isoprene,  $\alpha$ -  
38  
39561 pinene and naphthalene SOA particles experience glass transition and full deliquescence as a function of  
40  
41562 air parcel updraft velocity with implications for the potential ice nucleation pathways. The simulation  
42  
43  
44563 results indicate that for slow updraft velocities (lower humidification rates, dotted green lines) the po-  
45  
46564 tential heterogeneous freezing regime ( $RH_{ice} > 100\%$ ) starts at  $T < \sim 230, 235$  and  $240$  K for isoprene,  $\alpha$ -  
47  
48565 pinene and naphthalene SOA, respectively. Faster updrafts shift these conditions by 5-8 K to warmer  
49  
50  
51566 temperatures. Fig. 12 also demonstrates the impact of sulfates on SOA phase state, resulting in signifi-  
52  
53  
54567 cantly lower glass transition points and FDRH<sup>113-114</sup>, thus limiting the conditions where heterogeneous  
55  
56568 ice nucleation can proceed. The simulations suggest that the investigated biogenic SOA (Fig. 12A, B) do  
57  
58569 not act as INP for mixed-phase cloud conditions and likely will serve as INP only at lower temperatures  
59  
60 and faster updraft velocities. This is qualitatively in agreement with previous studies that based this con-

570 clusion on derived water diffusion coefficients in  $\alpha$ -pinene SOA particles<sup>118, 141</sup>. Naphthalene SOA  
1  
2 shows the highest FDRH values and as such has greatest potential to act as an INP under mixed-phase  
3  
4 cloud conditions. However, the simulations of naphthalene SOA neglect the potential of condensed-  
5  
6 phase oligomerization reactions that can proceed in SOA formation<sup>369-370</sup>. This may be the reason for the  
7  
8 disagreement with experimental data by Wang et al. (2012)<sup>105</sup>, who showed that naphthalene SOA can  
9  
10 act as INP in immersion mode for temperatures up to 240 K and close to water saturation. Wang et al.  
11  
12 (2012)<sup>105</sup> experimentally demonstrated that the glass transition point modulates the ice nucleation path-  
13  
14 way, resulting in either immersion freezing or deposition ice nucleation. The authors compared their la-  
15  
16 boratory data with ice nucleation observations from the MILAGRO and CalNex campaigns<sup>98, 101</sup>. These  
17  
18 ambient particles were all dominated by OM, likely due to SOA formation in these photochemically ac-  
19  
20 tive regions, and the T and S<sub>ice</sub> at which either deposition ice nucleation or immersion freezing occurred  
21  
22 were constrained by predicted naphthalene SOA glass transition as a function of a<sub>w</sub><sup>105</sup>. In summary, SOA  
23  
24 derived from heavier precursor gases such as naphthalene show higher glass transition points and there-  
25  
26 fore can act as INPs over a greater range of T and RH. This is in line with condensed-phase material  
27  
28 with higher molecular weight showing warmer glass transition temperatures<sup>113</sup>. Furthermore, SOA parti-  
29  
30 cle oxidation state and the presence of plasticizing material such as sulfates have a significant impact on  
31  
32 the conditions at which heterogeneous ice nucleation can proceed<sup>112-114, 119, 122</sup>.

#### 587 *Humic-Like Substances as INPs*

42588       Humic acids (HAs) and humic-like substances (HULIS) are a common Earth and atmospheric  
43  
44 constituent<sup>371</sup>. It has been demonstrated that those compounds can nucleate ice in the deposition and  
45  
46 immersion modes<sup>233, 372</sup> where the latter pathway follows a water activity description<sup>360, 373</sup>. In case of  
47  
48 immersion freezing, no correlation with droplet volume was observed<sup>360</sup>. Chemical aging<sup>374-375</sup> due to  
49  
50 ozone exposure of the HULIS compound leonardite resulted in a decrease in deposition ice nucleation  
51  
52 ability<sup>233</sup>. The authors hypothesized that this was due to alterations of hydrophobic and hydrophilic  
53  
54 functional groups on particle surfaces<sup>233</sup>. Investigations of solid ice nucleating soil organic particles  
55  
56  
57  
58  
59

1 595 (such as HULIS) were reviewed previously and in general agree that heat treatment and hydrogen per-  
2 596 oxide exposure of soils decreases their ice nucleation ability, which is thought to be a result of the or-  
3 597 ganic digestion, i.e., chemical modification or dissolution and removal of biogenic or organic from the  
4 598 soil particle surface<sup>53</sup>. However, it is important to note that ambient atmospheric HULIS may take up  
5 599 organic vapors such as toluene and benzyl alcohol in the presence of water vapor<sup>376</sup> and that chemical  
6 600 aging by OH radicals can impact HULIS particle composition by molecular fragmentation with conse-  
7 601 quences for particle hygroscopicity<sup>377</sup>. Smaller sized oxidized molecules, like C2 to C6 carboxylic acids  
8 602 dissolved in water, have not been found to affect ice nucleation<sup>353</sup> similar to previous studies employing  
9 603 dicarboxylic acids<sup>354</sup>.

20  
21 604 *Ice Nucleating Macromolecules*  
22

23 605 In contrast to ice nucleating solid organic substrates hundreds of nanometers to micrometers in  
24 606 size, INMs are on the order of  $10^2$  kDa or  $\sim 3$  nm in diameter<sup>44, 104, 110, 338-341, 343-344, 378-380</sup>. Pummer et al.  
25 607 (2012)<sup>340</sup> demonstrated that the water in which pollen was previously suspended retains ice nuclei after  
26 608 the pollen grains were removed and provided evidence that the responsible ice nucleating agents are  
27 609 polysaccharide macromolecules. Other studies have since confirmed this finding for the same type of  
28 610 pollen<sup>339, 343, 378</sup>. Observation of pollen and pollen derived components such as sugars and sugar-  
29 611 alcohols in atmospheric particles have been made<sup>381-383</sup> highlighting the potential relevance of INMs for  
30 612 atmospheric ice cloud formation. However, other biogenic particles such as fungal spores and bacteria  
31 613 can serve as a source of INMs<sup>104, 344, 379</sup> which may imply that INMs in general are derived from a varie-  
32 614 ty of biological or biogenic particles. Fig. 13 adapted from Pummer et al. (2015)<sup>104</sup> compiled INM size  
33 615 as a function of observed ice nucleation temperature and found that their relationship follows closely  
34 616 prediction of the critical ice cluster size given by CNT parameterized by Zobrist et al. (2007)<sup>108</sup>. It may  
35 617 be that the size of a single INM determines the temperature for it to nucleate ice. However, it should be  
36 618 noted that due to possibly different chemical properties of INMs or aggregation from filtration, total  
37 619 concentration of INMs are uncertain and lead to a range of ice nucleation temperatures<sup>104</sup>. For example,  
38 620 suspensions of INM at  $\leq 1000$  kDa derived from either the pollen *Betula pendula* or the fungus *Fusari-*  
39 621 *um* have been shown to have ice nucleation temperatures between -10°C and -15°C<sup>104</sup>.  
40 622

621 *um avenaceum* were observed to nucleate ice from 253-258 K and 248-267 K, respectively<sup>344</sup>, indicating  
622 that ice nucleation temperatures should also depend on the total concentration of INMs present<sup>104, 344</sup>.  
623 Dreischmeier et al. (2017)<sup>110</sup> observed not only heterogeneous ice nucleation from pollen washing wa-  
624 ter, but simultaneous ice binding properties, both initiated by polysaccharides bearing carboxylate  
625 groups where the former is due to macromolecules > 100 kDa and the latter < 100 kDa. Polysaccharides  
626 may be an atmospheric ice nucleating agent due to their ubiquity in organic and biogenic matter. X-ray  
627 micro-spectroscopic evidence has shown that ice nucleation can occur on atmospheric particles coated  
628 by OM<sup>96</sup> that has a similar chemical signature to that of atmospheric marine polysaccharide-like parti-  
629 cles<sup>384</sup>.

### 21630 *Marine Derived INPs*

22  
23 SSA particles composed of sea salts and OM may dominate numbers of INPs in regions where  
24 atmospheric dust loadings are relatively low<sup>337, 385-386</sup>. Fragments of marine phytoplankton cells, intact  
25 cells and associated exudate material nucleate ice, where immersion freezing followed solution water  
26 activity<sup>337, 387-390</sup>. Immersion freezing did not show a correlation with droplet volume<sup>387</sup>. Cellulose is a  
27 common constituent of cell walls in plants and algae in both the marine and terrestrial environment and  
28 was recently shown to nucleate ice as efficiently as desert dust<sup>352</sup>. The authors also claim that although  
29 airborne cellulose is less abundant than atmospheric minerals, it could play a role in cloud formation.  
30 Wilson et al.<sup>337</sup> found that droplets prepared from water sampled from the sea surface microlayer (the  
31 uppermost 1 to 1000 μm of the ocean surface) froze heterogeneously and provided evidence based on  
32 particle size, heat treatment, and X-ray micro-spectroscopy that the likely ice nucleating substrate  
33 stemmed from phytoplankton exudate material. This material, that can be polysaccharidic and protein-  
34 acous<sup>391</sup>, retained its ice nucleation propensity when filtering through a 0.2 μm filter adding to the class  
35 of water soluble INMs similar to findings of INMs derived from fungi, bacteria, and pollen<sup>104, 340, 378-380</sup>.  
36 DeMott et al.<sup>279</sup> and McCluskey et al.<sup>392</sup> showed that aerosolized particles from a laboratory wave flume  
37 containing cultures of phytoplankton and bacteria can also nucleate ice and suggested that numbers of  
38 INPs over remote marine regions may be linked to biological processes in the water.

647    *Organic Matter Mixed with Mineral Dust, Ammonium Sulfate, and Soot*

1  
2  
3    648       During atmospheric transport, mineral dust can be coated by inorganic material or OM. Recent  
4  
5    649       experimental studies generally agree that coated mineral dust (e.g., coated with sulfates, ammonium sul-  
6  
7    650       fate, ammonium bisulfate, nitric acid, levoglucosan, or succinic acid) show decreased ice nucleation  
8  
9    10651      ability below water saturation<sup>85, 87, 321, 361, 393-402</sup>. By increasing RH toward 100%, thereby diluting the  
11  
12    12652      coating material, ice nucleation temperatures approach those of uncoated mineral particles, indicative of  
13  
14    14653      a typical freezing point depression behavior<sup>188, 197, 356, 373, 395, 399</sup>. Modification of particle surfaces due to  
15  
16    17654      chemical reaction can significantly alter the ice nucleation behavior as shown, e.g., for sulfuric acid  
17  
18    19655      coated feldspar<sup>394</sup> and kaolinite<sup>88, 399</sup>. These laboratory studies demonstrate that aging of particles which  
19  
20    21656      acquire coatings can alter physical (solute effect) and chemical (surface site) particle properties resulting  
21  
22    23657      in different ice nucleation characteristics.

25  
26    26658      In the 2013 study by Schill and Tolbert<sup>324</sup>, heterogeneous ice nucleation was directly observed  
27  
28    28659      for mixed organic and ammonium sulfate particles, in which the organic was present as a glass coating  
29  
30    31660      the inorganic core. Fig. 14 shows optical images of ice nucleation with Raman spectra acquired along a  
31  
32    33661      cross section of the organic particle and ice crystal. Two organic components, 2, 2, 6, 6-  
33  
34    35662      tetrakis(hydroxymethyl) cyclohexanol and 1,2,6-hexanetriol referred to as C10 and C6, respectively,  
36  
37    38663      were mixed with ammonium sulfate. The optical microscopy image shows that ice nucleated on the sur-  
38  
39    40664      face of the mixed C6/C10 particle coating present in a glass-like state engulfing the ammonium sulfate  
41  
42    42665      core (Fig. 14, left panel). The Raman spectra show that the N-H and sulfate stretching modes are local-  
43  
44    44666      ized at the core while the C-H stretching modes encompasses the particle indicating that the organic is  
45  
46    47667      completely coating the inorganic particle core (Fig. 14, right panel). Ice (O-H stretching mode) is locat-  
47  
48    49668      ed on the glassy organic surface (C-H stretching mode). These observations directly demonstrate that a  
49  
50    51669      highly viscous organic surface can act as a substrate requirement for heterogeneous ice nucleation. Sur-  
52  
53    54670      rogate SOA material such as sucrose, citric acid, raffinose, and 4-hydroxy-3-methoxy mandelic acid  
55  
56    56671      among others can be glassy at UT temperatures and have been shown to nucleate ice<sup>168, 322-324, 358</sup>. Mur-  
57  
58  
59  
60

672 ray et al.<sup>322</sup> observed that aqueous citric acid aerosol can be solid under typical cirrus conditions induc-  
673 ing heterogeneous ice nucleation. The authors suggest that ice nucleation by organic-rich particles may  
674 explain observed low ice crystal numbers and high in-cloud humidity in the tropical tropopause layer.

675 Soot or BC is ubiquitous in the atmosphere as a result of biomass burning and fossil fuel  
676 combustion<sup>403</sup> and its ability to nucleate ice has been previously discussed in detail<sup>49-50, 53</sup>. During at-  
677 mospheric transport, soot can acquire OM impacting particle morphology and mixing state<sup>404-407</sup>. Re-  
678 cently, Ullrich et al. (2017)<sup>408</sup> evaluated the ice nucleation propensity of different types of soot using a  
679 cloud chamber. They observed that soot particles with higher OC content (>20%) showed lower deposi-  
680 tion ice nucleation efficiency than soot with lower OC content (<20%). Soot can be a more efficient INP  
681 compared to the investigated desert dust in deposition mode at temperatures between 215 and 235 K.  
682 Only a few studies have investigated the ice nucleation propensity of organic coated soot particles<sup>112, 409-</sup>  
683 <sup>412</sup>. Kulkarni et al. (2016)<sup>411</sup> emphasizes that despite the wealth of observations the effect of different  
684 atmospheric aging processes on the propensity of soot to nucleate ice is not well established. Aging pro-  
685 cesses will be discussed in more detail in the following section.

### 686 Biomass Burning Aerosol as INPs

687 Previous studies observed that INPs were present in only some prescribed laboratory burns of differ-  
688 ent biomass fuels reflecting southeastern and western U.S. flora<sup>364-365</sup>. Ice nucleation was observed at  
689 temperatures lower than 233 K, but only at the homogeneous freezing limit of aqueous solution<sup>364</sup>. The-  
690 se findings are similar to experimental ice nucleation results applying biomass burning surrogate spe-  
691 cies<sup>198-199</sup>. Levin et al. (2016) observed measurable INP concentrations at 243 K from combustion emis-  
692 sions from 13 of 22 different biomass fuel types<sup>366</sup>. When removing rBC via laser-induced incandes-  
693 cence<sup>311-312</sup>, they observed significant reductions in INP numbers emphasizing the role of rBC in INP  
694 for some biomass fuels.

### 695 The Effects of Atmospheric Aging, Coating, and Oxidation State on Ice Nucleation

696 Friedman et al. (2011)<sup>409</sup> investigated the effect of coatings of adipic, malic, and oleic acid on soot on  
697 ice nucleation. In addition, oleic acid coated soot particles were exposed to ozone to simulate atmos-

698 phetic oxidation. The authors did not observe heterogeneous freezing at 253 K and 243 K and only ho-  
699 mogeneous freezing at 233 K. Oxidation of oleic acid coated soot particles by ozone did not have a sig-  
700 nificant effect on ice nucleation. Chou et al. (2013)<sup>410</sup> did not observe changes in the ice nucleation effi-  
701 ciency of soot particles from a vehicle diesel engine that have been photochemically aged. However,  
702 addition of  $\alpha$ -pinene at 238 K led to a thicker organic coating with higher organic carbon (OC) to BC  
703 ratio, increased particle size and enhanced ice nucleation. Schill et al. (2016)<sup>412</sup> studied immersion  
704 freezing at 243 K from particles emitted by a diesel engine fueled with either petrodiesel and biodiesel.  
705 The exhaust was aged up to 1.5 photochemically equivalent days using an oxidative flow reactor. The  
706 authors found that aging of the diesel exhaust did not impact INP numbers and that exhaust of both fuels  
707 is not likely to contribute to atmospheric INP concentrations under mixed-phase cloud conditions. Kul-  
708 karni et al. (2016)<sup>411</sup> investigated the ice nucleation ability of fresh and aged diesel soot particles for  
709 temperatures between 223 K and 233 K. They employed transmission electron microscopy (TEM), X-  
710 ray photoelectron spectroscopy (XPS) and single particle mass spectrometry to track morphological and  
711 compositional changes of the soot particles. Bare, hydrated and compacted soot particles induced ice  
712 formation below the homogeneous freezing threshold, whereas soot particles coated with  $\alpha$ -pinene SOA  
713 nucleated ice at homogeneous freezing conditions in agreement with the study by Charnawskas et al.  
714 (2017)<sup>112</sup>. However, soot particles coated with a similar SOA formed at ~80% RH conditions (high RH)  
715 had an ice nucleation efficiency that was similar to that of bare soot particles<sup>411</sup>. This may be since the  
716  $\alpha$ -pinene SOA coating under those initial high RH conditions was chemically different compared to the  
717  $\alpha$ -pinene SOA coating generated under dry conditions. Another reason may be due to SOA volatility.  
718 Previous research has found that RH and T can impact SOA volatility<sup>33, 413-418</sup>, implying that if SOA  
719 coatings were to evaporate from soot particles, then their bare surface may be exposed after some time  
720 rendering their ice nucleation efficiency like the one of bare soot particles. This may point again to the  
721 importance of the SOA generation conditions and corresponding SOA phase state for understanding the  
722 potential ice nucleation pathways.

During atmospheric transport particles can age by condensation of inorganic compounds and OM and by multiphase chemical reactions involving, e.g., atmospheric oxidants and radicals such as O<sub>3</sub> and OH<sup>374-375, 419-424</sup>. The impact of heterogeneous or multiphase chemical oxidation of some organic substrates on ice nucleation has been previously investigated<sup>103, 233, 260, 409, 425</sup>. Exposure of soot surrogate material Lamp Black 101 to O<sub>3</sub> simulating about 2 weeks of atmospheric residence did not change the ice nucleation propensity in a temperature range from 242 to 257 K<sup>260</sup>. Friedman et al. (2011)<sup>409</sup> exposed bare soot and soot coated with oleic acid to O<sub>3</sub> simulating 3.5 days of atmospheric aging and did not observe a difference in the ice nucleation capability of either particle type. Wang and Knopf (2011)<sup>233</sup> exposed Leonardite, a humic acid, and Suwannee River fulvic acid (SRFA) to O<sub>3</sub> simulating about 2 weeks residence under remote conditions. In that study, they observed that O<sub>3</sub> oxidation led to a decrease in deposition nucleation efficiency and to water uptake at lower temperatures for Leonardite particles and to an increase in the lowest temperature at which deposition nucleation was observed for the SRFA particles. Brooks et al. (2014)<sup>425</sup> investigated ice nucleation in the contact mode using fresh and oxidized soot and polycyclic aromatic hydrocarbon (anthracene, pyrene, and phenanthrene) particles. O<sub>3</sub> exposure was conducted at ~80 ppm for 24 hrs. Exposure to ozone facilitated ice nucleation, on average, at 2–3 K warmer temperatures. For similar O<sub>3</sub> exposures, Collier and Brooks (2016)<sup>103</sup> examined the ice nucleating propensity of organic hydrocarbons including octacosane, squalane, and squalene in contact with water. The oxidized octacosane initiated contact freezing at 1.1 K warmer temperatures than the fresh one, the difference between these temperatures determined to be statistically significant. Oxidized squalane initiated freezing at ~2 K lower temperatures than the fresh one whereas freezing initiated by oxidized squalene did not differ from application of fresh squalene particles.

In all these experiments, chemical aging was conducted at room temperature under which the organic phase is likely semi-solid or liquid. However, particles acting as INP are likely to be found at higher altitudes and thus lower temperatures where particle oxidation may dominantly occur on solid organic phases. Chemical aging by oxidation of a solid particle versus a liquid particle will proceed differently<sup>426-429</sup> with different implications for the oxidized particles' cloud formation potential. Chem-

1      749      ical processing of an solid organic particle by atmospheric oxidants may be limited to the uppermost  
2      750      particle surface layers<sup>420, 428</sup> and may proceed via different reaction pathways, e.g., leading to higher de-  
3      751      grees of molecular fragmentation<sup>377, 426, 430-431</sup> thereby impacting hygroscopicity<sup>84, 377, 432-433</sup>. This in turn  
4      752      affects water uptake which is necessary for immersion freezing to proceed.  
5  
6  
7  
8

9      753      A few studies have examined SOA formation from precursor gases cyclohexene,  $\alpha$ -pinene, and limo-  
10     754      nene reacting with O<sub>3</sub> for temperatures as low as 243 K<sup>434-437</sup>. In general, these studies found that the  
11     755      SOA yield increases at lower temperatures due to lower vapor pressures and different particle chemical  
12     756      composition. For example, SOA particles from the ozonolysis of  $\alpha$ -pinene at 253 K had increased mass  
13     757      fraction of carboxylic acids and lower O:C compared to SOA formed at 293 K<sup>437</sup>. Furthermore, it was  
14     758      observed that dimer ester production was suppressed at lower temperatures. These observations point to  
15  
16     759      different chemical composition of SOA at lower formation temperatures that will likely impact particle  
17  
18     760      hygroscopicity, viscosity and reactivity towards atmospheric oxidants which in turn will affect ice nucle-  
19  
20     761      ation. Considering that during atmospheric transport OA is continuously exposed to atmospheric oxi-  
21  
22     762      dants and to condensing secondary OM both potentially altering the physicochemical properties of the  
23  
24     763      particle, more experimental and theoretical studies conducted at atmospherically relevant temperatures  
25  
26     764      investigating the impact of chemical aging under atmospherically relevant oxidant exposures and SOA  
27  
28     765      formation on INPs are warranted.  
29  
30  
31

32     766      Not explicitly discussed when describing the ice nucleation potential of SOA particles or coatings, is  
33     767      the fact that depending on the chemical formation pathway, SOA material has different O:C<sup>29, 33, 62, 420,</sup>  
34     768      <sup>438-440</sup>. Although T<sub>g</sub> is dominated by the molecular weight of the species<sup>113</sup>, O:C also impacts T<sub>g</sub><sup>122</sup>. Nu-  
35     769      merical diffusion modeling suggests that for  $\alpha$ -pinene SOA, increases of O:C increases T<sub>g</sub> whereas for  
36     770      naphthalene SOA, an increase in O:C results in a lower of T<sub>g</sub><sup>112, 119</sup>. The reason for this trend is based on  
37     771      the produced condensed-phase products accounted for in the model<sup>119</sup>. Composition determined changes  
38     772      in T<sub>g</sub> will also impact FDRH and thus the regime of potential ice nucleation pathways. Furthermore, a  
39     773      solid SOA particle phase state at room temperature is not a guarantee that this particle initiates ice nu-  
40     774      cleation at lower temperatures, as observed for the case of longifolene SOA<sup>112</sup>. A greater particle hygro-  
41  
42  
43  
44  
45  
46  
47  
48  
49  
50  
51  
52  
53  
54  
55  
56  
57  
58  
59  
60

1      775      scopicity likely accelerates the amorphous deliquescence and thus decreases the window in which im-  
2      776      mersion freezing can proceed. Clearly, the chemical composition, phase state, and hygroscopicity of  
3      777      SOA particles under typical mixed-phase and cirrus cloud conditions must be well characterized to pre-  
4      778      dict their potential to act as atmospheric INPs.  
5  
6  
7  
8  
9  
10  
11

## 12 780 ANALYSES OF ICE NUCLEATION DATA 13

### 14 781 *Current State of Ice Nucleation Data Analysis* 15

16  
17 782      How best to analyze heterogeneous ice nucleation data is currently debated, with more studies focus-  
18      783      ing on immersion freezing<sup>49-50, 328, 332, 373, 441-442</sup> than deposition ice nucleation<sup>221, 233, 333, 443</sup>. Commonly  
19      784      20 two approaches to explain the data are used, a stochastic description based on CNT and a deterministic  
21      785      22 or singular description. The stochastic description assumes that cluster formation leading up to ice nu-  
23      786      25 cleation occurs randomly over time on a substrate yielding a heterogeneous ice nucleation rate coeffi-  
24      787      27 cient,  $J_{\text{het}}(T)$ <sup>40, 108</sup>.  
25  
26

27  
28 788      By measuring  $J_{\text{het}}$ , CNT allows contact angles to be derived that can be parameterized in different  
29      789      30 ways to reflect the substrate's propensity to nucleate ice. Different parameterizations, however, result in  
31      790      32 different interpretation of the underlying nucleation mechanism<sup>40, 108, 328, 360</sup>. Theoretical calculation of  
32      791      34 any contact angle requires not only  $J_{\text{het}}$  observations, but also a choice in free energy of ice nucleus acti-  
33      792      36 vation. This in turn necessitates knowledge of thermodynamic and kinetic parameters relating to the  
34      793      38 critical water cluster and parameters such as supersaturation and temperature. A recent non-classical  
35      794      40 method to calculate free energy of critical cluster formation has been proposed based on changes in en-  
36      795      42 tropy as water molecules transition from the bulk to the ice cluster, rearranging their hydrogen bonding  
37      796      44 environment<sup>331</sup>.  
38  
39

40  
41 797      In contrast, the singular hypothesis assumes that there are a number of surface active sites on a parti-  
42      798      43 cle each of which has a different ice nucleating efficiency, depending on temperature only. This explana-  
43      799      45 tion neglects ice nucleation kinetics, i.e., fluxes of water molecules and fluctuations of ice embryo for-  
44  
45  
46  
47  
48  
49  
50  
51  
52  
53  
54  
55  
56  
57  
58  
59  
60

800 mation and currently lacks a physical basis of the observed events<sup>328, 444</sup>. The concept of ice active sites  
1  
2 801 has been used to parameterize ice nucleation data and implemented in CNT based analyses. These in-  
3 clude the multi-component model<sup>445</sup>, the time-dependent freezing rate parcel model<sup>446</sup>, parameteriza-  
4 tions of INPs per liter of air<sup>277</sup>, the probability density function (PDF) model<sup>447-448</sup>, the active site mod-  
5 el<sup>447-448</sup>, the surface-site based stochastic model<sup>442</sup>, the singular or modified-singular description<sup>387-388,</sup>  
6 10 804 445, 449-451, and the so-called soccer ball model<sup>444</sup>. However, due to the lack of observational characteriza-  
7 12 805 tion as discussed above, it remains to be seen whether active sites, though intriguing conceptually, are  
8 14 806 more than a mathematical construct to describe data. Furthermore, fitting parameters for these schemes  
9 16 807 applied to large scale atmospheric models are always implicitly dependent on the choice of laboratory  
10 18 808 defined thermodynamic and kinetic parameters<sup>441</sup>. In cloud resolving models the role of time, particle  
11 20 809 size, ice nucleation schemes or contact angle distributions on ice cloud formation have been investigated  
12 22 810 and are currently under scrutiny as to which are or are not appropriate to implement when predicting ice  
13 24 811 nucleation<sup>452-456</sup>.

29  
30 813 In the atmosphere, the aerosol population is physicochemically diverse and the chemical complexity  
31 32 814 of an entire aerosol population may need to be considered to predict ice nucleation<sup>96</sup>. A nucleation prob-  
33 34 815 ability dispersion function has been applied in a previous study that describes the deviation of individual  
35 36 816 particle ice nucleation coefficients from that of the average particle population, which was successful to  
37 38 817 represent laboratory freezing data and capable of predicting atmospheric ice nucleation<sup>333</sup>. Field meas-  
39 40 818 urements have indicated that INPs can belong to a major particle type class, where the few particles act-  
41 42 819 ing as INPs are chemically indistinguishable from the remaining inactive same particle types<sup>96, 98, 290</sup>.  
43  
44 820 This may be explained by the stochastic nature inherent to nucleation according to CNT or specific par-  
45 46 821 ticle features unresolvable with current techniques.

50  
51 822 During cloud activation which includes droplet activation and ice nucleation, OA particles can expe-  
52 53 823 rience amorphous phase transition (e.g., see Fig. 4) where the outer shell experiences changes in  $a_w$ <sup>119,</sup>  
54 55 824 <sup>130</sup>. Therefore, immersion freezing models that can account for changes in particle  $a_w$  would be desirable

825 to implicitly account for amorphous phase changes. The majority of parameterizations and models that  
826 apply the active sites concept do not consider particle  $a_w$ , though attempts have been made using fit  
827 functions<sup>399</sup>. Introduction of solution  $a_w$ <sup>355-356, 373</sup> renders  $J_{het}$  independent of the nature of the solute in  
828 the aqueous solution and interfacial energies. Thus, application of  $a_w$  avoids the capillary approximation,  
829 which is the main weakness of CNT<sup>40</sup>. Currently, the water activity based immersion freezing model  
830 (ABIFM)<sup>328, 373</sup> might present one approach to describe immersion freezing induced by amorphous OA  
831 particles.

### 16 832 *Illustration of Water Activity Based Model for Immersion Freezing*

19833 Previous reviews have discussed in detail various ice nucleation parameterizations<sup>49-50, 53</sup>. Here we  
20 briefly demonstrate predictions of the change in immersion freezing rate of inorganic particles coated by  
21 amorphous OM using ABIFM<sup>373</sup> as an alternative. These calculations only serve the purpose to demon-  
22 strate the prediction of INP numbers by immersion freezing, implicitly accounting for amorphous deli-  
23 quescence of the organic coating. Other cloud microphysical effects<sup>9, 457-458</sup>, including homogeneous ice  
24 nucleation, liquid droplet growth, water vapor depletion due to the Bergeron–Wegener–Findeisen pro-  
25 cess<sup>459-461</sup>, ice crystal growth, entrainment and mixing, and ice crystal sedimentation are neglected.  $J_{het}$   
26 is parameterized as a function of  $\Delta a_w$ <sup>197, 373</sup> where  $\Delta a_w$  is the difference between droplet solution  $a_w$  and  
27 the ice melting point,  $a_w(T) - a_{w,ice}(T)$ <sup>355</sup>. In equilibrium between gas-phase and condensed-phase,  $a_w$   
28 equals ambient RH<sup>197</sup>. It is assumed that during amorphous deliquescence a solid organic phase coexists  
29 with an aqueous organic solution.

44 45844 We simulate a particle population composed of illite mineral dust particles coated with Leonardite, a  
46 HA, serving as a surrogate of an amorphous HULIS depicted in Fig. 15a-c. For both components,  $J_{het}$   
47 has been determined in the laboratory<sup>360, 373, 462</sup>. Upon continuous cooling with  $0.1 \text{ K min}^{-1}$ , we assume  
48 that the HA in these mixed particles will pass the glass transition similar to a fulvic acid<sup>105</sup> at RH=93%  
49 at T=240 K and reach FDRH similar to other studied OA particle systems<sup>112-113, 119, 377</sup>. Prior to the glass  
50 transition, ice formation is only possible via deposition ice nucleation on the solid (glassy) HA coating  
51  
52  
53  
54  
55  
56  
57  
58

the illite dust. Beyond the FDRH, ice formation is only possible via immersion freezing on the mineral surface. Between  $T_g$  and FDRH an aqueous solution, some glassy HA and illite surface are present, and immersion freezing can occur on both organic and inorganic surfaces. The fractional coverage of solid HA,  $f_{org(s)}$ , is parameterized with a quadratic equation (see Fig. 13a, red line), where  $f_{org(s)} = 1$  prior to glass transition and  $f_{org(s)} = 0$  at a FDRH = 98%.  $J_{het}$  is calculated for illite and Leonardite following ABIFM<sup>373</sup>, displayed as blue and green lines, respectively, in Fig. 15a. The heterogeneous ice nucleation rate,  $\omega_{het}$ , for a population of HA/illite dust particles is shown in Fig. 15b as the red line, where  $\omega_{het} = J_{het,org} A_{org} + J_{het,dust} A_{dust}$ . This two-component system uses  $f_{org(s)}$  to calculate surface area, where the exposed solid HA surface area is  $A_{org} = A_p f_{org(s)}$ , the exposed illite dust surface area is  $A_{dust} = A_p (1-f_{org(s)})$  and the particle surface area is  $A_p$ . We employ  $A_p$  on the order of  $10^{-3} \text{ cm}^2$ , the total particle surface area in 1 L of air for assumed bimodal lognormally distributed spherical particles with mode parameters,  $N_1 = 95 \text{ cm}^{-3}$ ,  $\mu_1 = 100 \text{ nm}$ ,  $\sigma_1 = 0.5$  and  $N_2 = 5 \text{ cm}^{-3}$ ,  $\mu_2 = 800 \text{ nm}$ ,  $\sigma_2 = 1.0$ . This distribution is according to typical aerosol sizes and numbers in the troposphere having an enhanced accumulation mode with few coarse mode particles<sup>463-465</sup>, but the choice of aerosol size distribution will not affect the model findings.

Fig. 15b shows the contribution of the HA and illite dust to  $\omega_{het}$ , in addition to upper limits of the nucleation rate due to a particle population consisting of only solid organic or mineral dust.

At a humidity slightly higher than the glass transition, the solid HA and illite dust surface exposed to aqueous solution can nucleate ice with a combined rate  $\omega_{het} = 0.09 \text{ min}^{-1}$  at  $\Delta a_w = 0.2$ . At this condition,  $f_{org(s)} = 0.999$  and HA dominates  $\omega_{het}$  despite having lower  $J_{het}$  compared to illite as shown by the green and blue lines, respectively. At  $\Delta a_w = 0.24$  the contributions of HA and illite to  $\omega_{het}$  become equal indicated by the intersection of the green and blue lines. For  $\Delta a_w > 0.245$ , the contribution of the solid HA sharply decreases until FDRH is reached at  $\Delta a_w > 0.25$ , at which point no solid HA is present to nucleate ice. Overall, Fig. 15b shows that when  $\Delta a_w < 0.24$ , the solid HA acts as the INP and for  $\Delta a_w > 0.24$  the illite dust acts as INP. Knowledge of  $J_{het}$  and  $f_{org(s)}$  allows calculation of the number of ice crystals produced,  $N_{ice}$ , given in Fig. 15c. We assume individual binomial distributions to simulate freezing for

875 all  $10^5$  particles present in 1 L of air and time step of 10 sec. If a particle induces ice nucleation it is re-  
1 moved from the distribution and a record is kept of how many ice particles froze in the simulated vol-  
2 ume, or  $N_{ice}$ , with units of  $L^{-1}$ . Fig. 15c shows  $N_{ice}$  as a function of  $\Delta a_w$ . Freezing is simulated with a  
3 frost point,  $T_f = 243.5$  K. At conditions where solid HA dominates immersion freezing, indicated by the  
4 green arrow,  $N_{ice}$  increases from  $10^{-2}$  to  $10 L^{-1}$ . When illite particles dominate, as indicated by the blue  
5 arrow,  $N_{ice}$  continues to rise surpassing  $100 L^{-1}$  due to continued cooling and increasing  $J_{het}$  and  $\omega_{het}$ . We  
6 note that homogeneous ice nucleation is negligible here and becomes important only at  $\Delta a_w > 0.313^{197}$ ,  
7 14881  
8 355.  
9  
10  
11  
12  
13  
14  
15  
16  
17  
18  
19  
20  
21  
22  
23  
24  
25  
26  
27  
28  
29  
30  
31  
32  
33  
34  
35  
36  
37  
38  
39  
40  
41  
42  
43  
44  
45  
46  
47  
48  
49  
50  
51  
52  
53  
54  
55  
56  
57  
58  
59  
60

Repeating these simulations, each time sampling freezing from a binomial distribution and particle size from the bimodal lognormal distribution, yields 10<sup>th</sup> and 90<sup>th</sup> percentiles of  $N_{ice}$  to assess uncertainty ranges<sup>328</sup> shown as the shaded region in Fig. 15c. Stochastic freezing and random sampling of aerosol particle size distribution were the only contributors to this uncertainty estimate. At warm and dry conditions, e.g.,  $\Delta a_w < 0.21$ , the uncertainty in  $N_{ice}$  is more than 2 orders of magnitude since only few ice nucleation events occurred giving rise to a large statistical uncertainty. At colder and more humid conditions, more ice nucleation events are observed resulting in less uncertainty.

We use the above model to evaluate another immersion freezing system where natural dust particles are coated by OM as shown in Fig. 15d-f. Ice nucleation experiments performed by China et al. (2017)<sup>102</sup> employed ambient particles that were predominantly dust coated by OM. The authors suggested that the organic coating nucleated ice due to the fact it was the only common constituent among those particles individually identified and that all samples with organic coatings nucleated ice at similar RH and T. As an analogue to Fig. 15a-c, we assume  $J_{het}(\Delta a_w)$  from China et al. (2017)<sup>102</sup> in Fig. 13d-f as representative of ambient organic coatings. Natural dust<sup>466</sup> and its corresponding parameterization for  $J_{het}(\Delta a_w)$ <sup>328</sup> is used for simulating ice nucleation by the dust core. Fig. 15d displays  $J_{het}$  of the OM coated dust and natural dust particles where  $T_g$  and FDRH are assumed to proceed at 50% and 90% RH, respectively, based on water uptake measurements by China et al. (2017)<sup>102</sup>. Fig. 13e shows that OM dom-

1        inates  $\omega_{\text{het}}$  until ~80% RH. Fig. 15f displays the resulting  $N_{\text{ice}}$  as a function of  $\Delta a_w$ , RH,  $RH_{\text{ice}}$ , and T  
2        having applied  $T_f = 237$  K and same aerosol population (size and concentration) as in panels b and c.  
3        The particles with OM dominate ice nucleation up to  $N_{\text{ice}} = 3 \text{ L}^{-1}$  in the range indicated by the green ar-  
4        row in Fig. 15f. This region also exhibits the most stochastic uncertainty due to a low number of freez-  
5        ing events. At more humid conditions ( $\text{RH} > 80\%$ ), natural dust dominates ice nucleation indicated by  
6        the blue arrow and the stochastic uncertainty greatly reduces for  $N_{\text{ice}} = 10-10^3 \text{ L}^{-1}$ .  
7  
8  
9  
10  
11  
12  
13

14        Although the simulations in Fig. 15 do not represent real cloud or aerosol processes, the uncertainty  
15        estimate can yield understanding of observed ice nucleation. The uncertainty estimates imply that in-  
16        strumental uncertainty in T or RH may play a greater role than stochastic uncertainty when large num-  
17        bers of INP are measured. However, stochastic freezing uncertainty should be considered when inter-  
18        preting data in the case of low  $N_{\text{ice}}$ . For example, when ice crystals form in the atmosphere with  $N_{\text{ice}} =$   
19        0.2  $\text{L}^{-1}$ , then 80% of the time, due to randomly occurring freezing events and variability of particle size,  
20        actual  $N_{\text{ice}}$  varies between  $10^{-3}$  and  $10 \text{ L}^{-1}$  (Figures. 15c and f) which is a typical reported range in field  
21        measurements<sup>53, 277</sup>. Given that observed INP concentrations are commonly  $< 10 \text{ L}^{-1}$  and concentrations  
22        are often near the detection limit<sup>467</sup>, resulting  $N_{\text{ice}}$  concentrations should be expected to suffer from sto-  
23        chastic (nucleation theory) and random (aerosol statistics) uncertainty. Increasing the observed number  
24        of freezing events and improving particle surface area measurements could contribute to a resolution of  
25        this issue<sup>328</sup>. Although the simulations presented in Fig. 15 are highly idealized, they demonstrate that  
26        capturing the freezing efficiency, the glass transition, FDRH, and freezing point depression of OM  
27        should be important for quantifying atmospheric ice nucleation from chemically complex aerosol parti-  
28        cles.  
29  
30  
31  
32  
33  
34  
35  
36  
37  
38  
39  
40  
41  
42  
43  
44  
45  
46  
47  
48  
49  
50  
51  
52  
53  
54  
55  
56  
57  
58  
59  
60

## SUMMARY AND FUTURE RESEARCH DIRECTIONS

Recognizing the abundance of OM in the atmosphere, this article summarized recent findings dealing with the role of airborne OM as a potentially significant contributor of ice nucleating substrates. Con-

925 sidering the wide range of thermodynamic conditions present in the Earth's atmosphere, OM will impact  
1  
926 atmospheric ice nucleation in different ways compared to 'classically' regarded INPs such as insoluble  
2  
927 mineral dust particles. Despite the great advancements in understanding ice nucleation processes, many  
3  
928 challenges remain to assess the importance of OM and OA particles in atmospheric cloud glaciation. We  
4  
929 highlighted the peculiar physicochemical features of OM, which are modulated by changes in ambient  
5  
930 temperature and humidity, the current lack of molecular level understanding of ice nucleation, the chal-  
6  
931 lenges in analyses and measurements of INPs and IRs, and the necessity of descriptive physical and  
7  
932 chemical approaches that include OM specific processes. A multi-disciplinary approach is necessary  
8  
933 covering molecular, laboratory, field, and modeling scales to improve our predictive understanding of  
9  
934 atmospheric ice nucleation by OM. We have identified the following key points that, we feel, warrant  
10  
935 future research to fill knowledge gaps in ice nucleation by OM:  
11  
936

12  
937 1. Gain a sufficiently comprehensive molecular understanding of the interaction between liquid water  
13  
938 and water vapor with organic substrates of varying composition, morphology, viscosity, and surface  
14  
939 functional groups to confidently predict OM nucleating behavior. Establish the physical and chemical  
15  
940 interfacial features that initiate and govern the nucleation process. Molecular dynamic simulations and  
16  
941 Monte Carlo and density functional theory calculations have been shown to be promising approaches.  
17  
942 Further validation of those model results by carefully designed experiments, and applying controlled,  
18  
943 artificial substrates, will be required to confirm the insights gained on ice nucleation mechanisms.

19  
944 2. Further develop techniques to rapidly image the dynamic ice nucleation process and instrumenta-  
20  
945 tion to probe and characterize the interfaces that initiate ice nucleation at the sub-nanoscale. Comple-  
21  
946 mentary to current SEM and SFG methods, further development of instruments capable of measure-  
22  
947 ments of the ice nucleating sites with high temporal (since nucleation occurs rapidly) and spatial resolu-  
23  
948 tion is necessary. INP measurements will benefit from improvements in the detection limit, temporal  
24  
949 resolution of the ice nucleation event, and increases in the sampled number of ice nucleation events.

949        3. Expand direct measurements of OM and SOA viscosity and associated phase changes including  
1           liquid-liquid phase separation processes under thermodynamic conditions relevant for mixed-phase and  
2           cirrus clouds and relate those parameters to ice nucleation. Evaluate the competition between diffusion  
3           governed OM and SOA phase changes, ice nucleation pathways, and ice nucleation kinetics. This re-  
4           quires a rigorous humidity and temperature trajectory assessment in experiments and will need to be ap-  
5           plicable to actual cloud activation time scales.  
6  
7  
8  
9  
10  
11  
12  
13

14        4. Establish a better understanding of how chemical aging of OM by atmospheric oxidants and differ-  
15           ent SOA formations pathways (e.g., low or high NO<sub>x</sub> conditions, oligomerization reactions, SOA pre-  
16           cursor gases with higher molecular weight, etc.) impact ice nucleation by a combination of oxidant ex-  
17           posure ice nucleation experiments, theoretical model simulations, and field campaigns.  
18  
19  
20  
21  
22  
23

24        5. Expand measurements of INP spectra, i.e., for the entire particle size distribution covering the su-  
25           permicrometer mode, including the physicochemically characterization of ambient INPs containing OM  
26           in the planetary boundary layer and free troposphere in different environments and geological locations.  
27  
28           Assess the INPs' chemical complexity and mixing state. Identification of ice nucleating macromolecules  
29           in nanometer sizes and observation of high INP number concentrations in supermicrometer particle sizes  
30  
31           emphasize the need to expand the measured INP size spectrum.  
32  
33  
34  
35  
36  
37

38        6. Continue to develop uncertainty assessment methodologies for any employed measurement tech-  
39           nique, sufficient to rigorously establish statistical significance of gathered data. Low INP concentrations  
40           relative to detection limits are associated with a large data scatter irrespective of instrument accuracy. In  
41  
42           general, stochastic freezing and aerosol size variability can be meaningfully reduced when probing a  
43           larger number of INPs. Furthermore, best practices should be developed with regard to potential con-  
44           tamination issues by trace gas exposure and applied water sources.  
45  
46  
47  
48  
49  
50  
51

52        7. Further develop and evaluate descriptive approaches to ice nucleation (immersion, deposition, and  
53           contact modes), considering the insufficient knowledge about the physicochemical features of active  
54           sites. Theoretical models should represent the amorphous phase changes of OM and the varying ice nu-  
55  
56  
57  
58  
59  
60

974 cleation kinetics as OA particles are advected in a cloud system. Considering the kinetically driven  
1  
975 amorphous OM phase changes, evaluate the application of the time independent and time dependent ice  
2  
976 nucleation models. The kinetic flux model and a water activity based freezing description show promise  
3  
977 for a comprehensive representation of the amorphous phase-ice nucleation relationship. Approaches also  
4  
978 will depend on the applied scale, i.e., cloud microphysics versus large scale atmospheric models and  
5  
979 thus will differ in complexity. Future field measurements would benefit from being explicitly focused on  
6  
979 constraining global model predictions over a wide range of T and RH, ideally over the full range of INP  
7  
980 sizes.  
8  
981

19982 8. Better establish how important cloud recycling of organic INPs and associated particle morpholog-  
20  
19983 ical changes and pre-activation are as contributors to ice nucleation in the atmosphere. Establish the de-  
21  
984 gree to which pre-activation and associated changes in ice nucleation propensity may occur using labor-  
22  
985 atory particle surrogates. Identify atmospheric conditions under which those effects are expected and  
23  
985 can be confirmed in field observations.  
24  
986

31987 We hope that these suggestions spur novel and exciting research, ultimately resolving how OM can  
32  
33988 act as ice nucleating substrate in the atmosphere. There are likely many more discoveries to be made  
34  
35989 when probing multicomponent and multiphase OM or OA particles at supercooled temperatures and  
36  
37990 metastable conditions for their interaction with water.  
38  
39  
40991  
41  
42  
43992  
44  
45993  
46  
47  
48994  
49  
50995  
51  
52  
53996  
54  
55997  
56  
57  
58998  
59  
60

## 999 Nomenclature

ABIFM	Water activity based immersion freezing model
$A_{dust}$	Surface area of mineral dust, [cm <sup>2</sup> ]
$A_p$	Surface area of particle, [cm <sup>2</sup> ]
$A_{org}$	Surface area of organic compound, [cm <sup>2</sup> ]
$a_w$	Water activity
$a_{w,ice}$	Ice melting point as a function of water activity
CalNex	California Research at the Nexus of Air Quality and Climate Change
CARES	Carbonaceous Aerosols and Radiative Effects Study
CCSEM/EDX	Computer controlled scanning electron microscopy with an energy dispersive X-ray analysis
CFDC	Continuous flow diffusion chamber
CNT	Classical nucleation theory
CVI	Counterflow-virtual-impactor
$\Delta a_w$	Water activity criterion
ELV-OOA	Extremely LV-OOA
FD	Full deliquescence
FDRH	Full deliquescence relative humidity
$f_{ice}$	Number of nucleated ice crystals/aerosol particle number
$f_{org(s)}$	Fractional coverage of solid
HA	Humic acid
HOA	Hydrocarbon-like OA

HULIS	Humic-like substances
Ice-CVI	Ice counterflow-virtual-impactor
INM	Ice nucleating macromolecule
INP	Ice nucleating particle
ISDAC	Indirect and Semi-Direct Aerosol Campaign
ISI	Ice selective inlet
$J_{\text{het}}$	Heterogeneous ice nucleation rate coefficient, [ $\text{cm}^{-2}\text{s}^{-1}$ ]
$J_{\text{het,dust}}$ <sup>1]</sup>	Heterogeneous ice nucleation rate coefficient of mineral dust, [ $\text{cm}^{-2}\text{s}^{-1}$ ]
$J_{\text{het,org}}$	Heterogeneous ice nucleation rate coefficient of organic compound, [ $\text{cm}^{-2}\text{s}^{-1}$ ]
$J_{\text{hom}}$	Homogeneous ice nucleation rate coefficient, [ $\text{cm}^{-3}\text{s}^{-1}$ ]
LLPS	Liquid-liquid phase separation
LV-OOA	Low-volatile oxygenated OA
MD	Molecular dynamics
MILAGRO	The Megacity Initiative: Local and Global Research Observations
$\mu_1, \mu_2$	Location parameter of log-normal distribution
$N_1, N_2$	Particle numbers in bimodal log-normal size distribution
$N_{\text{ice}}$	Number of ice crystals, [ $\text{L}^{-1}$ ]
O:C	Atomic oxygen to carbon ratio
OA	Organic aerosol
OC	Organic carbon

1	OM	Organic matter
2	$\omega_{\text{het}}$	Heterogeneous ice nucleation rate, [ $\text{s}^{-1}$ ]
3	PALMS	Particle Ablation by Laser Mass Spectrometry
4	PD	Partial deliquescence
5	PDF	Probability density function
6	POA	Primary organic aerosol
7	rBC	Refractory black carbon
8	RH	Relative humidity, [%]
9	$\text{RH}_{\text{ice}}$	Relative humidity with respect to ice, [%]
10	$\sigma_1, \sigma_2$	Scale parameter of log-normal distribution
11	SFG	Sum frequency generation spectroscopy
12	SHG	Second-harmonic generation spectroscopy
13	$S_{\text{ice}}$	Supersaturation with respect to ice
14	SOA	Secondary organic aerosol
15	SRFA	Suwannee River fluvic acid
16	SSA	Sea spray aerosol
17	STXM/NEXAFS	Scanning transmission X-ray microscopy coupled with near edge X-ray absorption fine structure spectroscopy
18	SV-OA	Semi-volatile
19	$\tau_{\text{cd}}$	Characteristic timescale of bulk diffusion
20	TEM	Transmission electron microscopy
21	TEM/EDX	Transmission electron microscopy/energy dispersive X-ray analysis

1	T	Temperature, [K]
2	T <sub>f</sub>	Frost point, [K]
3	T <sub>g</sub>	Glass transition temperature
4	UT/LS	Upper troposphere and lower stratosphere
5	VOC	Volatile organic compound
6	XPS	X-ray photoelectron spectroscopy

16000  
17  
18  
19001  
20002  
21  
22003  
23  
24  
25004  
26  
27  
28005  
29  
30  
31006  
32  
33  
34  
35007  
36  
37  
38008  
39  
40  
41009  
42  
43  
44010  
45  
46  
47011  
48  
49  
50012  
51  
52  
53013  
54  
55  
56014  
57  
58  
59  
60

1015   **AUTHOR INFORMATION**

1

31016   **Corresponding Author**

4

5  
6 1017 \*Daniel A. Knopf, Email: Daniel.Knopf@stonybrook.edu

7

8  
9 1018   **Author Contributions**

10

11019 The manuscript was written through contributions of all authors. All authors have given approval to the  
12  
13 1020 final version of the manuscript.

14

15  
16 1021   **Funding Sources**

17

18  
19 1022 This work was funded by the U.S. Department of Energy, Office of Science (BER), Atmospheric Sys-  
20  
21 2023 tem Research (DE-SC0016370) and U.S. National Science Foundation grants AGS 1446286 and AGS  
22  
23 2024 1232203, European Union's Horizon 2020 research and innovation program grant agreement No.  
24  
25 2025 701647, National Science Foundation of China (No. 41775133), the Fundamental Research Funds for  
26  
27 2026 the Central Universities (No. 20720160111), and the Recruitment Program of Global Youth Experts of  
28  
29  
30 2027 China.

31

32  
33 1028   **Notes**

34

35 1029 The authors declare no competing financial interest.

36

37  
38 1030   **ACKNOWLEDGMENTS**

39

40  
41 1031 This work was funded by the U.S. Department of Energy, Office of Science (BER), Atmospheric Sys-  
42  
43 1032 tem Research (DE-SC0016370) and U.S. National Science Foundation grants AGS 1446286 and AGS  
44  
45 1033 1232203. P. A. acknowledges support from the European Union's Horizon 2020 research and innova-  
46  
47 1034 tion program under the Marie Skłodowska-Curie grant agreement No. 701647. B. W. acknowledge the  
48  
49 1035 support by the National Science Foundation of China (No. 41775133), the Fundamental Research Funds  
50  
51 1036 for the Central Universities (No. 20720160111), and the Recruitment Program of Global Youth Experts  
52  
53 1037 of China. The authors are grateful to J. Aller and A. Fridlind for reading the manuscript and providing  
54  
55 1038 helpful comments.

56

57

58 1039

59

60

1040  
1041 REFERENCES  
1042  
1043  
1044  
1045  
1046  
1047  
1048  
1049  
1050  
1051  
1052  
1053  
1054  
1055  
1056  
1057  
1058  
1059  
1060  
1061  
1062  
1063  
1064  
1065  
1066  
1067  
1068  
1069  
1070  
1071  
1072  
1073  
1074  
1075  
1076  
1077  
1078  
1079  
1080  
1081  
1082  
1083  
1084  
1085  
1086  
1087  
1088  
58  
59  
60

1. Smith, P. H.; Tamppari, L. K.; Arvidson, R. E.; Bass, D.; Blaney, D.; Boynton, W. V.; Carswell, A.; Catling, D. C.; Clark, B. C.; Duck, T.; DeJong, E.; Fisher, D.; Goetz, W.; Gunnlaugsson, H. P.; Hecht, M. H.; Hipkin, V.; Hoffman, J.; Hviid, S. F.; Keller, H. U.; Kounaves, S. P.; Lange, C. F.; Lemmon, M. T.; Madsen, M. B.; Markiewicz, W. J.; Marshall, J.; McKay, C. P.; Mellon, M. T.; Ming, D. W.; Morris, R. V.; Pike, W. T.; Renno, N.; Staufer, U.; Stoker, C.; Taylor, P.; Whiteway, J. A.; Zent, A. P., H<sub>2</sub>O at the Phoenix Landing Site. *Science* **2009**, *325* (5936), 58-61.
2. Whiteway, J. A.; Komguem, L.; Dickinson, C.; Cook, C.; Illnicky, M.; Seabrook, J.; Popovici, V.; Duck, T. J.; Davy, R.; Taylor, P. A.; Pathak, J.; Fisher, D.; Carswell, A. I.; Daly, M.; Hipkin, V.; Zent, A. P.; Hecht, M. H.; Wood, S. E.; Tamppari, L. K.; Renno, N.; Moores, J. E.; Lemmon, M. T.; Daerden, F.; Smith, P. H., Mars Water-Ice Clouds and Precipitation. *Science* **2009**, *325* (5936), 68-70.
3. Carr, M. H.; Belton, M. J. S.; Chapman, C. R.; Davies, A. S.; Geissler, P.; Greenberg, R.; McEwen, A. S.; Tufts, B. R.; Greeley, R.; Sullivan, R.; Head, J. W.; Pappalardo, R. T.; Klaasen, K. P.; Johnson, T. V.; Kaufman, J.; Senske, D.; Moore, J.; Neukum, G.; Schubert, G.; Burns, J. A.; Thomas, P.; Veverka, J., Evidence for a subsurface ocean on Europa. *Nature* **1998**, *391* (6665), 363-365.
4. Scipioni, F.; Schenk, P.; Tosi, F.; D'Aversa, E.; Clark, R.; Combe, J. P.; Ore, C. M. D., Deciphering sub-micron ice particles on Enceladus surface. *Icarus* **2017**, *290*, 183-200.
5. Fisher, E. A.; Lucey, P. G.; Lemelin, M.; Greenhagen, B. T.; Siegler, M. A.; Mazarico, E.; Aharonson, O.; Williams, J. P.; Hayne, P. O.; Neumann, G. A.; Paige, D. A.; Smith, D. E.; Zuber, M. T., Evidence for surface water ice in the lunar polar regions using reflectance measurements from the Lunar Orbiter Laser Altimeter and temperature measurements from the Diviner Lunar Radiometer Experiment. *Icarus* **2017**, *292*, 74-85.
6. Ball, P., *Life's Matrix: A Biography of Water*. 1st edition ed.; University of California Press: 2001.
7. Boucher, O.; Randall, D.; Artaxo, P.; Bretherton, C.; Feingold, G.; Forster, P.; Kerminen, V.-M.; Kondo, Y.; Liao, H.; Lohmann, U.; Rasch, P.; Satheesh, S. K.; Sherwood, S.; Stevens, B.; Zhang, X. Y., Clouds and Aerosols. In *Climate Change 2013: The Physical Science Basis. Contribution of Working Group I to the Fifth Assessment Report of the Intergovernmental Panel on Climate Change*, Stocker, T. F.; Qin, D.; Plattner, G.-K.; Tignor, M.; Allen, S. K.; Boschung, J.; Nauels, A.; Xia, Y.; Bex, V.; Midgley, P. M., Eds. Cambridge University Press: Cambridge, United Kingdom and New York, NY, USA, 2013.
8. Storelvmo, T., Aerosol Effects on Climate via Mixed-Phase and Ice Clouds. In *Annual Review of Earth and Planetary Sciences*, Vol 45, Jeanloz, R.; Freeman, K. H., Eds. 2017; Vol. 45, pp 199-222.
9. Baker, M. B.; Peter, T., Small-scale cloud processes and climate. *Nature* **2008**, *451* (7176), 299-300.
10. Baker, M. B., Cloud microphysics and climate. *Science* **1997**, *276* (5315), 1072-1078.
11. Lohmann, U.; Feichter, J., Global indirect aerosol effects: a review. *Atmos. Chem. Phys.* **2005**, *5*, 715-737.
12. Rosenfeld, D.; Sherwood, S.; Wood, R.; Donner, L., Climate effects of aerosol-cloud interactions. *Science* **2014**, *343* (6169), 379-380.
13. Lau, K. M.; Wu, H. T., Warm rain processes over tropical oceans and climate implications. *Geophys. Res. Lett.* **2003**, *30* (24), 2290.
14. Mulmenstadt, J.; Sourdeval, O.; Delanoe, J.; Quaas, J., Frequency of occurrence of rain from liquid-, mixed-, and ice-phase clouds derived from A-Train satellite retrievals. *Geophys. Res. Lett.* **2015**, *42* (15), 6502-6509.
15. Brewer, A. W., Evidence for a world circulation provided by the measurements of helium and water vapour distribution in the stratosphere. *Q. J. Roy. Meteor. Soc.* **1949**, *75* (326), 351-363.
16. Holton, J. R.; Haynes, P. H.; McIntyre, M. E.; Douglass, A. R.; Rood, R. B.; Pfister, L., Stratosphere-troposphere exchange. *Rev. Geophys.* **1995**, *33* (4), 403-439.

- 1089 17. Lohmann, U.; Roeckner, E.; Collins, W. D.; Heymsfield, A. J.; McFarquhar, G. M.; Barnett, T.  
1090 P., The role of water vapor and convection during the Central Equatorial Pacific Experiment from  
1091 observations and model simulations. *J. Geophys. Res.* **1995**, *100* (D12), 26229-26245.
- 1092 18. Held, I. M.; Soden, B. J., Water vapor feedback and global warming. *Annu. Rev. Energ. Env.*  
1093 **2000**, *25*, 441-475.
- 1094 19. Krämer, M.; Schiller, C.; Voigt, C.; Schlager, H.; Popp, P. J., A climatological view of HNO<sub>3</sub>  
1095 partitioning in cirrus clouds. *Q. J. R. Meteorol. Soc.* **2008**, *134* (633), 905-912.
- 1096 20. Popp, P. J.; Marcy, T. P.; Watts, L. A.; Gao, R. S.; Fahey, D. W.; Weinstock, E. M.; Smith, J. B.;  
1097 Herman, R. L.; Troy, R. F.; Webster, C. R.; Christensen, L. E.; Baumgardner, D. G.; Voigt, C.; Karcher,  
1098 B.; Wilson, J. C.; Mahoney, M. J.; Jensen, E. J.; Bui, T. P., Condensed-phase nitric acid in a tropical  
1099 subvisible cirrus cloud. *Geophys. Res. Lett.* **2007**, *34* (24), 5.
- 1100 21. Voigt, C.; Schlager, H.; Ziereis, H.; Karcher, B.; Luo, B. P.; Schiller, C.; Kramer, M.; Popp, P.  
1101 J.; Irie, H.; Kondo, Y., Nitric acid in cirrus clouds. *Geophys. Res. Lett.* **2006**, *33* (5), 4.
- 1102 22. Forster, P.; Ramaswamy, V.; Artaxo, P.; Berntsen, T.; Betts, R.; Fahey, D. W.; Haywood, J.;  
1103 Lean, J.; Lowe, D. C.; Myhre, G.; Nganga, J.; Prinn, R.; Raga, G.; Schulz, M.; Van Dorland, R., Chapter  
1104 2: Changes in Atmospheric Constituents and in Radiative Forcing. In *Climate Change 2007: The  
1105 Physical Science Basis. Contribution of Working Group I to the Fourth Assessment Report of the  
1106 Intergovernmental Panel on Climate Change*, Solomon, S.; Qin, D.; Manning, M.; Chen, Z.; Marquis,  
1107 M.; Averyt, K. B.; Tignor, M.; Miller, H. L., Eds. Cambridge University Press: Cambridge, United  
1108 Kingdom and New York, NY, USA, 2007; pp 129-234.
- 1109 23. Field, P. R.; Lawson, P.; Brown, R. A.; Lloyd, G.; Westbrook, C.; Moisseev, D.; Miltenberger,  
1110 A.; Nenes, A.; Blyth, A.; Choularton, T.; Connolly, P.; Buehl, J.; Crosier, J.; Cui, Z.; Dearden, C.;  
1111 Demott, P.; Flossmann, A.; Heymsfield, A.; Huang, Y.; Kalesse, H.; Kanji, Z. A.; Korolev, A.;  
1112 Kirchgaessner, A.; Lasher-Trapp, S.; Leisner, T.; Mcfarquhar, G.; Phillips, V.; Stith, J.; Sullivan, S.,  
1113 Secondary Ice Production: Current State of the Science and Recommendations for the Future. In *Ice  
1114 Formation and Evolution in Clouds and Precipitation: Measurement and Modeling Challenges*,  
1115 American Meteorological Society: 2017; Vol. 58, pp 7.1-7.20.
- 1116 24. Hallett, J.; Mossop, S. C., Production of secondary ice particles during riming process. *Bull.  
1117 Amer. Meteorol. Soc.* **1974**, *55* (6), 679-679.
- 1118 25. Ladino, L. A.; Korolev, A.; Heckman, I.; Wolde, M.; Fridlind, A. M.; Ackerman, A. S., On the  
1119 role of ice-nucleating aerosol in the formation of ice particles in tropical mesoscale convective systems.  
1120 *Geophys. Res. Lett.* **2017**, *44* (3), 1574-1582.
- 1121 26. Fridlind, A. M.; Li, X. W.; Wu, D.; van Lier-Walqui, M.; Ackerman, A. S.; Tao, W. K.;  
1122 McFarquhar, G. M.; Wu, W.; Dong, X. Q.; Wang, J. Y.; Ryzhkov, A.; Zhang, P. F.; Poellot, M. R.;  
1123 Neumann, A.; Tomlinson, J. M., Derivation of aerosol profiles for MC3E convection studies and use in  
1124 simulations of the 20 May squall line case. *Atmos. Chem. Phys.* **2017**, *17* (9), 5947-5972.
- 1125 27. Kanakidou, M.; Seinfeld, J. H.; Pandis, S. N.; Barnes, I.; Dentener, F. J.; Facchini, M. C.; Van  
1126 Dingenen, R.; Ervens, B.; Nenes, A.; Nielsen, C. J.; Swietlicki, E.; Putaud, J. P.; Balkanski, Y.; Fuzzi,  
1127 S.; Horth, J.; Moortgat, G. K.; Winterhalter, R.; Myhre, C. E. L.; Tsigaridis, K.; Vignati, E.; Stephanou,  
1128 E. G.; Wilson, J., Organic aerosol and global climate modelling: a review. *Atmos. Chem. Phys.* **2005**, *5*,  
1129 1053-1123.
- 1130 28. Hallquist, M.; Wenger, J. C.; Baltensperger, U.; Rudich, Y.; Simpson, D.; Claeys, M.; Dommen,  
1131 J.; Donahue, N. M.; George, C.; Goldstein, A. H.; Hamilton, J. F.; Herrmann, H.; Hoffmann, T.; Iinuma,  
1132 Y.; Jang, M.; Jenkin, M. E.; Jimenez, J. L.; Kiendler-Scharr, A.; Maenhaut, W.; McFiggans, G.; Mentel,  
1133 T. F.; Monod, A.; Prevot, A. S. H.; Seinfeld, J. H.; Surratt, J. D.; Szmigielski, R.; Wildt, J., The  
1134 formation, properties and impact of secondary organic aerosol: current and emerging issues. *Atmos.  
1135 Chem. Phys.* **2009**, *9* (14), 5155-5236.
- 1136 29. Jimenez, J. L.; Canagaratna, M. R.; Donahue, N. M.; Prevot, A. S. H.; Zhang, Q.; Kroll, J. H.;  
1137 DeCarlo, P. F.; Allan, J. D.; Coe, H.; Ng, N. L.; Aiken, A. C.; Docherty, K. S.; Ulbrich, I. M.; Grieshop,  
1138 A. P.; Robinson, A. L.; Duplissy, J.; Smith, J. D.; Wilson, K. R.; Lanz, V. A.; Hueglin, C.; Sun, Y. L.;  
1139 Tian, J.; Laaksonen, A.; Raatikainen, T.; Rautiainen, J.; Vaattovaara, P.; Ehn, M.; Kulmala, M.;

- 1140 Tomlinson, J. M.; Collins, D. R.; Cubison, M. J.; Dunlea, E. J.; Huffman, J. A.; Onasch, T. B.; Alfarra,  
1141 M. R.; Williams, P. I.; Bower, K.; Kondo, Y.; Schneider, J.; Drewnick, F.; Borrmann, S.; Weimer, S.;  
1142 Demerjian, K.; Salcedo, D.; Cottrell, L.; Griffin, R.; Takami, A.; Miyoshi, T.; Hatakeyama, S.;  
1143 Shimo, A.; Sun, J. Y.; Zhang, Y. M.; Dzepina, K.; Kimmel, J. R.; Sueper, D.; Jayne, J. T.; Herndon,  
1144 S. C.; Trimborn, A. M.; Williams, L. R.; Wood, E. C.; Middlebrook, A. M.; Kolb, C. E.; Baltensperger,  
1145 U.; Worsnop, D. R., Evolution of Organic Aerosols in the Atmosphere. *Science* **2009**, *326* (5959), 1525-  
1146 1529.
- 1147 30. Heald, C. L.; Goldstein, A. H.; Allan, J. D.; Aiken, A. C.; Apel, E.; Atlas, E. L.; Baker, A. K.;  
1148 Bates, T. S.; Beyersdorf, A. J.; Blake, D. R.; Campos, T.; Coe, H.; Crounse, J. D.; DeCarlo, P. F.; de  
1149 Gouw, J. A.; Dunlea, E. J.; Flocke, F. M.; Fried, A.; Goldan, P.; Griffin, R. J.; Herndon, S. C.;  
1150 Holloway, J. S.; Holzinger, R.; Jimenez, J. L.; Junkermann, W.; Kuster, W. C.; Lewis, A. C.; Meinardi,  
1151 S.; Millet, D. B.; Onasch, T.; Polidori, A.; Quinn, P. K.; Riemer, D. D.; Roberts, J. M.; Salcedo, D.;  
1152 Sive, B.; Swanson, A. L.; Talbot, R.; Warneke, C.; Weber, R. J.; Weibring, P.; Wennberg, P. O.;  
1153 Worsnop, D. R.; Wittig, A. E.; Zhang, R.; Zheng, J.; Zheng, W., Total observed organic carbon (TOOC)  
1154 in the atmosphere: a synthesis of North American observations. *Atmos. Chem. Phys.* **2008**, *8* (7), 2007-  
1155 2025.
- 1156 31. Zhang, Q.; Jimenez, J. L.; Canagaratna, M. R.; Allan, J. D.; Coe, H.; Ulbrich, I.; Alfarra, M. R.;  
1157 Takami, A.; Middlebrook, A. M.; Sun, Y. L.; Dzepina, K.; Dunlea, E.; Docherty, K.; DeCarlo, P. F.;  
1158 Salcedo, D.; Onasch, T.; Jayne, J. T.; Miyoshi, T.; Shimo, A.; Hatakeyama, S.; Takegawa, N.; Kondo,  
1159 Y.; Schneider, J.; Drewnick, F.; Borrmann, S.; Weimer, S.; Demerjian, K.; Williams, P.; Bower, K.;  
1160 Bahreini, R.; Cottrell, L.; Griffin, R. J.; Rautiainen, J.; Sun, J. Y.; Zhang, Y. M.; Worsnop, D. R.,  
1161 Ubiquity and dominance of oxygenated species in organic aerosols in anthropogenically-influenced  
1162 Northern Hemisphere midlatitudes. *Geophys. Res. Lett.* **2007**, *34* (13), L13801.
- 1163 32. Ehn, M.; Thornton, J. A.; Kleist, E.; Sipila, M.; Junninen, H.; Pullinen, I.; Springer, M.; Rubach,  
1164 F.; Tillmann, R.; Lee, B.; Lopez-Hilfiker, F.; Andres, S.; Acir, I. H.; Rissanen, M.; Jokinen, T.;  
1165 Schobesberger, S.; Kangasluoma, J.; Kontkanen, J.; Nieminen, T.; Kurten, T.; Nielsen, L. B.; Jorgensen,  
1166 S.; Kjaergaard, H. G.; Canagaratna, M.; Dal Maso, M.; Berndt, T.; Petaja, T.; Wahner, A.; Kerminen, V.  
1167 M.; Kulmala, M.; Worsnop, D. R.; Wildt, J.; Mentel, T. F., A large source of low-volatility secondary  
1168 organic aerosol. *Nature* **2014**, *506* (7489), 476-479.
- 1169 33. Shrivastava, M.; Cappa, C. D.; Fan, J. W.; Goldstein, A. H.; Guenther, A. B.; Jimenez, J. L.;  
1170 Kuang, C.; Laskin, A.; Martin, S. T.; Ng, N. L.; Petaja, T.; Pierce, J. R.; Rasch, P. J.; Roldin, P.;  
1171 Seinfeld, J. H.; Shilling, J.; Smith, J. N.; Thornton, J. A.; Volkamer, R.; Wang, J.; Worsnop, D. R.;  
1172 Zaveri, R. A.; Zelenyuk, A.; Zhang, Q., Recent advances in understanding secondary organic aerosol:  
1173 Implications for global climate forcing. *Rev. Geophys.* **2017**, *55* (2), 509-559.
- 1174 34. Turpin, B. J.; Lim, H. J., Species contributions to PM2.5 mass concentrations: Revisiting  
1175 common assumptions for estimating organic mass. *Aerosol Sci. Tech.* **2001**, *35* (1), 602-610.
- 1176 35. Murphy, D. M.; Cziczo, D. J.; Froyd, K. D.; Hudson, P. K.; Matthew, B. M.; Middlebrook, A.  
1177 M.; Peltier, R. E.; Sullivan, A.; Thomson, D. S.; Weber, R. J., Single-particle mass spectrometry of  
1178 tropospheric aerosol particles. *J. Geophys. Res.* **2006**, *111* (D23), D23S32.
- 1179 36. Heald, C. L.; Jacob, D. J.; Park, R. J.; Russell, L. M.; Huebert, B. J.; Seinfeld, J. H.; Liao, H.;  
1180 Weber, R. J., A large organic aerosol source in the free troposphere missing from current models.  
1181 *Geophys. Res. Lett.* **2005**, *32* (18), L18809.
- 1182 37. Volkamer, R.; Jimenez, J. L.; San Martini, F.; Dzepina, K.; Zhang, Q.; Salcedo, D.; Molina, L.  
1183 T.; Worsnop, D. R.; Molina, M. J., Secondary organic aerosol formation from anthropogenic air  
1184 pollution: Rapid and higher than expected. *Geophys. Res. Lett.* **2006**, *33* (17), L17811.
- 1185 38. Goldstein, A. H.; Galbally, I. E., Known and unexplored organic constituents in the earth's  
1186 atmosphere. *Environ. Sci. Technol.* **2007**, *41* (5), 1514-1521.
- 1187 39. de Gouw, J. A.; Middlebrook, A. M.; Warneke, C.; Goldan, P. D.; Kuster, W. C.; Roberts, J. M.;  
1188 Fehsenfeld, F. C.; Worsnop, D. R.; Canagaratna, M. R.; Pszenny, A. A. P.; Keene, W. C.; Marchewka,  
1189 M.; Bertman, S. B.; Bates, T. S., Budget of organic carbon in a polluted atmosphere: Results from the  
1190 New England Air Quality Study in 2002. *J. Geophys. Res.* **2005**, *110* (D16), D16305.

- 1191 40. Pruppacher, H. R.; Klett, J. D., *Microphysics of Clouds and Precipitation*. Kluwer Academic  
1192 Publishers: Dordrecht, 1997.
- 1193 41. Morris, C. E.; Georgakopoulos, D. G.; Sands, D. C., Ice nucleation active bacteria and their  
1194 potential role in precipitation. *J. Phys. IV* **2004**, *121*, 87-103.
- 1195 42. Schnell, R. C.; Vali, G., Biogenic Ice Nuclei: Part I. Terrestrial and Marine Sources. *J. Atmos.*  
6196 *Sci.* **1976**, *33* (8), 1554-1564.
- 7197 43. Vali, G.; Christensen, M.; Fresh, R. W.; Galyan, E. L.; Maki, L. R.; Schnell, R. C., Biogenic Ice  
8198 Nuclei. Part II: Bacterial Sources. *J. Atmos. Sci.* **1976**, *33* (8), 1565-1570.
- 9199 44. Fröhlich-Nowoisky, J.; Kampf, C. J.; Weber, B.; Huffman, J. A.; Pöhlker, C.; Andreae, M. O.;  
10200 Lang-Yona, N.; Burrows, S. M.; Gunthe, S. S.; Elbert, W.; Su, H.; Hoor, P.; Thines, E.; Hoffmann, T.;  
11201 Despres, V. R.; Poschl, U., Bioaerosols in the Earth system: Climate, health, and ecosystem interactions.  
12202 *Atmos. Res.* **2016**, *182*, 346-376.
- 13203 45. Huffman, J. A.; Prenni, A. J.; DeMott, P. J.; Pöhlker, C.; Mason, R. H.; Robinson, N. H.;  
14204 Fröhlich-Nowoisky, J.; Tobo, Y.; Despres, V. R.; Garcia, E.; Gochis, D. J.; Harris, E.; Mueller-  
15205 Germann, I.; Ruzene, C.; Schmer, B.; Sinha, B.; Day, D. A.; Andreae, M. O.; Jimenez, J. L.; Gallagher,  
16206 M.; Kreidenweis, S. M.; Bertram, A. K.; Pöschl, U., High concentrations of biological aerosol particles  
17207 and ice nuclei during and after rain. *Atmos. Chem. Phys.* **2013**, *13* (13), 6151-6164.
- 18208 46. Despres, V. R.; Huffman, J. A.; Burrows, S. M.; Hoose, C.; Safatov, A. S.; Buryak, G.; Fröhlich-  
19209 Nowoisky, J.; Elbert, W.; Andreae, M. O.; Pöschl, U.; Jaenicke, R., Primary biological aerosol particles  
20210 in the atmosphere: a review. *Tellus B* **2012**, *64*, 1-58.
- 21211 47. Fröhlich-Nowoisky, J.; Burrows, S. M.; Xie, Z.; Engling, G.; Solomon, P. A.; Fraser, M. P.;  
22212 Mayol-Bracero, O. L.; Artaxo, P.; Begerow, D.; Conrad, R.; Andreae, M. O.; Despres, V. R.; Pöschl, U.,  
23213 Biogeography in the air: fungal diversity over land and oceans. *Biogeosciences* **2012**, *9* (3), 1125-1136.
- 24214 48. Hegg, D. A.; Baker, M. B., Nucleation in the atmosphere. *Rep. Prog. Phys.* **2009**, *72* (5),  
25215 056801.
- 26216 49. Murray, B. J.; O'Sullivan, D.; Atkinson, J. D.; Webb, M. E., Ice nucleation by particles  
27217 immersed in supercooled cloud droplets. *Chem. Soc. Rev.* **2012**, *41* (19), 6519-6554.
- 28218 50. Hoose, C.; Möhler, O., Heterogeneous ice nucleation on atmospheric aerosols: a review of  
29219 results from laboratory experiments. *Atmos. Chem. Phys.* **2012**, *12* (20), 9817-9854.
- 30220 51. Cantrell, W.; Heymsfield, A., Production of ice in tropospheric clouds - A review. *Bull. Amer.*  
31221 *Meteorol. Soc.* **2005**, *86* (6), 795-807.
- 32222 52. DeMott, P. J.; Möhler, O.; Stetzer, O.; Vali, G.; Levin, Z.; Petters, M. D.; Murakami, M.;  
33223 Leisner, T.; Bundke, U.; Klein, H.; Kanji, Z. A.; Cotton, R.; Jones, H.; Benz, S.; Brinkmann, M.;  
34224 Rzesanke, D.; Saathoff, H.; Nicolet, M.; Saito, A.; Nillius, B.; Bingemer, H.; Abbatt, J.; Ardon, K.;  
35225 Ganor, E.; Georgakopoulos, D. G.; Saunders, C., Resurgence in ice nuclei measurement research. *Bull.*  
36226 *Amer. Meteorol. Soc.* **2011**, *92* (12), 1623-1635.
- 37227 53. Kanji, Z. A.; Ladino, L. A.; Wex, H.; Boose, Y.; Burkert-Kohn, M.; Cziczo, D. J.; Krämer, M.,  
38228 Overview of Ice Nucleating Particles. In *Ice Formation and Evolution in Clouds and Precipitation:*  
39229 *Measurement and Modeling Challenges*, American Meteorological Society: 2017; Vol. 58, pp 1.1-1.33.
- 40230 54. Cziczo, D. J.; Ladino, L. A.; Boose, Y.; Kanji, Z. A.; Kupiszewski, P.; Lance, S.; Mertes, S.;  
41231 Wex, H., Measurements of Ice Nucleating Particles and Ice Residuals. In *Ice Formation and Evolution*  
42232 *in Clouds and Precipitation: Measurement and Modeling Challenges*, American Meteorological  
43233 Society: 2017; Vol. 58, pp 8.1-8.13.
- 44234 55. Coluzzi, I.; Creamean, J.; Rossi, M. J.; Wex, H.; Alpert, P. A.; Bianco, V.; Boose, Y.; Dellago,  
45235 C.; Felgitsch, L.; Fröhlich-Nowoisky, J.; Herrmann, H.; Jungblut, S.; Kanji, Z. A.; Menzl, G.; Moffett,  
46236 B.; Moritz, C.; Mutzel, A.; Pöschl, U.; Schauperl, M.; Scheel, J.; Stopelli, E.; Stratmann, F.; Grothe, H.;  
47237 Schmale III, D. G., Perspectives on the Future of Ice Nucleation Research: Research Needs and  
48238 Unanswered Questions Identified from Two International Workshops. *Atmosphere* **2017**, *8* (138), 1-28.
- 49239 56. Ariya, P. A.; Sun, J.; Eltouny, N. A.; Hudson, E. D.; Hayes, C. T.; Kos, G., Physical and  
50240 chemical characterization of bioaerosols - Implications for nucleation processes. *Int. Rev. Phys. Chem.*  
51241 **2009**, *28* (1), 1-32.

- 1242 57. Salameh, A.; Daskalakis, V., Atmospheric Ice Nucleation by Glassy Organic Compounds: A  
1243 Review. *Chemi. Compil. J.* **2017**, *1*, 13-23.
- 1244 58. Vali, G.; DeMott, P. J.; Möhler, O.; Whale, T. F., Technical Note: A proposal for ice nucleation  
1245 terminology. *Atmos. Chem. Phys.* **2015**, *15* (18), 10263-10270.
- 1246 59. Heald, C. L.; Coe, H.; Jimenez, J. L.; Weber, R. J.; Bahreini, R.; Middlebrook, A. M.; Russell,  
1247 L. M.; Jolley, M.; Fu, T.-M.; Allan, J. D.; Bower, K. N.; Capes, G.; Crosier, J.; Morgan, W. T.;  
1248 Robinson, N. H.; Williams, P. I.; Cubison, M. J.; DeCarlo, P. F.; Dunlea, E. J., Exploring the vertical  
1249 profile of atmospheric organic aerosol: comparing 17 aircraft field campaigns with a global model.  
1250 *Atmos. Chem. Phys.* **2011**, *11* (24), 12673.
- 1251 60. Donahue, N. M.; Epstein, S. A.; Pandis, S. N.; Robinson, A. L., A two-dimensional volatility  
1252 basis set: 1. organic-aerosol mixing thermodynamics. *Atmos. Chem. Phys.* **2011**, *11* (7), 3303-3318.
- 1253 61. Kroll, J. H.; Donahue, N. M.; Jimenez, J. L.; Kessler, S. H.; Canagaratna, M. R.; Wilson, K. R.;  
1254 Altieri, K. E.; Mazzoleni, L. R.; Wozniak, A. S.; Bluhm, H.; Mysak, E. R.; Smith, J. D.; Kolb, C. E.;  
1255 Worsnop, D. R., Carbon oxidation state as a metric for describing the chemistry of atmospheric organic  
1256 aerosol. *Nat Chem* **2011**, *3* (2), 133-139.
- 1257 62. Li, Y.; Pöschl, U.; Shiraiwa, M., Molecular corridors and parameterizations of volatility in the  
1258 chemical evolution of organic aerosols. *Atmos. Chem. Phys.* **2016**, *16* (5), 3327-3344.
- 1259 63. Hoyle, C. R.; Boy, M.; Donahue, N. M.; Fry, J. L.; Glasius, M.; Guenther, A.; Hallar, A. G.;  
1260 Hartz, K. H.; Petters, M. D.; Petaja, T.; Rosenoern, T.; Sullivan, A. P., A review of the anthropogenic  
1261 influence on biogenic secondary organic aerosol. *Atmos. Chem. Phys.* **2011**, *11* (1), 321-343.
- 1262 64. Ervens, B.; Turpin, B. J.; Weber, R. J., Secondary organic aerosol formation in cloud droplets  
1263 and aqueous particles (aqSOA): a review of laboratory, field and model studies. *Atmos. Chem. Phys.*  
1264 **2011**, *11* (21), 11069-11102.
- 1265 65. Lim, Y. B.; Tan, Y.; Perri, M. J.; Seitzinger, S. P.; Turpin, B. J., Aqueous chemistry and its role  
1266 in secondary organic aerosol (SOA) formation. *Atmos. Chem. Phys.* **2010**, *10* (21), 10521-10539.
- 1267 66. Altieri, K. E.; Carlton, A. G.; Lim, H. J.; Turpin, B. J.; Seitzinger, S. P., Evidence for oligomer  
1268 formation in clouds: Reactions of isoprene oxidation products. *Environ. Sci. Technol.* **2006**, *40* (16),  
1269 4956-4960.
- 1270 67. Lim, H. J.; Carlton, A. G.; Turpin, B. J., Isoprene forms secondary organic aerosol through cloud  
1271 processing: Model simulations. *Environ. Sci. Technol.* **2005**, *39* (12), 4441-4446.
- 1272 68. Ervens, B., Modeling the Processing of Aerosol and Trace Gases in Clouds and Fogs. *Chem.  
1273 Rev.* **2015**, *115* (10), 4157-4198.
- 1274 69. Moffet, R. C.; O'Brien, R. E.; Alpert, P. A.; Kelly, S. T.; Pham, D. Q.; Gilles, M. K.; Knopf, D.  
1275 A.; Laskin, A., Morphology and mixing of black carbon particles collected in central California during  
1276 the CARES field study. *Atmos. Chem. Phys.* **2016**, *16* (22), 14515-14525.
- 1277 70. Laskin, A.; Gilles, M. K.; Knopf, D. A.; Wang, B.; China, S., Progress in the Analysis of  
1278 Complex Atmospheric Particles. *Annu. Rev. Anal. Chem.* **2016**, *9* (1), 117-143.
- 1279 71. Pöhlker, C.; Wiedemann, K. T.; Sinha, B.; Shiraiwa, M.; Gunthe, S. S.; Smith, M.; Su, H.;  
1280 Artaxo, P.; Chen, Q.; Cheng, Y. F.; Elbert, W.; Gilles, M. K.; Kilcoyne, A. L. D.; Moffet, R. C.;  
1281 Weigand, M.; Martin, S. T.; Pöschl, U.; Andreae, M. O., Biogenic Potassium Salt Particles as Seeds for  
1282 Secondary Organic Aerosol in the Amazon. *Science* **2012**, *337* (6098), 1075-1078.
- 1283 72. Moffet, R. C.; Tivanski, A. V.; Gilles, M. K., Scanning X-ray Transmission Microscopy:  
1284 Applications in Atmospheric Aerosol Research. In *Fundamentals and Applications in Aerosol  
1285 Spectroscopy*, Signorell, R.; Reid, J. P., Eds. Taylor and Francis Books, Inc.: 2010; pp 419-462.
- 1286 73. Gilles, M. K.; Moffet, R. C.; Laskin, A., Spectro-microscopy of carbonaceous particulates.  
1287 *Geochim. Cosmochim. Ac.* **2010**, *74* (12), A332-A332.
- 1288 74. Moffet, R. C.; Henn, T. R.; Tivanski, A. V.; Hopkins, R. J.; Desyaterik, Y.; Kilcoyne, A. L. D.;  
1289 Tyliszczak, T.; Fast, J.; Barnard, J.; Shuthanandan, V.; Cliff, S. S.; Perry, K. D.; Laskin, A.; Gilles, M.  
1290 K., Microscopic characterization of carbonaceous aerosol particle aging in the outflow from Mexico  
1291 City. *Atmos. Chem. Phys.* **2010**, *10*, 961-976.

- 1292 75. Adachi, K.; Freney, E. J.; Buseck, P. R., Shapes of internally mixed hygroscopic aerosol  
1293 particles after deliquescence, and their effect on light scattering. *Geophys. Res. Lett.* **2011**, *38*, L13804.  
1294 76. Posfai, M.; Gelencser, A.; Simonics, R.; Arato, K.; Li, J.; Hobbs, P. V.; Buseck, P. R.,  
1295 Atmospheric tar balls: Particles from biomass and biofuel burning. *J. Geophys. Res.* **2004**, *109* (D6),  
1296 D06213.  
1297 77. Li, J.; Posfai, M.; Hobbs, P. V.; Buseck, P. R., Individual aerosol particles from biomass burning  
1298 in southern Africa: 2, Compositions and aging of inorganic particles. *J. Geophys. Res.* **2003**, *108* (D13),  
1299 8484.  
1300 78. Buseck, P. R.; Posfai, M., Airborne minerals and related aerosol particles: Effects on climate and  
1301 the environment. *P. Natl. Acad. Sci. USA* **1999**, *96* (7), 3372-3379.  
1302 79. Laskin, A.; Laskin, J.; Nizkorodov, S. A., Chemistry of Atmospheric Brown Carbon. *Chem. Rev.*  
1303 **2015**, *115* (10), 4335-4382.  
1304 80. Solomon, P. A.; Sioutas, C., Continuous and semicontinuous monitoring techniques for  
1305 particulate matter mass and chemical components: A synthesis of findings from EPA's particulate matter  
1306 supersites program and related studies. *J. Air Waste Manage. Assoc.* **2008**, *58* (2), 164-195.  
1307 81. Hersey, S. P.; Craven, J. S.; Metcalf, A. R.; Lin, J.; Lathem, T.; Suski, K. J.; Cahill, J. F.; Duong,  
1308 H. T.; Sorooshian, A.; Jonsson, H. H.; Shiraiwa, M.; Zuend, A.; Nenes, A.; Prather, K. A.; Flagan, R.  
1309 C.; Seinfeld, J. H., Composition and hygroscopicity of the Los Angeles Aerosol: CalNex. *Journal of  
21310 Geophysical Research* **2013**, *118* (7), 3016-3036.  
21311 82. Hidy, G. M., Surface-Level Fine Particle Mass Concentrations: From Hemispheric Distributions  
21312 to Megacity Sources. *J. Air Waste Manage. Assoc.* **2009**, *59* (7), 770-789.  
21313 83. Bond, T. C.; Doherty, S. J.; Fahey, D. W.; Forster, P. M.; Berntsen, T.; DeAngelo, B. J.; Flanner,  
21314 M. G.; Ghan, S.; Karcher, B.; Koch, D.; Kinne, S.; Kondo, Y.; Quinn, P. K.; Sarofim, M. C.; Schultz,  
21315 M. G.; Schulz, M.; Venkataraman, C.; Zhang, H.; Zhang, S.; Bellouin, N.; Guttikunda, S. K.; Hopke, P.  
21316 K.; Jacobson, M. Z.; Kaiser, J. W.; Klimont, Z.; Lohmann, U.; Schwarz, J. P.; Shindell, D.; Storelvmo,  
21317 T.; Warren, S. G.; Zender, C. S., Bounding the role of black carbon in the climate system: A scientific  
31318 assessment. *J. Geophys. Res.* **2013**, *118* (11), 5380-5552.  
31319 84. Farmer, D. K.; Cappa, C. D.; Kreidenweis, S. M., Atmospheric Processes and Their Controlling  
31320 Influence on Cloud Condensation Nuclei Activity. *Chem. Rev.* **2015**, *115* (10), 4199-4217.  
31321 85. Sullivan, R. C.; Petters, M. D.; DeMott, P. J.; Kreidenweis, S. M.; Wex, H.; Niedermeier, D.;  
31322 Hartmann, S.; Clauss, T.; Stratmann, F.; Reitz, P.; Schneider, J.; Sierau, B., Irreversible loss of ice  
31323 nucleation active sites in mineral dust particles caused by sulphuric acid condensation. *Atmos. Chem.  
31324 Phys.* **2010**, *10* (23), 11471-11487.  
31325 86. Sullivan, R. C.; Minambres, L.; DeMott, P. J.; Prenni, A. J.; Carrico, C. M.; Levin, E. J. T.;  
31326 Kreidenweis, S. M., Chemical processing does not always impair heterogeneous ice nucleation of  
40327 mineral dust particles. *Geophys. Res. Lett.* **2010**, *37*, L24805.  
41328 87. Niedermeier, D.; Hartmann, S.; Clauss, T.; Wex, H.; Kiselev, A.; Sullivan, R. C.; DeMott, P. J.;  
42329 Petters, M. D.; Reitz, P.; Schneider, J.; Mikhailov, E.; Sierau, B.; Stetzer, O.; Reimann, B.; Bundke, U.;  
43330 Shaw, R. A.; Buchholz, A.; Mentel, T. F.; Stratmann, F., Experimental study of the role of  
44331 physicochemical surface processing on the IN ability of mineral dust particles. *Atmos. Chem. Phys.*  
45332 **2011**, *11* (21), 11131-11144.  
46333 88. Sihvonen, S. K.; Schill, G. P.; Lyktey, N. A.; Veghte, D. P.; Tolbert, M. A.; Freedman, M. A.,  
47334 Chemical and Physical Transformations of Aluminosilicate Clay Minerals Due to Acid Treatment and  
48335 Consequences for Heterogeneous Ice Nucleation. *J. Phys. Chem. A* **2014**, *118* (38), 8787-8796.  
49336 89. Fierce, L.; Riemer, N.; Bond, T. C., Toward reduced representation of mixing state for  
50337 simulating aerosol effects on climate. *Bull. Amer. Meteorol. Soc.* **2017**, *98* (5), 971-980.  
51338 90. Ching, J.; Zaveri, R. A.; Easter, R. C.; Riemer, N.; Fast, J. D., A three-dimensional sectional  
52339 representation of aerosol mixing state for simulating optical properties and cloud condensation nuclei. *J.  
53340 Geophys. Res.* **2016**, *121* (10), 5912-5929.  
54341 91. Riemer, N.; West, M., Quantifying aerosol mixing state with entropy and diversity measures.  
55342 *Atmos. Chem. Phys.* **2013**, *13* (22), 11423-11439.

- 1343  
1344 92. Riemer, N.; West, M.; Zaveri, R. A.; Easter, R. C., Simulating the evolution of soot mixing state  
1345 with a particle-resolved aerosol model. *J. Geophys. Res.* **2009**, *114*, D09202.  
1346 93. Cziczo, D. J.; Froyd, K. D.; Hoose, C.; Jensen, E. J.; Diao, M. H.; Zondlo, M. A.; Smith, J. B.;  
1347 Twohy, C. H.; Murphy, D. M., Clarifying the Dominant Sources and Mechanisms of Cirrus Cloud  
51347 Formation. *Science* **2013**, *340* (6138), 1320-1324.  
1348 94. Froyd, K. D.; Cziczo, D. J.; Hoose, C.; Jensen, E. J.; Diao, M. H.; Zondlo, M. A.; Smith, J. B.;  
71349 Twohy, C. H.; Murphy, D. M., Cirrus cloud formation and the role of heterogeneous ice nuclei. In  
81350 *Nucleation and Atmospheric Aerosols*, DeMott, P. J.; Odowd, C. D., Eds. Amer. Inst. Physics: Melville,  
91351 10 2013; Vol. 1527, pp 976-978.  
11352 95. O'Brien, R. E.; Wang, B. B.; Laskin, A.; Riemer, N.; West, M.; Zhang, Q.; Sun, Y. L.; Yu, X.  
12353 Y.; Alpert, P.; Knopf, D. A.; Gilles, M. K.; Moffet, R. C., Chemical imaging of ambient aerosol  
13354 particles: Observational constraints on mixing state parameterization. *J. Geophys. Res.* **2015**, *120* (18),  
14355 9591-9605.  
15356 96. Knopf, D. A.; Alpert, P. A.; Wang, B.; O'Brien, R. E.; Kelly, S. T.; Laskin, A.; Gilles, M. K.;  
16357 Moffet, R. C., Microspectroscopic imaging and characterization of individually identified ice nucleating  
17358 particles from a case field study. *J. Geophys. Res.* **2014**, *119*, 10365-10381.  
18359 97. Moffet, R. C.; Rodel, T. C.; Kelly, S. T.; Yu, X. Y.; Carroll, G. T.; Fast, J.; Zaveri, R. A.;  
20360 Laskin, A.; Gilles, M. K., Spectro-microscopic measurements of carbonaceous aerosol aging in Central  
21361 California. *Atmos. Chem. Phys.* **2013**, *13* (20), 10445-10459.  
22362 98. Wang, B.; Laskin, A.; Roedel, T.; Gilles, M. K.; Moffet, R. C.; Tivanski, A. V.; Knopf, D. A.,  
23363 Heterogeneous ice nucleation and water uptake by field-collected atmospheric particles below 273 K. *J.  
24364 Geophys. Res.* **2012**, *117*, D00V19.  
25365 99. Laskin, A.; Moffet, R. C.; Gilles, M. K.; Fast, J. D.; Zaveri, R. A.; Wang, B. B.; Nigge, P.;  
26366 Shutthanandan, J., Tropospheric chemistry of internally mixed sea salt and organic particles: Surprising  
27367 reactivity of NaCl with weak organic acids. *J. Geophys. Res.* **2012**, *117*, D15302.  
28368 100. Moffet, R. C.; Henn, T.; Laskin, A.; Gilles, M. K., Automated Chemical Analysis of Internally  
29369 Mixed Aerosol Particles Using X-ray Spectromicroscopy at the Carbon K-Edge. *Anal. Chem.* **2010**, *82*  
30370 (19), 7906-7914.  
31371 101. Knopf, D. A.; Wang, B.; Laskin, A.; Moffet, R. C.; Gilles, M. K., Heterogeneous nucleation of  
32372 ice on anthropogenic organic particles collected in Mexico City. *Geophys. Res. Lett.* **2010**, *37*, L11803.  
33373 102. China, S.; Alpert, P. A.; Zhang, B.; Schum, S.; Dzepina, K.; Wright, K.; Owen, R. C.; Fialho, P.;  
34374 Mazzoleni, L. R.; Mazzoleni, C.; Knopf, D. A., Ice cloud formation potential by free tropospheric  
35375 particles from long-range transport over the Northern Atlantic Ocean. *J. Geophys. Res.* **2017**, *122* (5),  
36376 3065-3079.  
37377 103. Collier, K. N.; Brooks, S. D., Role of organic hydrocarbons in atmospheric ice formation via  
38378 contact freezing. *J. Phys. Chem. A* **2016**, *120* (51), 10169-10180.  
39379 104. Pummer, B. G.; Budke, C.; Augustin-Bauditz, S.; Niedermeier, D.; Felgitsch, L.; Kampf, C. J.;  
40380 Huber, R. G.; Liedl, K. R.; Loerting, T.; Moschen, T.; Schauperl, M.; Tollinger, M.; Morris, C. E.; Wex,  
41381 H.; Grothe, H.; Pöschl, U.; Koop, T.; Fröhlich-Nowoisky, J., Ice nucleation by water-soluble  
42382 macromolecules. *Atmos. Chem. Phys.* **2015**, *15* (8), 4077-4091.  
43383 105. Wang, B. B.; Lambe, A. T.; Massoli, P.; Onasch, T. B.; Davidovits, P.; Worsnop, D. R.; Knopf,  
44384 D. A., The deposition ice nucleation and immersion freezing potential of amorphous secondary organic  
45385 aerosol: Pathways for ice and mixed-phase cloud formation. *J. Geophys. Res.* **2012**, *117*, D16209.  
46386 106. Cantrell, W.; Robinson, C., Heterogeneous freezing of ammonium sulfate and sodium chloride  
51387 solutions by long chain alcohols. *Geophys. Res. Lett.* **2006**, *33* (7), L07802.  
52388 107. Ochshorn, E.; Cantrell, W., Towards understanding ice nucleation by long chain alcohols. *J.  
53389 Chem. Phys.* **2006**, *124* (5), 054714.  
54390 108. Zobrist, B.; Koop, T.; Luo, B. P.; Marcolli, C.; Peter, T., Heterogeneous ice nucleation rate  
55391 coefficient of water droplets coated by a nonadecanol monolayer. *J. Phys. Chem. C* **2007**, *111* (5), 2149-  
56392 2155.

- 1393 109. Knopf, D. A.; Forrester, S. M., Freezing of Water and Aqueous NaCl Droplets Coated by  
1394 Organic Monolayers as a Function of Surfactant Properties and Water Activity. *J. Phys. Chem. A* **2011**,  
1395 *115* (22), 5579-5591.
- 1396 110. Dreischmeier, K.; Budke, C.; Wiedemeier, L.; Kottke, T.; Koop, T., Boreal pollen contain ice-  
1397 nucleating as well as ice-binding ‘antifreeze’ polysaccharides. *Sci. Rep.* **2017**, *7*, 41890.
- 61398 111. Gavish, M.; Popovitzbiro, R.; Lahav, M.; Leiserowitz, L., Ice Nucleation by Alcohols Arranged  
71399 in Monolayers at the Surface of Water Drops. *Science* **1990**, *250* (4983), 973-975.
- 81400 112. Charnawskas, J. C.; Alpert, P. A.; Lambe, A. T.; Berkemeier, T.; O'Brien, R. E.; Massoli, P.;  
91401 Onasch, T. B.; Shiraiwa, M.; Moffet, R. C.; Gilles, M. K.; Davidovits, P.; Worsnop, D. R.; Knopf, D.  
101402 A., Condensed-phase biogenic-anthropogenic interactions with implications for cold cloud formation.  
111403 *Faraday Discuss.* **2017**, *200*, 164-195.
- 13404 113. Koop, T.; Bookhold, J.; Shiraiwa, M.; Pöschl, U., Glass transition and phase state of organic  
14405 compounds: dependency on molecular properties and implications for secondary organic aerosols in the  
15406 atmosphere. *Phys. Chem. Chem. Phys.* **2011**, *13* (43), 19238-19255.
- 16407 114. Saukko, E.; Lambe, A. T.; Massoli, P.; Koop, T.; Wright, J. P.; Croasdale, D. R.; Pedernera, D.  
17408 A.; Onasch, T. B.; Laaksonen, A.; Davidovits, P.; Worsnop, D. R.; Virtanen, A., Humidity-dependent  
18409 phase state of SOA particles from biogenic and anthropogenic precursors. *Atmos. Chem. Phys.* **2012**, *12*  
20410 (16), 7517-7529.
- 21411 115. Virtanen, A.; Kannisto, J.; Kuuluvainen, H.; Arffman, A.; Joutsensaari, J.; Saukko, E.; Hao, L.;  
22412 Yli-Pirila, P.; Tiitta, P.; Holopainen, J. K.; Keskinen, J.; Worsnop, D. R.; Smith, J. N.; Laaksonen, A.,  
23413 Bounce behavior of freshly nucleated biogenic secondary organic aerosol particles. *Atmos. Chem. Phys.*  
24414 **2011**, *11* (16), 8759-8766.
- 25415 116. Virtanen, A.; Joutsensaari, J.; Koop, T.; Kannisto, J.; Yli-Pirila, P.; Leskinen, J.; Makela, J. M.;  
26416 Holopainen, J. K.; Pöschl, U.; Kulmala, M.; Worsnop, D. R.; Laaksonen, A., An amorphous solid state  
27417 of biogenic secondary organic aerosol particles. *Nature* **2010**, *467* (7317), 824-827.
- 28418 117. Martin, S. T., Phase transitions of aqueous atmospheric particles. *Chem. Rev.* **2000**, *100* (9),  
29419 3403-3453.
- 30420 118. Lienhard, D. M.; Huisman, A. J.; Krieger, U. K.; Rudich, Y.; Marcolli, C.; Luo, B. P.; Bones, D.  
31421 L.; Reid, J. P.; Lambe, A. T.; Canagaratna, M. R.; Davidovits, P.; Onasch, T. B.; Worsnop, D. R.;  
32422 Steimer, S. S.; Koop, T.; Peter, T., Viscous organic aerosol particles in the upper troposphere:  
33423 diffusivity-controlled water uptake and ice nucleation? *Atmos. Chem. Phys.* **2015**, *15* (23), 13599-  
34424 13613.
- 35425 119. Berkemeier, T.; Shiraiwa, M.; Pöschl, U.; Koop, T., Competition between water uptake and ice  
36426 nucleation by glassy organic aerosol particles. *Atmos. Chem. Phys.* **2014**, *14* (22), 12513-12531.
- 37427 120. Angell, C. A., Formation of Glasses from Liquids and Biopolymers. *Science* **1995**, *267* (5206),  
38428 1924-1935.
- 39429 121. Zobrist, B.; Soonsin, V.; Luo, B. P.; Krieger, U. K.; Marcolli, C.; Peter, T.; Koop, T., Ultra-slow  
40430 water diffusion in aqueous sucrose glasses. *Phys. Chem. Chem. Phys.* **2011**, *13* (8), 3514-3526.
- 41431 122. Shiraiwa, M.; Li, Y.; Tsimpidi, A. P.; Karydis, V. A.; Berkemeier, T.; Pandis, S. N.; Lelieveld,  
42432 J.; Koop, T.; Pöschl, U., Global distribution of particle phase state in atmospheric secondary organic  
43433 aerosols. *Nat. Commun.* **2017**, *8*, 15002.
- 44434 123. Wylie, D.; Jackson, D. L.; Menzel, W. P.; Bates, J. J., Trends in global cloud cover in two  
45435 decades of HIRS observations. *J. Clim.* **2005**, *18* (15), 3021-3031.
- 46436 124. Yang, S.; Zou, X., Lapse rate characteristics in ice clouds inferred from GPS RO and CloudSat  
51437 observations. *Atmos. Res.* **2017**, *197*, 105-112.
- 47438 125. McFarquhar, G. M.; Ghan, S.; Verlinde, J.; Korolev, A.; Strapp, J. W.; Schmid, B.; Tomlinson,  
48439 J. M.; Wolde, M.; Brooks, S. D.; Cziczo, D.; Dubey, M. K.; Fan, J.; Flynn, C.; Gultepe, I.; Hubbe, J.;  
49440 Gilles, M. K.; Laskin, A.; Lawson, P.; Leaitch, W. R.; Liu, P.; Liu, X.; Lubin, D.; Mazzoleni, C.;  
50441 Macdonald, A.-M.; Moffet, R. C.; Morrison, H.; Ovchinnikov, M.; Shupe, M. D.; Turner, D. D.; Xie, S.;  
51442 Zelenyuk, A.; Bae, K.; Freer, M.; Glen, A., Indirect and Semi-Direct Aerosol Campaign: The Impact of  
52443 Arctic Aerosols on Clouds. *Bull. Amer. Meteorol. Soc.* **2011**, *92* (2), 183-201.

- 1444 126. Verlinde, J.; Harrington, J. Y.; McFarquhar, G. M.; Yannuzzi, V. T.; Avramov, A.; Greenberg,  
1445 S.; Johnson, N.; Zhang, G.; Poellot, M. R.; Mather, J. H.; Turner, D. D.; Eloranta, E. W.; Zak, B. D.;  
1446 Prenni, A. J.; Daniel, J. S.; Kok, G. L.; Tobin, D. C.; Holz, R.; Sassen, K.; Spangenberg, D.; Minnis, P.;  
1447 Tooman, T. P.; Ivey, M. D.; Richardson, S. J.; Bahrman, C. P.; Shupe, M.; DeMott, P. J.; Heymsfield,  
1448 A. J.; Schofield, R., The mixed-phase Arctic cloud experiment. *Bull. Amer. Meteorol. Soc.* **2007**, 88 (2),  
1449 205-221.
- 1450 127. Lawson, R. P.; Baker, B. A.; Schmitt, C. G.; Jensen, T. L., An overview of microphysical  
1451 properties of Arctic clouds observed in May and July 1998 during FIRE ACE. *J. Geophys. Res.* **2001**,  
1452 106 (D14), 14989-15014.
- 1453 128. Morrison, H.; de Boer, G.; Feingold, G.; Harrington, J.; Shupe, M. D.; Sulia, K., Resilience of  
1454 persistent Arctic mixed-phase clouds. *Nat. Geosci.* **2012**, 5 (1), 11-17.
- 1455 129. Shiraiwa, M.; Seinfeld, J. H., Equilibration timescale of atmospheric secondary organic aerosol  
1456 partitioning. *Geophys. Res. Lett.* **2012**, 39, L24801.
- 1457 130. Mikhailov, E.; Vlasenko, S.; Martin, S. T.; Koop, T.; Pöschl, U., Amorphous and crystalline  
1458 aerosol particles interacting with water vapor: conceptual framework and experimental evidence for  
1459 restructuring, phase transitions and kinetic limitations. *Atmos. Chem. Phys.* **2009**, 9 (24), 9491-9522.
- 1460 131. Moreno, L. A. L.; Stetzer, O.; Lohmann, U., Contact freezing: a review of experimental studies.  
1461 *Atmos. Chem. Phys.* **2013**, 13 (19), 9745-9769.
- 1462 132. Durant, A. J.; Shaw, R. A., Evaporation freezing by contact nucleation inside-out. *Geophys. Res.*  
1463 *Lett.* **2005**, 32 (20), L20814.
- 1464 133. Wex, H.; DeMott, P. J.; Tobo, Y.; Hartmann, S.; Roesch, M.; Clauss, T.; Tomsche, L.;  
1465 Niedermeier, D.; Stratmann, F., Kaolinite particles as ice nuclei: learning from the use of different  
1466 kaolinite samples and different coatings. *Atmos. Chem. Phys.* **2014**, 14 (11), 5529-5546.
- 1467 134. Ansmann, A.; Baars, H.; Tesche, M.; Mueller, D.; Althausen, D.; Engelmann, R.; Pauliquevis,  
1468 T.; Artaxo, P., Dust and smoke transport from Africa to South America: Lidar profiling over Cape  
1469 Verde and the Amazon rainforest. *Geophys. Res. Lett.* **2009**, 36, L11802.
- 1470 135. de Boer, G.; Morrison, H.; Shupe, M. D.; Hildner, R., Evidence of liquid dependent ice  
1471 nucleation in high-latitude stratiform clouds from surface remote sensors. *Geophys. Res. Lett.* **2011**, 38,  
1472 L01803.
- 1473 136. Wiacek, A.; Peter, T.; Lohmann, U., The potential influence of Asian and African mineral dust  
1474 on ice, mixed-phase and liquid water clouds. *Atmos. Chem. Phys.* **2010**, 10 (18), 8649-8667.
- 1475 137. Hande, L. B.; Hoose, C., Partitioning the primary ice formation modes in large eddy simulations  
1476 of mixed-phase clouds. *Atmos. Chem. Phys.* **2017**, 17 (22), 14105-14118.
- 1477 138. Shaw, R. A.; Durant, A. J.; Mi, Y., Heterogeneous surface crystallization observed in  
1478 undercooled water. *J. Phys. Chem. B* **2005**, 109 (20), 9865-9868.
- 1479 139. Hoffmann, N.; Duft, D.; Kiselev, A.; Leisner, T., Contact freezing efficiency of mineral dust  
1480 aerosols studied in an electrodynamic balance: quantitative size and temperature dependence for illite  
1481 particles. *Faraday Discuss.* **2013**, 165, 383-390.
- 1482 140. Zobrist, B.; Marcolli, C.; Pedernera, D. A.; Koop, T., Do atmospheric aerosols form glasses?  
1483 *Atmos. Chem. Phys.* **2008**, 8 (17), 5221-5244.
- 1484 141. Price, H. C.; Mattsson, J.; Zhang, Y.; Bertram, A. K.; Davies, J. F.; Grayson, J. W.; Martin, S.  
1485 T.; O'Sullivan, D.; Reid, J. P.; Rickards, A. M. J.; Murray, B. J., Water diffusion in atmospherically  
1486 relevant alpha-pinene secondary organic material. *Chem. Sci.* **2015**, 6 (8), 4876-4883.
- 1487 142. Herrmann, H.; Schaefer, T.; Tilgner, A.; Styler, S. A.; Weller, C.; Teich, M.; Otto, T.,  
1488 Tropospheric Aqueous-Phase Chemistry: Kinetics, Mechanisms, and Its Coupling to a Changing Gas  
1489 Phase. *Chem. Rev.* **2015**, 115 (10), 4259-4334.
- 1490 143. Thomson, W., On the equilibrium of vapour at a curved surface of liquid. *Philosoph. Mag.* **1871**,  
1491 42 (282), 448-452.
- 1492 144. Hatch, C. D.; Greenaway, A. L.; Christie, M. J.; Baltrusaitis, J., Water adsorption constrained  
1493 Frenkel-Halsey-Hill adsorption activation theory: Montmorillonite and illite. *Atmos. Environ.* **2014**, 87,  
1494 26-33.

- 1495 145. Hatch, C. D.; Gierlus, K. M.; Shuttlefield, J. D.; Grassian, V. H., Water adsorption and cloud  
1496 condensation nuclei activity of calcite and calcite coated with model humic and fulvic acids. *Atmos.*  
1497 *Environ.* **2008**, 42 (22), 5672-5684.
- 1498 146. Vlasenko, A.; Sjogren, S.; Weingartner, E.; Gaggeler, H. W.; Ammann, M., Generation of  
1499 submicron Arizona test dust aerosol: Chemical and hygroscopic properties. *Aerosol Sci. Technol.* **2005**,  
61500 39 (5), 452-460.
- 1501 147. Gustafsson, R. J.; Orlov, A.; Badger, C. L.; Griffiths, P. T.; Cox, R. A.; Lambert, R. M., A  
81502 comprehensive evaluation of water uptake on atmospherically relevant mineral surfaces: DRIFT  
91503 spectroscopy, thermogravimetric analysis and aerosol growth measurements. *Atmos. Chem. Phys.* **2005**,  
101504 5, 3415-3421.
- 1505 148. Herich, H.; Tritscher, T.; Wiacek, A.; Gysel, M.; Weingartner, E.; Lohmann, U.; Baltensperger,  
1506 U.; Cziczo, D. J., Water uptake of clay and desert dust aerosol particles at sub- and supersaturated water  
1507 vapor conditions. *Phys. Chem. Chem. Phys.* **2009**, 11 (36), 7804-7809.
- 1508 149. Koehler, K. A.; Kreidenweis, S. M.; DeMott, P. J.; Petters, M. D.; Prenni, A. J.; Carrico, C. M.,  
1509 Hygroscopicity and cloud droplet activation of mineral dust aerosol. *Geophys. Res. Lett.* **2009**, 36,  
1510 L08805.
- 1511 150. Koehler, K. A.; Kreidenweis, S. M.; DeMott, P. J.; Prenni, A. J.; Petters, M. D., Potential impact  
20512 of Owens (dry) Lake dust on warm and cold cloud formation. *J. Geophys. Res.* **2007**, 112 (D12),  
21513 D12210.
- 21514 151. Kumar, P.; Sokolik, I. N.; Nenes, A., Measurements of cloud condensation nuclei activity and  
21515 droplet activation kinetics of fresh unprocessed regional dust samples and minerals. *Atmos. Chem. Phys.*  
21516 **2011**, 11 (7), 3527-3541.
- 21517 152. Kumar, P.; Nenes, A.; Sokolik, I. N., Importance of adsorption for CCN activity and  
21518 hygroscopic properties of mineral dust aerosol. *Geophys. Res. Lett.* **2009**, 36, L24804.
- 21519 153. Sullivan, R. C.; Moore, M. J. K.; Petters, M. D.; Kreidenweis, S. M.; Qafoku, O.; Laskin, A.;  
21520 Roberts, G. C.; Prather, K. A., Impact of Particle Generation Method on the Apparent Hygroscopicity of  
30521 Insoluble Mineral Particles. *Aerosol Sci. Technol.* **2010**, 44 (10), 830-846.
- 31522 154. Garimella, S.; Huang, Y. W.; Seewald, J. S.; Cziczo, D. J., Cloud condensation nucleus activity  
31523 comparison of dry- and wet-generated mineral dust aerosol: the significance of soluble material. *Atmos.*  
33524 *Chem. Phys.* **2014**, 14 (12), 6003-6019.
- 33525 155. Hung, H. M.; Wang, K. C.; Chen, J. P., Adsorption of nitrogen and water vapor by insoluble  
36526 particles and the implication on cloud condensation nuclei activity. *J. Aerosol. Sci.* **2015**, 86, 24-31.
- 37527 156. Gibson, E. R.; Gierlus, K. M.; Hudson, P. K.; Grassian, V. H., Generation of internally mixed  
38528 insoluble and soluble aerosol particles to investigate the impact of atmospheric aging and heterogeneous  
39529 processing on the CCN activity of mineral dust aerosol. *Aerosol Sci. Technol.* **2007**, 41 (10), 914-924.
- 40530 157. Tang, M. J.; Whitehead, J.; Davidson, N. M.; Pope, F. D.; Alfarra, M. R.; McFiggans, G.;  
41531 Kalberer, M., Cloud condensation nucleation activities of calcium carbonate and its atmospheric ageing  
42532 products. *Phys. Chem. Chem. Phys.* **2015**, 17 (48), 32194-32203.
- 43533 158. Cziczo, D. J.; Froyd, K. D.; Gallavardin, S. J.; Möhler, O.; Benz, S.; Saathoff, H.; Murphy, D.  
44534 M., Deactivation of ice nuclei due to atmospherically relevant surface coatings. *Environ. Res. Lett.*  
45535 **2009**, 4 (4), 044013.
- 46536 159. Knopf, D. A.; Koop, T., Heterogeneous nucleation of ice on surrogates of mineral dust. *J.*  
47537 *Geophys. Res.* **2006**, 111 (D12), D12201.
- 48538 160. Bogdan, A.; Molina, M. J., Physical Chemistry of the Freezing Process of Atmospheric Aqueous  
50539 Drops. *J. Phys. Chem. A* **2017**, 121 (16), 3109-3116.
- 51540 161. Bogdan, A.; Molina, M. J.; Tenhu, H., Freezing and glass transitions upon cooling and warming  
52541 and ice/freeze-concentration-solution morphology of emulsified aqueous citric acid. *Eur. J. Pharm.*  
53542 *Biopharm.* **2016**, 109, 49-60.
- 54543 162. Bogdan, A.; Molina, M. J.; Tenhu, H.; Loerting, T., Multiple glass transitions and freezing  
55544 events of aqueous citric acid. *J. Phys. Chem. A* **2015**, 119 (19), 4515-4523.

- 1545  
1546 163. Bogdan, A.; Loerting, T., Phase separation during freezing upon warming of aqueous solutions.  
J. Chem. Phys. **2014**, *141* (18), 4.
- 1547  
1548 164. Bogdan, A.; Molina, M. J.; Tenhu, H.; Bertel, E.; Bogdan, N.; Loerting, T., Visualization of  
Freezing Process in situ upon Cooling and Warming of Aqueous Solutions. Sci Rep **2014**, *4*, 6.
- 1549  
1550 165. Adler, G.; Koop, T.; Haspel, C.; Taraniuk, I.; Moise, T.; Koren, I.; Heiblum, R. H.; Rudich, Y.,  
Formation of highly porous aerosol particles by atmospheric freeze-drying in ice clouds. P. Natl. Acad.  
Sci. USA **2013**, *110* (51), 20414-20419.
- 1552  
1553 166. Adler, G.; Haspel, C.; Moise, T.; Rudich, Y., Optical extinction of highly porous aerosol  
following atmospheric freeze drying. Journal of Geophysical Research **2014**, *119* (11), 6768-6787.
- 1554  
1555 167. Wagner, R.; Höhler, K.; Huang, W.; Kiselev, A.; Möhler, O.; Mohr, C.; Pajunoja, A.; Saathoff,  
H.; Schiebel, T.; Shen, X.; Virtanen, A., Heterogeneous ice nucleation of  $\alpha$ -pinene SOA particles before  
and after ice cloud processing. J. Geophys. Res. **2017**, *122* (9), 4924-4943.
- 1557  
1558 168. Wagner, R.; Möhler, O.; Saathoff, H.; Schnaiter, M.; Skrotzki, J.; Leisner, T.; Wilson, T. W.;  
Malkin, T. L.; Murray, B. J., Ice cloud processing of ultra-viscous/glassy aerosol particles leads to  
enhanced ice nucleation ability. Atmos. Chem. Phys. **2012**, *12* (18), 8589-8610.
- 1560  
1561 169. Wagner, R.; Mohler, O.; Saathoff, H.; Schnaiter, M., Enhanced high-temperature ice nucleation  
ability of crystallized aerosol particles after preactivation at low temperature. J. Geophys. Res. **2014**,  
*119* (13), 19.
- 21563  
21564 170. Nangia, A., Conformational polymorphism in organic crystals. Accounts Chem. Res. **2008**, *41*  
(5), 595-604.
- 23565  
24566 171. Stahly, G. P., Diversity in single- and multiple-component crystals. The search for and  
prevalence of polymorphs and cocrystals. Cryst. Growth Des. **2007**, *7* (6), 1007-1026.
- 25567  
26568 172. Davey, R. J.; Schroeder, S. L. M.; ter Horst, J. H., Nucleation of Organic CrystalsA Molecular  
Perspective. Angew. Chem.-Int. Edit. **2013**, *52* (8), 2166-2179.
- 28569  
29570 173. Threlfall, T. L., Analysis of organic polymorphs - a review. Analyst **1995**, *120* (10), 2435-2460.
- 30571  
31572 174. Suzuki, M.; Ogaki, T.; Sato, K., Crystallization and transformation mechanisms of alpha,beta-  
polymorphs and gamma-polymorphs of ultra-pure oleic-acid. J. Am. Oil Chem. Soc. **1985**, *62* (11),  
1600-1604.
- 32573  
33574 175. Inoue, T.; Hisatsugu, Y.; Yamamoto, R.; Suzuki, M., Solid-liquid phase behavior of binary fatty  
acid mixtures 1. Oleic acid stearic acid and oleic acid behenic acid mixtures. Chem. Phys. Lipids **2004**,  
*127* (2), 143-152.
- 34575  
35576 176. Inoue, T.; Hisatsugu, Y.; Ishikawa, R.; Suzuki, M., Solid-liquid phase behavior of binary fatty  
acid mixtures 2. Mixtures of oleic acid with lauric acid, myristic acid, and palmitic acid. Chem. Phys.  
Lipids **2004**, *127* (2), 161-173.
- 36577  
37578 177. Knopf, D. A.; Anthony, L. M.; Bertram, A. K., Reactive uptake of O-3 by multicomponent and  
multiphase mixtures containing oleic acid. J. Phys. Chem. A **2005**, *109* (25), 5579-5589.
- 38579  
39580 178. Marcolli, C.; Luo, B. P.; Peter, T., Mixing of the organic aerosol fractions: Liquids as the  
thermodynamically stable phases. J. Phys. Chem. A **2004**, *108* (12), 2216-2224.
- 40581  
41582 179. Pöhlker, C.; Saturno, J.; Kruger, M. L.; Forster, J. D.; Weigand, M.; Wiedemann, K. T.; Bechtel,  
M.; Artaxo, P.; Andreae, M. O., Efflorescence upon humidification? X-ray microspectroscopic in situ  
observation of changes in aerosol microstructure and phase state upon hydration. Geophys. Res. Lett.  
**2014**, *41* (10), 3681-3689.
- 42583  
43584 180. Bertram, A. K.; Martin, S. T.; Hanna, S. J.; Smith, M. L.; Bodsworth, A.; Chen, Q.; Kuwata, M.;  
Liu, A.; You, Y.; Zorn, S. R., Predicting the relative humidities of liquid-liquid phase separation,  
efflorescence, and deliquescence of mixed particles of ammonium sulfate, organic material, and water  
using the organic-to-sulfate mass ratio of the particle and the oxygen-to-carbon elemental ratio of the  
organic component. Atmos. Chem. Phys. **2011**, *11* (21), 10995-11006.
- 44585  
45586 181. You, Y.; Bertram, A. K., Effects of molecular weight and temperature on liquid-liquid phase  
separation in particles containing organic species and inorganic salts. Atmos. Chem. Phys. **2015**, *15* (3),  
1351-1365.

- 1595 182. O'Brien, R. E.; Wang, B. B.; Kelly, S. T.; Lundt, N.; You, Y.; Bertram, A. K.; Leone, S. R.;  
1596 Laskin, A.; Gilles, M. K., Liquid-Liquid Phase Separation in Aerosol Particles: Imaging at the  
1597 Nanometer Scale. *Environ. Sci. Technol.* **2015**, *49* (8), 4995-5002.  
1598 183. Zuend, A.; Marcolli, C.; Peter, T.; Seinfeld, J. H., Computation of liquid-liquid equilibria and  
1599 phase stabilities: implications for RH-dependent gas/particle partitioning of organic-inorganic aerosols.  
61600 *Atmos. Chem. Phys.* **2010**, *10* (16), 7795-7820.  
71601 184. Renbaum-Wolff, L.; Song, M. J.; Marcolli, C.; Zhang, Y.; Liu, P. F. F.; Grayson, J. W.; Geiger,  
81602 F. M.; Martin, S. T.; Bertram, A. K., Observations and implications of liquid-liquid phase separation at  
91603 high relative humidities in secondary organic material produced by alpha-pinene ozonolysis without  
101604 inorganic salts. *Atmos. Chem. Phys.* **2016**, *16* (12), 7969-7979.  
11605 185. Song, M.; Liu, P.; Martin, S. T.; Bertram, A. K., Liquid-liquid phase separation in particles  
12606 containing secondary organic material free of inorganic salts. *Atmos. Chem. Phys.* **2017**, *17*, 11261–  
13607 11271.  
14608 186. Song, M.; Marcolli, C.; Krieger, U. K.; Zuend, A.; Peter, T., Liquid-liquid phase separation in  
15609 aerosol particles: Dependence on O:C, organic functionalities, and compositional complexity. *Geophys.  
16610 Res. Lett.* **2012**, *39*, 5.  
17611 187. Ovadnevaite, J.; Zuend, A.; Laaksonen, A.; Sanchez, K. J.; Roberts, G.; Ceburnis, D.; Decesari,  
18612 S.; Rinaldi, M.; Hodas, N.; Facchini, M. C.; Seinfeld, J. H.; Dowd, C. O., Surface tension prevails over  
21613 solute effect in organic-influenced cloud droplet activation. *Nature* **2017**, *546* (7660), 637-641.  
22614 188. Rasmussen, D. H., Ice Formation in Aqueous Systems. *J. Microsc. - Oxford* **1982**, *128* (NOV),  
23615 167-174.  
24616 189. Rasmussen, D. H., Thermodynamics and Nucleation Phenomena - a Set of Experimental-  
25617 Observations. *J Cryst Growth* **1982**, *56* (1), 56-66.  
26618 190. Koop, T., Homogeneous Ice Nucleation in Water and Aqueous Solutions. *Z. Phys. Chem.* **2004**,  
27619 *218*, 1231-1258.  
28620 191. Koop, T.; Murray, B. J., A physically constrained classical description of the homogeneous  
29621 nucleation of ice in water. *J. Chem. Phys.* **2016**, *145* (21), 211915.  
30622 192. Herbert, R. J.; Murray, B. J.; Dobbie, S. J.; Koop, T., Sensitivity of liquid clouds to homogenous  
31623 freezing parameterizations. *Geophys. Res. Lett.* **2015**, *42* (5), 1599-1605.  
32624 193. Lupi, L.; Hudait, A.; Peters, B.; Grunwald, M.; Mullen, R. G.; Nguyen, A. H.; Molinero, V.,  
33625 Role of stacking disorder in ice nucleation. *Nature* **2017**, *551* (7679), 218-222.  
34626 194. Murray, B. J.; Knopf, D. A.; Bertram, A. K., The formation of cubic ice under conditions  
35627 relevant to Earth's atmosphere. *Nature* **2005**, *434* (7030), 202-205.  
36628 195. Malkin, T. L.; Murray, B. J.; Brukhno, A. V.; Anwar, J.; Salzmann, C. G., Structure of ice  
37629 crystallized from supercooled water. *P. Natl. Acad. Sci. USA* **2012**, *109* (4), 1041-1045.  
38630 196. Zobrist, B.; Weers, U.; Koop, T., Ice nucleation in aqueous solutions of poly[ethylene glycol]  
39631 with different molar mass. *J. Chem. Phys.* **2003**, *118* (22), 10254-10261.  
40632 197. Koop, T.; Luo, B. P.; Tsias, A.; Peter, T., Water activity as the determinant for homogeneous ice  
41633 nucleation in aqueous solutions. *Nature* **2000**, *406* (6796), 611-614.  
42634 198. Knopf, D. A.; Rigg, Y. J., Homogeneous Ice Nucleation From Aqueous Inorganic/Organic  
43635 Particles Representative of Biomass Burning: Water Activity, Freezing Temperatures, Nucleation Rates.  
44636 *J. Phys. Chem. A* **2011**, *115* (5), 762-773.  
45637 199. Knopf, D. A.; Lopez, M. D., Homogeneous ice freezing temperatures and ice nucleation rates of  
46638 aqueous ammonium sulfate and aqueous levoglucosan particles for relevant atmospheric conditions.  
47639 *Phys. Chem. Chem. Phys.* **2009**, *11* (36), 8056-8068.  
48640 200. Bullock, G.; Molinero, V., Low-density liquid water is the mother of ice: on the relation between  
49641 mesostructure, thermodynamics and ice crystallization in solutions. *Faraday Discuss.* **2013**, *167*, 371-  
50642 388.  
51643 201. Murata, K.; Tanaka, H., General nature of liquid-liquid transition in aqueous organic solutions.  
52644 *Nat. Commun.* **2013**, *4*, 2844.

- 1645 202. Baker, M. B.; Baker, M., A new look at homogeneous freezing of water. *Geophys. Res. Lett.*  
1646 **2004**, *31* (19), L19102.  
1647 203. Ganbavale, G.; Marcolli, C.; Krieger, U. K.; Zuend, A.; Stratmann, G.; Peter, T., Experimental  
1648 determination of the temperature dependence of water activities for a selection of aqueous organic  
1649 solutions. *Atmos. Chem. Phys.* **2014**, *14* (18), 9993-10012.  
1650 204. Wexler, A. S.; Clegg, S. L., Atmospheric aerosol models for systems including the ions H<sup>+</sup>,  
1651 NH<sub>4</sub><sup>+</sup>, Na<sup>+</sup>, SO<sub>4</sub><sup>2-</sup>, NO<sub>3</sub><sup>-</sup>, Cl<sup>-</sup>, Br<sup>-</sup>, and H<sub>2</sub>O. *J. Geophys. Res.* **2002**, *107* (D14), 4207.  
1652 205. Carslaw, K. S.; Clegg, S. L.; Brimblecombe, P., A Thermodynamic Model of the System HCl-  
1653 HNO<sub>3</sub>-H<sub>2</sub>SO<sub>4</sub>-H<sub>2</sub>O, Including Solubilities of HBr, from Less-Than-200 to 328 K. *J. Phys. Chem.* **1995**,  
1654 *99* (29), 11557-11574.  
1655 206. Clegg, S. L.; Brimblecombe, P., Comment on the "Thermodynamic dissociation constant of the  
1656 bisulfate ion from Raman and ion interaction modeling studies of aqueous sulfuric acid at low  
1657 temperatures". *J. Phys. Chem. A* **2005**, *109* (11), 2703-2706.  
1658 207. Massucci, M.; Clegg, S. L.; Brimblecombe, P., Equilibrium partial pressures, thermodynamic  
1659 properties of aqueous and solid phases, and Cl<sub>2</sub> production from aqueous HCl and HNO<sub>3</sub> and their  
1660 mixtures. *J. Phys. Chem. A* **1999**, *103* (21), 4209-4226.  
1661 208. Knopf, D. A.; Luo, B. P.; Krieger, U. K.; Koop, T., Reply to "Comment on the 'Thermodynamic  
20662 dissociation constant of the bisulfate ion from Raman and ion interaction modeling studies of aqueous  
21663 sulfuric acid at low temperatures'". *J. Phys. Chem. A* **2005**, *109* (11), 2707-2709.  
21664 209. Knopf, D. A.; Luo, B. P.; Krieger, U. K.; Koop, T., Thermodynamic dissociation constant of the  
21665 bisulfate ion from Raman and ion interaction modeling studies of aqueous sulfuric acid at low  
21666 temperatures. *J. Phys. Chem. A* **2003**, *107* (21), 4322-4332.  
21667 210. Friese, E.; Ebel, A., Temperature Dependent Thermodynamic Model of the System H<sup>+</sup>-NH<sub>4</sub><sup>+</sup>-  
21668 Na<sup>+</sup>-SO<sub>4</sub><sup>2-</sup>-NO<sub>3</sub><sup>-</sup>-Cl<sup>-</sup>-H<sub>2</sub>O. *J. Phys. Chem. A* **2010**, *114* (43), 11595-11631.  
21669 211. Ganbavale, G.; Zuend, A.; Marcolli, C.; Peter, T., Improved AIOMFAC model parameterisation  
21670 of the temperature dependence of activity coefficients for aqueous organic mixtures. *Atmos. Chem.  
21671 Phys.* **2015**, *15* (1), 447-493.  
21672 212. Tabazadeh, A.; Djikaev, Y. S.; Reiss, H., Surface crystallization of supercooled water in clouds.  
21673 *P. Natl. Acad. Sci. USA* **2002**, *99* (25), 15873-15878.  
21674 213. Djikaev, Y. S.; Tabazadeh, A.; Hamill, P.; Reiss, H., Thermodynamic conditions for the surface-  
21675 stimulated crystallization of atmospheric droplets. *J. Phys. Chem. A* **2002**, *106* (43), 10247-10253.  
21676 214. Duft, D.; Leisner, T., Laboratory evidence for volume-dominated nucleation of ice in  
21677 supercooled water microdroplets. *Atmos. Chem. Phys.* **2004**, *4*, 1997-2000.  
21678 215. Djikaev, Y. S.; Ruckenstein, E., Dependence of homogeneous crystal nucleation in water  
21679 droplets on their radii and its implication for modeling the formation of ice particles in cirrus clouds.  
21680 *Phys. Chem. Chem. Phys.* **2017**, *19*, 20075-20081.  
21681 216. Pluharova, E.; Vrbka, L.; Jungwirth, P., Effect of Surface Pollution on Homogeneous Ice  
21682 Nucleation: A Molecular Dynamics Study. *J. Phys. Chem. C* **2010**, *114* (17), 7831-7838.  
21683 217. Vrbka, L.; Jungwirth, P., Homogeneous freezing of water starts in the subsurface. *J. Phys.  
21684 Chem. B* **2006**, *110* (37), 18126-18129.  
21685 218. Haji-Akbari, A.; Debenedetti, P. G., Computational investigation of surface freezing in a  
21686 molecular model of water. *Proc. Natl. Acad. Sci. U. S. A.* **2017**, *114* (13), 3316-3321.  
21687 219. Wang, B.; Knopf, D. A.; China, S.; Arey, B. W.; Harder, T. H.; Gilles, M. K.; Laskin, A., Direct  
21688 observation of ice nucleation events on individual atmospheric particles. *Phys. Chem. Chem. Phys.*  
21689 **2016**, *18* (43), 29721-29731.  
21690 220. Kiselev, A.; Bachmann, F.; Pedevilla, P.; Cox, S. J.; Michaelides, A.; Gerthsen, D.; Leisner, T.,  
21691 Active sites in heterogeneous ice nucleation—the example of K-rich feldspars. *Science* **2017**, *355*  
21692 (6323), 367-371.  
21693 221. Marcolli, C., Deposition nucleation viewed as homogeneous or immersion freezing in pores and  
21694 cavities. *Atmos. Chem. Phys.* **2014**, *14* (4), 2071-2104.  
21695 222. Layton, R. G.; Harris, F. S., Nucleation of ice on mica. *J. Atmos. Sci.* **1963**, *20* (2), 142-148.

- 1696 223. Campbell, J. M.; Meldrum, F. C.; Christenson, H. K., Observing the formation of ice and  
1697 organic crystals in active sites. *Proc. Natl. Acad. Sci. U. S. A.* **2017**, *114* (5), 810-815.  
1698 224. Campbell, J. M.; Meldrum, F. C.; Christenson, H. K., Characterization of Preferred Crystal  
1699 Nucleation Sites on Mica Surfaces. *Cryst. Growth Des.* **2013**, *13* (5), 1915-1925.  
1700 225. Christenson, H. K., Two-step crystal nucleation via capillary condensation. *Crystengcomm* **2013**,  
1701 *15* (11), 2030-2039.  
1702 226. Kovacs, T.; Christenson, H. K., A two-step mechanism for crystal nucleation without  
1703 supersaturation. *Faraday Discuss.* **2012**, *159*, 123-138.  
1704 227. Hofmann, S., *Auger- and X-Ray Photoelectron Spectroscopy in Materials Science A User-*  
1705 *Oriented Guide*. Springer Berlin Heidelberg: Berlin, 2013; Vol. 49.  
1706 228. Barr, T. L.; Seal, S., Nature of the use of adventitious carbon as a binding energy standard. *J.*  
1707 *Vac. Sci. Technol. A* **1995**, *13* (3), 1239-1246.  
1708 229. Bzdek, B. R.; Power, R. M.; Simpson, S. H.; Reid, J. P.; Royall, C. P., Precise, contactless  
1709 measurements of the surface tension of picolitre aerosol droplets. *Chem. Sci.* **2016**, *7* (1), 274-285.  
1710 230. Kirkby, J.; Curtius, J.; Almeida, J.; Dunne, E.; Duplissy, J.; Ehrhart, S.; Franchin, A.; Gagne, S.;  
1711 Ickes, L.; Kurten, A.; Kupc, A.; Metzger, A.; Riccobono, F.; Rondo, L.; Schobesberger, S.;  
1712 Tsagkogeorgas, G.; Wimmer, D.; Amorim, A.; Bianchi, F.; Breitenlechner, M.; David, A.; Dommen, J.;  
1713 Downard, A.; Ehn, M.; Flagan, R. C.; Haider, S.; Hansel, A.; Hauser, D.; Jud, W.; Junninen, H.; Kreissl,  
1714 F.; Kvashin, A.; Laaksonen, A.; Lehtipalo, K.; Lima, J.; Lovejoy, E. R.; Makhmutov, V.; Mathot, S.;  
1715 Mikkila, J.; Minginette, P.; Mogo, S.; Nieminen, T.; Onnela, A.; Pereira, P.; Petaja, T.; Schnitzhofer, R.;  
1716 Seinfeld, J. H.; Sipila, M.; Stozhkov, Y.; Stratmann, F.; Tome, A.; Vanhanen, J.; Viisanen, Y.; Vrtala,  
1717 A.; Wagner, P. E.; Walther, H.; Weingartner, E.; Wex, H.; Winkler, P. M.; Carslaw, K. S.; Worsnop, D.  
1718 R.; Baltensperger, U.; Kulmala, M., Role of sulphuric acid, ammonia and galactic cosmic rays in  
1719 atmospheric aerosol nucleation. *Nature* **2011**, *476* (7361), 429-433.  
1720 231. Bianchi, F.; Dommen, J.; Mathot, S.; Baltensperger, U., On-line determination of ammonia at  
1721 low pptv mixing ratios in the CLOUD chamber. *Atmos. Meas. Tech.* **2012**, *5* (7), 1719-1725.  
1722 232. Schnitzhofer, R.; Metzger, A.; Breitenlechner, M.; Jud, W.; Heinritzi, M.; De Menezes, L. P.;  
1723 Duplissy, J.; Guida, R.; Haider, S.; Kirkby, J.; Mathot, S.; Minginette, P.; Onnela, A.; Walther, H.;  
1724 Wasem, A.; Hansel, A.; Team, C., Characterisation of organic contaminants in the CLOUD chamber at  
1725 CERN. *Atmos. Meas. Tech.* **2014**, *7* (7), 2159-2168.  
1726 233. Wang, B.; Knopf, D. A., Heterogeneous ice nucleation on particles composed of humic-like  
1727 substances impacted by O<sub>3</sub>. *J. Geophys. Res.* **2011**, *116*, D03205.  
1728 234. Riechers, B.; Wittbracht, F.; Hutten, A.; Koop, T., The homogeneous ice nucleation rate of water  
1729 droplets produced in a microfluidic device and the role of temperature uncertainty. *Phys. Chem. Chem.*  
1730 *Phys.* **2013**, *15* (16), 5873-5887.  
1731 235. Sosso, G. C.; Chen, J.; Cox, S. J.; Fitzner, M.; Pedevilla, P.; Zen, A.; Michaelides, A., Crystal  
1732 Nucleation in Liquids: Open Questions and Future Challenges in Molecular Dynamics Simulations.  
1733 *Chem. Rev.* **2016**, *116* (12), 7078-7116.  
1734 236. Zielke, S. A.; Bertram, A. K.; Patey, G. N., Simulations of Ice Nucleation by Model AgI Disks  
1735 and Plates. *J. Phys. Chem. B* **2016**, *120* (9), 2291-2299.  
1736 237. Zielke, S. A.; Bertram, A. K.; Patey, G. N., Simulations of Ice Nucleation by Kaolinite (001)  
1737 with Rigid and Flexible Surfaces. *J. Phys. Chem. B* **2016**, *120* (8), 1726-1734.  
1738 238. Zielke, S. A.; Bertram, A. K.; Patey, G. N., A Molecular Mechanism of Ice Nucleation on Model  
1739 AgI Surfaces. *J. Phys. Chem. B* **2015**, *119* (29), 9049-9055.  
1740 239. Croteau, T.; Bertram, A. K.; Patey, G. N., Water Adsorption on Kaolinite Surfaces Containing  
1741 Trenches. *J. Phys. Chem. A* **2010**, *114* (5), 2171-2178.  
1742 240. Croteau, T.; Bertram, A. K.; Patey, G. N., Simulation of Water Adsorption on Kaolinite under  
1743 Atmospheric Conditions. *J. Phys. Chem. A* **2009**, *113* (27), 7826-7833.  
1744 241. Croteau, T.; Bertram, A. K.; Patey, G. N., Adsorption and Structure of Water on Kaolinite  
1745 Surfaces: Possible Insight into Ice Nucleation from Grand Canonical Monte Carlo Calculations. *J. Phys.*  
1746 *Chem. A* **2008**, *112* (43), 10708-10712.

- 1747 242. Cox, S. J.; Kathmann, S. M.; Slater, B.; Michaelides, A., Molecular simulations of  
1748 heterogeneous ice nucleation. II. Peeling back the layers. *J. Chem. Phys.* **2015**, *142* (18), 184705.  
1749 243. Cox, S. J.; Kathmann, S. M.; Slater, B.; Michaelides, A., Molecular simulations of  
1750 heterogeneous ice nucleation. I. Controlling ice nucleation through surface hydrophilicity. *J. Chem.*  
1751 *Phys.* **2015**, *142* (18), 184704.  
1752 244. Cox, S. J.; Raza, Z.; Kathmann, S. M.; Slater, B.; Michaelides, A., The microscopic features of  
1753 heterogeneous ice nucleation may affect the macroscopic morphology of atmospheric ice crystals.  
1754 *Faraday Discuss.* **2013**, *167*, 389-403.  
1755 245. Sosso, G. C.; Tribello, G. A.; Zen, A.; Pedevilla, P.; Michaelides, A., Ice formation on kaolinite:  
1756 Insights from molecular dynamics simulations. *J. Chem. Phys.* **2016**, *145* (21), 10.  
1757 246. Liu, J.; Zhu, C.; Liu, K.; Jiang, Y.; Song, Y.; Francisco, J. S.; Cheng, X. C.; Wang, J., Distinct  
1758 ice patterns on solid surfaces with various wettabilities. *Proc. Natl. Acad. Sci. USA* **2017**, Early Edition.  
1759 247. Yan, J. Y.; Overduin, S. D.; Patey, G. N., Understanding electrofreezing in water simulations. *J.*  
1760 *Chem. Phys.* **2014**, *141* (7), 074501.  
1761 248. Yan, J. Y.; Patey, G. N., Ice nucleation by electric surface fields of varying range and geometry.  
1762 *J. Chem. Phys.* **2013**, *139* (14), 144501.  
1763 249. Yan, J. Y.; Patey, G. N., Molecular Dynamics Simulations of Ice Nucleation by Electric Fields.  
1764 *J. Phys. Chem. A* **2012**, *116* (26), 7057-7064.  
1765 250. Yan, J. Y.; Patey, G. N., Heterogeneous Ice Nucleation Induced by Electric Fields. *J. Phys.*  
1766 *Chem. Lett.* **2011**, *2* (20), 2555-2559.  
1767 251. Pedevilla, P.; Cox, S. J.; Slater, B.; Michaelides, A., Can Ice-Like Structures Form on Non-Ice-  
1768 Like Substrates? The Example of the K-feldspar Microcline. *J. Phys. Chem. C* **2016**, *120* (12), 6704-  
1769 6713.  
1770 252. Fitzner, M.; Sosso, G. C.; Cox, S. J.; Michaelides, A., The Many Faces of Heterogeneous Ice  
1771 Nucleation: Interplay Between Surface Morphology and Hydrophobicity. *J. Am. Chem. Soc.* **2015**, *137*  
1772 (42), 13658-13669.  
1773 253. Cox, S. J.; Kathmann, S. M.; Purton, J. A.; Gillan, M. J.; Michaelides, A., Non-hexagonal ice at  
1774 hexagonal surfaces: the role of lattice mismatch. *Phys. Chem. Chem. Phys.* **2012**, *14* (22), 7944-7949.  
1775 254. Fitzner, M.; Sosso, G. C.; Pietrucci, F.; Pipolo, S.; Michaelides, A., Pre-critical fluctuations and  
1776 what they disclose about heterogeneous crystal nucleation. *Nat. Commun.* **2017**, *8*, 2257.  
1777 255. Lupi, L.; Peters, B.; Molinero, V., Pre-ordering of interfacial water in the pathway of  
1778 heterogeneous ice nucleation does not lead to a two-step crystallization mechanism. *J. Chem. Phys.*  
1779 **2016**, *145* (21), 10.  
1780 256. Lupi, L.; Kastelowitz, N.; Molinero, V., Vapor deposition of water on graphitic surfaces:  
1781 Formation of amorphous ice, bilayer ice, ice I, and liquid water. *J. Chem. Phys.* **2014**, *141* (18), 11.  
1782 257. Lupi, L.; Molinero, V., Does Hydrophilicity of Carbon Particles Improve Their Ice Nucleation  
1783 Ability? *J. Phys. Chem. A* **2014**, *118* (35), 7330-7337.  
1784 258. Lupi, L.; Hudait, A.; Molinero, V., Heterogeneous Nucleation of Ice on Carbon Surfaces. *J. Am.*  
1785 *Chem. Soc.* **2014**, *136* (8), 3156-3164.  
1786 259. Cabriolu, R.; Li, T. S., Ice nucleation on carbon surface supports the classical theory for  
1787 heterogeneous nucleation. *Phys. Rev. E* **2015**, *91* (5), 052402.  
1788 260. Dymarska, M.; Murray, B. J.; Sun, L. M.; Eastwood, M. L.; Knopf, D. A.; Bertram, A. K.,  
1789 Deposition ice nucleation on soot at temperatures relevant for the lower troposphere. *J. Geophys. Res.*  
1790 **2006**, *111* (D4), D04204.  
1791 261. Pedevilla, P.; Fitzner, M.; Michaelides, A., What makes a good descriptor for heterogeneous ice  
1792 nucleation on OH-patterned surfaces. *Phys. Rev. B* **2017**, *96* (11), 115441.  
1793 262. Seeley, L. H.; Seidler, G. T., Two-dimensional nucleation of ice from supercooled water. *Phys.*  
1794 *Rev. Lett.* **2001**, *8705* (5), 055702.  
1795 263. Seeley, L. H.; Seidler, G. T., Preactivation in the nucleation of ice by Langmuir films of  
1796 aliphatic alcohols. *J. Chem. Phys.* **2001**, *114* (23), 10464-10470.

- 1797 264. Qiu, Y. Q.; Odendahl, N.; Hudait, A.; Mason, R.; Bertram, A. K.; Paesani, F.; DeMott, P. J.;  
1798 Molinero, V., Ice Nucleation Efficiency of Hydroxylated Organic Surfaces Is Controlled by Their  
1799 Structural Fluctuations and Mismatch to Ice. *J. Am. Chem. Soc.* **2017**, *139* (8), 3052-3064.
- 1800 265. Zou, A.; Chanana, A.; Agrawal, A.; Wayner, P. C.; Maroo, S. C., Steady State Vapor Bubble in  
51801 Pool Boiling. *Sci. Rep.* **2016**, *6*, 20240.
- 61802 266. Sear, R. P., Nucleation at contact lines where fluid-fluid interfaces meet solid surfaces. *J. Phys.-*  
71803 *Condes. Matter* **2007**, *19* (46), 466106.
- 81804 267. Yang, F.; Shaw, R. A.; Gurganus, C. W.; Chong, S. K.; Yap, Y. K., Ice nucleation at the contact  
91805 line triggered by transient electrowetting fields. *Appl. Phys. Lett.* **2015**, *107* (26), 264101.
- 101806 268. Gurganus, C. W.; Charnawskas, J. C.; Kostinski, A. B.; Shaw, R. A., Nucleation at the Contact  
111807 Line Observed on Nanotextured Surfaces. *Phys. Rev. Lett.* **2014**, *113* (23), 235701.
- 121808 269. Gurganus, C.; Kostinski, A. B.; Shaw, R. A., High-Speed Imaging of Freezing Drops: Still No  
131809 Preference for the Contact Line. *J. Phys. Chem. C* **2013**, *117* (12), 6195-6200.
- 141810 270. Gurganus, C.; Kostinski, A. B.; Shaw, R. A., Fast Imaging of Freezing Drops: No Preference for  
151811 Nucleation at the Contact Line. *J. Phys. Chem. Letters* **2011**, *2* (12), 1449-1454.
- 161812 271. Pandey, R.; Usui, K.; Livingstone, R. A.; Fischer, S. A.; Pfaendtner, J.; Backus, E. H. G.;  
171813 Nagata, Y.; Fröhlich-Nowoisky, J.; Schmuser, L.; Mauri, S.; Scheel, J. F.; Knopf, D. A.; Pöschl, U.;  
201814 Bonn, M.; Weidner, T., Ice-nucleating bacteria control the order and dynamics of interfacial water. *Sci. Adv.* **2016**, *2* (4), e1501630.
- 211815 272. Djikaev, Y. S.; Ruckenstein, E., Thermodynamics of Heterogeneous Crystal Nucleation in  
221817 Contact and Immersion Modes. *J. Phys. Chem. A* **2008**, *112* (46), 11677-11687.
- 231818 273. Fu, Q. T.; Liu, E. J.; Wilson, P.; Chen, Z., Ice nucleation behaviour on sol-gel coatings with  
241819 different surface energy and roughness. *Phys. Chem. Chem. Phys.* **2015**, *17* (33), 21492-21500.
- 251820 274. Carvalho, J. L.; Dalnoki-Veress, K., Homogeneous Bulk, Surface, and Edge Nucleation in  
261821 Crystalline Nanodroplets. *Phys. Rev. Lett.* **2010**, *105* (23), 237801.
- 271822 275. Abdelmonem, A.; Backus, E. H. G.; Hoffmann, N.; Sanchez, M. A.; Cyran, J. D.; Kiselev, A.;  
281823 Bonn, M., Surface-charge-induced orientation of interfacial water suppresses heterogeneous ice  
291824 nucleation on alpha-alumina (0001). *Atmos. Chem. Phys.* **2017**, *17* (12), 7827-7837.
- 301825 276. Abdelmonem, A.; Lutzenkirchen, J.; Leisner, T., Probing ice-nucleation processes on the  
311826 molecular level using second harmonic generation spectroscopy. *Atmos. Meas. Tech.* **2015**, *8* (8), 3519-  
321827 3526.
- 331828 277. DeMott, P. J.; Prenni, A. J.; Liu, X.; Kreidenweis, S. M.; Petters, M. D.; Twohy, C. H.;  
341829 Richardson, M. S.; Eidhammer, T.; Rogers, D. C., Predicting global atmospheric ice nuclei distributions  
351830 and their impacts on climate. *P. Natl. Acad. Sci. USA* **2010**, *107* (25), 11217-11222.
- 361831 278. DeMott, P. J.; Cziczo, D. J.; Prenni, A. J.; Murphy, D. M.; Kreidenweis, S. M.; Thomson, D. S.;  
371832 Borys, R.; Rogers, D. C., Measurements of the concentration and composition of nuclei for cirrus  
381833 formation. *P. Natl. Acad. Sci. USA* **2003**, *100* (25), 14655-14660.
- 391834 279. DeMott, P. J.; Hill, T. C. J.; McCluskey, C. S.; Prather, K. A.; Collins, D. B.; Sullivan, R. C.;  
401835 Ruppel, M. J.; Mason, R. H.; Irish, V. E.; Lee, T.; Hwang, C. Y.; Rhee, T. S.; Snider, J. R.; McMeeking,  
411836 G. R.; Dhaniyala, S.; Lewis, E. R.; Wentzell, J. J. B.; Abbatt, J.; Lee, C.; Sultana, C. M.; Ault, A. P.;  
421837 Axson, J. L.; Diaz Martinez, M.; Venero, I.; Santos-Figueroa, G.; Stokes, M. D.; Deane, G. B.; Mayol-  
431838 Bracero, O. L.; Grassian, V. H.; Bertram, T. H.; Bertram, A. K.; Moffett, B. F.; Franc, G. D., Sea spray  
441839 aerosol as a unique source of ice nucleating particles. *P. Natl. Acad. Sci.* **2016**, *113* (21), 5797-5803.
- 451840 280. Schrod, J.; Weber, D.; Drücke, J.; Keleshis, C.; Pikridas, M.; Ebert, M.; Cvetković, B.;  
461841 Nickovic, S.; Marinou, E.; Baars, H.; Ansmann, A.; Vrekoussis, M.; Mihalopoulos, N.; Sciare, J.;  
471842 Curtius, J.; Bingemer, H. G., Ice nucleating particles over the Eastern Mediterranean measured by  
481843 unmanned aircraft systems. *Atmos. Chem. Phys.* **2017**, *17* (7), 4817-4835.
- 491844 281. DeMott, P. J.; Hill, T. C. J.; Petters, M. D.; Bertram, A. K.; Tobo, Y.; Mason, R. H.; Suski, K. J.;  
501845 McCluskey, C. S.; Levin, E. J. T.; Schill, G. P.; Boose, Y.; Rauker, A. M.; Miller, A. J.; Zaragoza, J.;  
511846 Rocci, K.; Rothfuss, N. E.; Taylor, H. P.; Hader, J. D.; Chou, C.; Huffman, J. A.; Pöschl, U.; Prenni, A.  
521847 J.; Kreidenweis, S. M., Comparative measurements of ambient atmospheric concentrations of ice

- 1848 nucleating particles using multiple immersion freezing methods and a continuous flow diffusion  
1849 chamber. *Atmos. Chem. Phys.* **2017**, *17* (18), 11227-11245.
- 1850 282. Conen, F.; Eckhardt, S.; Gundersen, H.; Stohl, A.; Yttri, K. E., Rainfall drives atmospheric ice-  
1851 nucleating particles in the coastal climate of southern Norway. *Atmos. Chem. Phys.* **2017**, *17* (18),  
1852 11065-11073.
- 1853 283. Belosi, F.; Rinaldi, M.; Decesari, S.; Tarozzi, L.; Nicosia, A.; Santachiara, G., Ground level ice  
1854 nuclei particle measurements including Saharan dust events at a Po Valley rural site (San Pietro  
1855 Capofiume, Italy). *Atmos. Res.* **2017**, *186*, 116-126.
- 1856 284. Jiang, H.; Yin, Y.; Wang, X.; Gao, R.; Yuan, L.; Chen, K.; Shan, Y., The measurement and  
1857 parameterization of ice nucleating particles in different backgrounds of China. *Atmos. Res.* **2016**, *181*,  
1858 72-80.
- 1859 285. Yin, J.; Wang, D.; Zhai, G., An Evaluation of Ice Nuclei Characteristics from the Long-term  
1860 Measurement Data over North China. *Asia-Pac. J. Atmos. Sci.* **2012**, *48* (2), 197-204.
- 1861 286. Twohy, C. H.; Poellot, M. R., Chemical characteristics of ice residual nuclei in anvil cirrus  
1862 clouds: evidence for homogeneous and heterogeneous ice formation. *Atmos. Chem. Phys.* **2005**, *5*, 2289-  
1863 2297.
- 1864 287. Baustian, K. J.; Cziczo, D. J.; Wise, M. E.; Pratt, K. A.; Kulkarni, G.; Hallar, A. G.; Tolbert, M.  
1865 A., Importance of aerosol composition, mixing state, and morphology for heterogeneous ice nucleation:  
21866 A combined field and laboratory approach. *J. Geophys. Res.* **2012**, *117*, D06217.
- 1867 288. Hiranuma, N.; Brooks, S. D.; Moffet, R. C.; Glen, A.; Laskin, A.; Gilles, M. K.; Liu, P.;  
1868 Macdonald, A. M.; Strapp, J. W.; McFarquhar, G. M., Chemical characterization of individual particles  
1869 and residuals of cloud droplets and ice crystals collected on board research aircraft in the ISDAC 2008  
1870 study. *J. Geophys. Res.* **2013**, *118* (12), 6564-6579.
- 1871 289. Chen, Y. L.; Kreidenweis, S. M.; McInnes, L. M.; Rogers, D. C.; DeMott, P. J., Single particle  
1872 analyses of ice nucleating aerosols in the upper troposphere and lower stratosphere. *Geophys. Res. Lett.*  
1873 **1998**, *25* (9), 1391-1394.
- 1874 290. Froyd, K. D.; Murphy, D. M.; Lawson, P.; Baumgardner, D.; Herman, R. L., Aerosols that form  
1875 subvisible cirrus at the tropical tropopause. *Atmos. Chem. Phys.* **2010**, *10* (1), 209-218.
- 1876 291. Cziczo, D. J.; Froyd, K. D., Sampling the composition of cirrus ice residuals. *Atmos. Res.* **2014**,  
1877 *142*, 15-31.
- 1878 292. McCluskey, C. S.; DeMott, P. J.; Prenni, A. J.; Levin, E. J. T.; McMeeking, G. R.; Sullivan, A.  
1879 P.; Hill, T. C. J.; Nakao, S.; Carrico, C. M.; Kreidenweis, S. M., Characteristics of atmospheric ice  
1880 nucleating particles associated with biomass burning in the US: Prescribed burns and wildfires. *J.  
1881 Geophys. Res.* **2014**, *119* (17), 10458-10470.
- 1882 293. Pratt, K. A.; DeMott, P. J.; French, J. R.; Wang, Z.; Westphal, D. L.; Heymsfield, A. J.; Twohy,  
1883 C. H.; Prenni, A. J.; Prather, K. A., In situ detection of biological particles in cloud ice-crystals. *Nat.  
1884 Geosci.* **2009**, *2* (6), 397-400.
- 1885 294. Pratt, K. A.; Murphy, S. M.; Subramanian, R.; DeMott, P. J.; Kok, G. L.; Campos, T.; Rogers,  
1886 D. C.; Prenni, A. J.; Heymsfield, A. J.; Seinfeld, J. H.; Prather, K. A., Flight-based chemical  
1887 characterization of biomass burning aerosols within two prescribed burn smoke plumes. *Atmos. Chem.  
1888 Phys.* **2011**, *11* (24), 12549-12565.
- 1889 295. Prenni, A. J.; DeMott, P. J.; Sullivan, A. P.; Sullivan, R. C.; Kreidenweis, S. M.; Rogers, D. C.,  
1890 Biomass burning as a potential source for atmospheric ice nuclei: Western wildfires and prescribed  
1891 burns. *Geophys. Res. Lett.* **2012**, *39*, L11805.
- 1892 296. Prenni, A. J.; Petters, M. D.; Kreidenweis, S. M.; Heald, C. L.; Martin, S. T.; Artaxo, P.;  
1893 Garland, R. M.; Wollny, A. G.; Pöschl, U., Relative roles of biogenic emissions and Saharan dust as ice  
1894 nuclei in the Amazon basin. *Nat. Geosci.* **2009**, *2* (6), 401-404.
- 1895 297. Prenni, A. J.; Demott, P. J.; Rogers, D. C.; Kreidenweis, S. M.; McFarquhar, G. M.; Zhang, G.;  
1896 Poellot, M. R., Ice nuclei characteristics from M-PACE and their relation to ice formation in clouds.  
1897 *Tellus B* **2009**, *61* (2), 436-448.

- 1898 298. Rogers, D. C.; DeMott, P. J.; Kreidenweis, S. M., Airborne measurements of tropospheric ice-  
1899 nucleating aerosol particles in the Arctic spring. *J. Geophys. Res.* **2001**, *106* (D14), 15053-15063.  
1900 299. Schmidt, S.; Schneider, J.; Klimach, T.; Mertes, S.; Schenk, L. P.; Kupiszewski, P.; Curtius, J.;  
1901 Borrman, S., Online single particle analysis of ice particle residuals from mountain-top mixed-phase  
1902 clouds using laboratory derived particle type assignment. *Atmos. Chem. Phys.* **2017**, *17* (1), 575-594.  
1903 300. Ebert, M.; Worringen, A.; Benker, N.; Mertes, S.; Weingartner, E.; Weinbruch, S., Chemical  
1904 composition and mixing-state of ice residuals sampled within mixed phase clouds. *Atmos. Chem. Phys.*  
1905 **2011**, *11* (6), 2805-2816.  
1906 301. Worringen, A.; Kandler, K.; Benker, N.; Dirsch, T.; Mertes, S.; Schenk, L.; Kastner, U.; Frank,  
1907 F.; Nillius, B.; Bundke, U.; Rose, D.; Curtius, J.; Kupiszewski, P.; Weingartner, E.; Vochezer, P.;  
1908 Schneider, J.; Schmidt, S.; Weinbruch, S.; Ebert, M., Single-particle characterization of ice-nucleating  
1909 particles and ice particle residuals sampled by three different techniques. *Atmos. Chem. Phys.* **2015**, *15*  
1910 (8), 4161-4178.  
1911 302. Kupiszewski, P.; Zanatta, M.; Mertes, S.; Vochezer, P.; Lloyd, G.; Schneider, J.; Schenk, L.;  
1912 Schnaiter, M.; Baltensperger, U.; Weingartner, E.; Gysel, M., Ice residual properties in mixed-phase  
1913 clouds at the high-alpine Jungfraujoch site. *J. Geophys. Res.* **2016**, *121* (20), 12343-12362.  
1914 303. Corbin, J. C.; Rehbein, P. J. G.; Evans, G. J.; Abbatt, J. P. D., Combustion particles as ice nuclei  
1915 in an urban environment: Evidence from single-particle mass spectrometry. *Atmos. Environ.* **2012**, *51*,  
21916 286-292.  
1917 304. Froyd, K. D.; Murphy, S. M.; Murphy, D. M.; de Gouw, J. A.; Eddingsaas, N. C.; Wennberg, P.  
1918 O., Contribution of isoprene-derived organosulfates to free tropospheric aerosol mass. *P. Natl. Acad.*  
1919 *Sci. USA* **2010**, *107* (50), 21360-21365.  
1920 305. Surratt, J. D.; Chan, A. W. H.; Eddingsaas, N. C.; Chan, M.; Loza, C. L.; Kwan, A. J.; Hersey, S.  
1921 P.; Flagan, R. C.; Wennberg, P. O.; Seinfeld, J. H., Reactive intermediates revealed in secondary  
1922 organic aerosol formation from isoprene. *P. Natl. Acad. Sci. USA* **2010**, *107* (15), 6640-6645.  
1923 306. Claeys, M., Comment on "Unexpected Epoxide Formation in the Gas-Phase Photooxidation of  
1924 Isoprene". *Science* **2010**, *327* (5966), 644-645.  
1925 307. Paulot, F.; Crounse, J. D.; Kjaergaard, H. G.; Kuerten, A.; St Clair, J. M.; Seinfeld, J. H.;  
1926 Wennberg, P. O., Unexpected Epoxide Formation in the Gas-Phase Photooxidation of Isoprene. *Science*  
1927 **2009**, *325* (5941), 730-733.  
1928 308. Molina, L. T.; Madronich, S.; Gaffney, J. S.; Apel, E.; de Foy, B.; Fast, J.; Ferrare, R.; Herndon,  
1929 S.; Jimenez, J. L.; Lamb, B.; Osornio-Vargas, A. R.; Russell, P.; Schauer, J. J.; Stevens, P. S.;  
1930 Volkamer, R.; Zavala, M., An overview of the MILAGRO 2006 Campaign: Mexico City emissions and  
1931 their transport and transformation. *Atmos. Chem. Phys.* **2010**, *10* (18), 8697-8760.  
1932 309. Ryerson, T. B.; Andrews, A. E.; Angevine, W. M.; Bates, T. S.; Brock, C. A.; Cairns, B.; Cohen,  
1933 R. C.; Cooper, O. R.; de Gouw, J. A.; Fehsenfeld, F. C.; Ferrare, R. A.; Fischer, M. L.; Flagan, R. C.;  
1934 Goldstein, A. H.; Hair, J. W.; Hardesty, R. M.; Hostetler, C. A.; Jimenez, J. L.; Langford, A. O.;  
1935 McCauley, E.; McKeen, S. A.; Molina, L. T.; Nenes, A.; Oltmans, S. J.; Parrish, D. D.; Pederson, J. R.;  
1936 Pierce, R. B.; Prather, K.; Quinn, P. K.; Seinfeld, J. H.; Senff, C. J.; Sorooshian, A.; Stutz, J.; Surratt, J.  
1937 D.; Trainer, M.; Volkamer, R.; Williams, E. J.; Wofsy, S. C., The 2010 California Research at the  
1938 Nexus of Air Quality and Climate Change (CalNex) field study. *J. Geophys. Res.* **2013**, *118* (11), 5830-  
1939 5866.  
1940 310. Rogers, D. C., Measurements of natural ice nuclei with a continuous flow diffusion chamber.  
1941 *Atmos. Res.* **1993**, *29* (3-4), 209-228.  
1942 311. Aiken, A. C.; McMeeking, G. R.; Levin, E. J. T.; Dubey, M. K.; DeMott, P. J.; Kreidenweis, S.  
1943 M., Quantification of online removal of refractory black carbon using laser-induced incandescence in  
1944 the single particle soot photometer. *Aerosol Sci. Technol.* **2016**, *50* (7), 679-692.  
1945 312. Levin, E. J. T.; McMeeking, G. R.; DeMott, P. J.; McCluskey, C. S.; Stockwell, C. E.; Yokelson,  
1946 R. J.; Kreidenweis, S. M., A New Method to Determine the Number Concentrations of Refractory Black  
1947 Carbon Ice Nucleating Particles. *Aerosol Sci. Technol.* **2014**, *48* (12), 1264-1275.

- 1948 313. McFarquhar, G. M.; Ghan, S.; Verlinde, J.; Korolev, A.; Strapp, J. W.; Schmid, B.; Tomlinson,  
1949 J. M.; Wolde, M.; Brooks, S. D.; Cziczo, D.; Dubey, M. K.; Fan, J. W.; Flynn, C.; Gultepe, I.; Hubbe,  
1950 J.; Gilles, M. K.; Laskin, A.; Lawson, P.; Leaitch, W. R.; Liu, P.; Liu, X. H.; Lubin, D.; Mazzoleni, C.;  
1951 Macdonald, A. M.; Moffet, R. C.; Morrison, H.; Ovchinnikov, M.; Shupe, M. D.; Turner, D. D.; Xie, S.  
1952 C.; Zelenyuk, A.; Bae, K.; Freer, M.; Glen, A., Indirect and Semi-Direct Aerosol Campaign: The Impact  
61953 of Arctic Aerosols on Clouds. *Bull. Amer. Meteorol. Soc.* **2011**, 92 (2), 183-201.
- 1954 314. Zaveri, R. A.; Shaw, W. J.; Cziczo, D. J.; Schmid, B.; Ferrare, R. A.; Alexander, M. L.;  
1955 Alexandrov, M.; Alvarez, R. J.; Arnott, W. P.; Atkinson, D. B.; Baidar, S.; Banta, R. M.; Barnard, J. C.;  
1956 Beranek, J.; Berg, L. K.; Brechtel, F.; Brewer, W. A.; Cahill, J. F.; Cairns, B.; Cappa, C. D.; Chand, D.;  
1957 China, S.; Comstock, J. M.; Dubey, M. K.; Easter, R. C.; Erickson, M. H.; Fast, J. D.; Floerchinger, C.;  
1958 Flowers, B. A.; Fortner, E.; Gaffney, J. S.; Gilles, M. K.; Gorkowski, K.; Gustafson, W. I.; Gyawali, M.;  
1959 Hair, J.; Hardesty, R. M.; Harworth, J. W.; Herndon, S.; Hiranuma, N.; Hostetler, C.; Hubbe, J. M.;  
1960 Jayne, J. T.; Jeong, H.; Jobson, B. T.; Kassianov, E. I.; Kleinman, L. I.; Kluzek, C.; Knighton, B.;  
1961 Kolesar, K. R.; Kuang, C.; Kubatova, A.; Langford, A. O.; Laskin, A.; Laulainen, N.; Marchbanks, R.  
1962 D.; Mazzoleni, C.; Mei, F.; Moffet, R. C.; Nelson, D.; Obland, M. D.; Oetjen, H.; Onasch, T. B.; Ortega,  
1963 I.; Ottaviani, M.; Pekour, M.; Prather, K. A.; Radney, J. G.; Rogers, R. R.; Sandberg, S. P.; Sedlacek,  
1964 A.; Senff, C. J.; Senum, G.; Setyan, A.; Shilling, J. E.; Shrivastava, M.; Song, C.; Springston, S. R.;  
2065 Subramanian, R.; Suski, K.; Tomlinson, J.; Volkamer, R.; Wallace, H. W.; Wang, J.; Weickmann, A.  
21966 M.; Worsnop, D. R.; Yu, X. Y.; Zelenyuk, A.; Zhang, Q., Overview of the 2010 Carbonaceous Aerosols  
24967 and Radiative Effects Study (CARES). *Atmos. Chem. Phys.* **2012**, 12 (16), 7647-7687.
- 23968 315. Mason, R. H.; Si, M.; Li, J.; Chou, C.; Dickie, R.; Toom-Sauntry, D.; Pöhlker, C.; Yakobi-  
24969 Hancock, J. D.; Ladino, L. A.; Jones, K.; Leaitch, W. R.; Schiller, C. L.; Abbatt, J. P. D.; Huffman, J.  
25970 A.; Bertram, A. K., Ice nucleating particles at a coastal marine boundary layer site: correlations with  
27971 aerosol type and meteorological conditions. *Atmos. Chem. Phys.* **2015**, 15 (21), 12547-12566.
- 28972 316. Mason, R. H.; Chou, C.; McCluskey, C. S.; Levin, E. J. T.; Schiller, C. L.; Hill, T. C. J.;  
29973 Huffman, J. A.; DeMott, P. J.; Bertram, A. K., The micro-orifice uniform deposit impactor-droplet  
30974 freezing technique (MOUDI-DFT) for measuring concentrations of ice nucleating particles as a function  
31975 of size: improvements and initial validation. *Atmos. Meas. Tech.* **2015**, 8 (6), 2449-2462.
- 32976 317. Mason, R. H.; Si, M.; Chou, C.; Irish, V. E.; Dickie, R.; Elizondo, P.; Wong, R.; Brintnell, M.;  
33977 Elsasser, M.; Lassar, W. M.; Pierce, K. M.; Leaitch, W. R.; MacDonald, A. M.; Platt, A.; Toom-  
34978 Sauntry, D.; Sarda-Esteve, R.; Schiller, C. L.; Suski, K. J.; Hill, T. C. J.; Abbatt, J. P. D.; Huffman, J.  
35979 A.; DeMott, P. J.; Bertram, A. K., Size-resolved measurements of ice-nucleating particles at six  
36980 locations in North America and one in Europe. *Atmos. Chem. Phys.* **2016**, 16 (3), 1637-1651.
- 37981 318. Jiang, H.; Yin, Y.; Su, H.; Shan, Y. P.; Gao, R. J., The characteristics of atmospheric ice nuclei  
38982 measured at the top of Huangshan (the Yellow Mountains) in Southeast China using a newly built static  
39983 vacuum water vapor diffusion chamber. *Atmos. Res.* **2015**, 153, 200-208.
- 40984 319. Jiang, H.; Yin, Y.; Yang, L.; Yang, S. Z.; Su, H.; Chen, K., The Characteristics of Atmospheric  
41985 Ice Nuclei Measured at Different Altitudes in the Huangshan Mountains in Southeast China. *Adv.  
44986 Atmos. Sci.* **2014**, 31 (2), 396-406.
- 45987 320. Rinaldi, M.; Santachiara, G.; Nicosia, A.; Piazza, M.; Decesari, S.; Gilardoni, S.; Paglione, M.;  
46988 Cristofanelli, P.; Marinoni, A.; Bonasoni, P.; Belosi, F., Atmospheric Ice Nucleating Particle  
47989 measurements at the high mountain observatory Mt. Cimone (2165 m a.s.l., Italy). *Atmos. Env.* **2017**,  
48990 accepted.
- 49991 321. Möhler, O.; Benz, S.; Saathoff, H.; Schnaiter, M.; Wagner, R.; Schneider, J.; Walter, S.; Ebert,  
50992 V.; Wagner, S., The effect of organic coating on the heterogeneous ice nucleation efficiency of mineral  
51993 dust aerosols. *Environ. Res. Lett.* **2008**, 3 (2), 025007.
- 52994 322. Murray, B. J.; Wilson, T. W.; Dobbie, S.; Cui, Z. Q.; Al-Jumur, S. M. R. K.; Möhler, O.;  
53995 Schnaiter, M.; Wagner, R.; Benz, S.; Niemand, M.; Saathoff, H.; Ebert, V.; Wagner, S.; Kärcher, B.,  
54996 Heterogeneous nucleation of ice particles on glassy aerosols under cirrus conditions. *Nat. Geosci.* **2010**,  
55997 3 (4), 233-237.

- 1998 323. Baustian, K. J.; Wise, M. E.; Jensen, E. J.; Schill, G. P.; Freedman, M. A.; Tolbert, M. A., State  
1999 transformations and ice nucleation in amorphous (semi-)solid organic aerosol. *Atmos. Chem. Phys.*  
2000 **2013**, 13 (11), 5615-5628.  
2001 324. Schill, G. P.; Tolbert, M. A., Heterogeneous ice nucleation on phase-separated organic-sulfate  
2002 particles: effect of liquid vs. glassy coatings. *Atmos. Chem. Phys.* **2013**, 13 (9), 4681-4695.  
2003 325. Schill, G. P.; De Haan, D. O.; Tolbert, M. A., Heterogeneous Ice Nucleation on Simulated  
2004 Secondary Organic Aerosol. *Environ. Sci. Technol.* **2014**, 48 (3), 1675-1682.  
2005 326. Ladino, L. A.; Zhou, S.; Yakobi-Hancock, J. D.; Aljawahary, D.; Abbatt, J. P. D., Factors  
2006 controlling the ice nucleating abilities of alpha-pinene SOA particles. *J. Geophys. Res.* **2014**, 119 (14),  
2007 9041-9051.  
2008 327. Ignatius, K.; Kristensen, T. B.; Jarvinen, E.; Nichman, L.; Fuchs, C.; Gordon, H.; Herenz, P.;  
2009 Hoyle, C. R.; Duplissy, J.; Garimella, S.; Dias, A.; Frege, C.; Hoppel, N.; Troestl, J.; Wagner, R.; Yan,  
2010 C.; Amorim, A.; Baltensperger, U.; Curtius, J.; Donahue, N. M.; Gallagher, M. W.; Kirkby, J.; Kulmala,  
2011 M.; Möhler, O.; Saathoff, H.; Schnaiter, M.; Tome, A.; Virtanen, A.; Worsnop, D.; Stratmann, F.,  
2012 Heterogeneous ice nucleation of viscous secondary organic aerosol produced from ozonolysis of  $\alpha$ -  
2013 pinene. *Atmos. Chem. Phys.* **2016**, 16 (10), 6495-6509.  
2014 328. Alpert, P. A.; Knopf, D. A., Analysis of isothermal and cooling-rate-dependent immersion  
2015 freezing by a unifying stochastic ice nucleation model. *Atmos. Chem. Phys.* **2016**, 16 (4), 2083-2107.  
2016 329. Riechers, B.; Wittbracht, F.; Hutten, A.; Koop, T., The homogeneous ice nucleation rate of water  
2017 droplets produced in a microfluidic device and the role of temperature uncertainty. *Phys. Chem. Chem.  
2018 Phys.* **2013**, 15 (16), 5873-5887.  
2019 330. Hiranuma, N.; Augustin-Bauditz, S.; Bingemer, H.; Budke, C.; Curtius, J.; Danielczok, A.;  
2020 Diehl, K.; Dreischmeier, K.; Ebert, M.; Frank, F.; Hoffmann, N.; Kandler, K.; Kiselev, A.; Koop, T.;  
2021 Leisner, T.; Möhler, O.; Nillius, B.; Peckhaus, A.; Rose, D.; Weinbruch, S.; Wex, H.; Boose, Y.;  
2022 DeMott, P. J.; Hader, J. D.; Hill, T. C. J.; Kanji, Z. A.; Kulkarni, G.; Levin, E. J. T.; McCluskey, C. S.;  
2023 Murakami, M.; Murray, B. J.; Niedermeier, D.; Petters, M. D.; O'Sullivan, D.; Saito, A.; Schill, G. P.;  
2024 Tajiri, T.; Tolbert, M. A.; Welti, A.; Whale, T. F.; Wright, T. P.; Yamashita, K., A comprehensive  
2025 laboratory study on the immersion freezing behavior of illite NX particles: a comparison of 17 ice  
2026 nucleation measurement techniques. *Atmos. Chem. Phys.* **2015**, 15 (5), 2489-2518.  
2027 331. Barahona, D., Thermodynamic derivation of the activation energy for ice nucleation. *Atmos.  
2028 Chem. Phys.* **2015**, 15 (24), 13819-13831.  
2029 332. Barahona, D., Analysis of the effect of water activity on ice formation using a new  
2030 thermodynamic framework. *Atmos. Chem. Phys.* **2014**, 14 (14), 7665-7680.  
2031 333. Barahona, D., On the ice nucleation spectrum. *Atmos. Chem. Phys.* **2012**, 12 (8), 3733-3752.  
2032 334. Lovering, K. A.; Bertram, A. K.; Chou, K. C., Transient Phase of Ice Observed by Sum  
2033 Frequency Generation at the Water/Mineral Interface During Freezing. *J. Phys. Chem. Lett.* **2017**, 8 (4),  
2034 871-875.  
2035 335. Zimmermann, F.; Ebert, M.; Worringen, A.; Schutz, L.; Weinbruch, S., Environmental scanning  
2036 electron microscopy (ESEM) as a new technique to determine the ice nucleation capability of individual  
2037 atmospheric aerosol particles. *Atmos. Environ.* **2007**, 41 (37), 8219-8227.  
2038 336. Magee, N. B.; Miller, A.; Amaral, M.; Cumiskey, A., Mesoscopic surface roughness of ice  
2039 crystals pervasive across a wide range of ice crystal conditions. *Atmos. Chem. Phys.* **2014**, 14 (22),  
2040 12357-12371.  
2041 337. Wilson, T. W.; Ladino, L. A.; Alpert, P. A.; Breckels, M. N.; Brooks, I. M.; Browne, J.;  
2042 Burrows, S. M.; Carslaw, K. S.; Huffman, J. A.; Judd, C.; Kilthau, W. P.; Mason, R. H.; McFiggans, G.;  
2043 Miller, L. A.; Najera, J. J.; Polishchuk, E.; Rae, S.; Schiller, C. L.; Si, M.; Temprado, J. V.; Whale, T.  
2044 F.; Wong, J. P. S.; Wurl, O.; Yakobi-Hancock, J. D.; Abbatt, J. P. D.; Aller, J. Y.; Bertram, A. K.;  
2045 Knopf, D. A.; Murray, B. J., A marine biogenic source of atmospheric ice-nucleating particles. *Nature*  
2046 **2015**, 525 (7568), 234-238.  
2047  
2048  
2049  
2050  
2051  
2052  
2053  
2054  
2055  
2056  
2057  
2058  
2059  
2060

- 2047 338. von Blohn, N.; Mitra, S. K.; Diehl, K.; Borrmann, S., The ice nucleating ability of pollen. Part  
12048 III: New laboratory studies in immersion and contact freezing modes including more pollen types.  
2049 *Atmos. Res.* **2005**, 78 (3), 182-189.
- 42050 339. Tong, H. J.; Ouyang, B.; Nikolovski, N.; Lienhard, D. M.; Pope, F. D.; Kalberer, M., A new  
52051 electrodynamic balance (EDB) design for low-temperature studies: application to immersion freezing of  
62052 pollen extract bioaerosols. *Atmos. Meas. Tech.* **2015**, 8 (3), 1183-1195.
- 72053 340. Pummer, B. G.; Bauer, H.; Bernardi, J.; Bleicher, S.; Grothe, H., Suspendable macromolecules  
82054 are responsible for ice nucleation activity of birch and conifer pollen. *Atmos. Chem. Phys.* **2012**, 12 (5),  
92055 2541-2550.
- 10 341. Hader, J. D.; Wright, T. P.; Petters, M. D., Contribution of pollen to atmospheric ice nuclei  
11 concentrations. *Atmos. Chem. Phys.* **2014**, 14 (11), 5433-5449.
- 12056 342. Augustin, S.; Wex, H.; Niedermeier, D.; Pummer, B.; Grothe, H.; Hartmann, S.; Tomsche, L.;  
12059 Clauss, T.; Voigtländer, J.; Ignatius, K.; Stratmann, F., Immersion freezing of birch pollen washing  
12060 water. *Atmos. Chem. Phys.* **2013**, 13 (21), 10989-11003.
- 16061 343. Augustin-Bauditz, S.; Wex, H.; Denjean, C.; Hartmann, S.; Schneider, J.; Schmidt, S.; Ebert, M.;  
17062 Stratmann, F., Laboratory-generated mixtures of mineral dust particles with biological substances:  
18063 characterization of the particle mixing state and immersion freezing behavior. *Atmos. Chem. Phys.* **2016**,  
19064 16 (9), 5531-5543.
- 22065 344. O'Sullivan, D.; Murray, B. J.; Ross, J. F.; Whale, T. F.; Price, H. C.; Atkinson, J. D.; Umo, N. S.;  
22066 Webb, M. E., The relevance of nanoscale biological fragments for ice nucleation in clouds. *Sci Rep*  
23067 **2015**, 5, 8082.
- 24068 345. Tobo, Y.; DeMott, P. J.; Hill, T. C. J.; Prenni, A. J.; Swoboda-Colberg, N. G.; Franc, G. D.;  
25069 Kreidenweis, S. M., Organic matter matters for ice nuclei of agricultural soil origin. *Atmos. Chem. Phys.*  
26070 **2014**, 14 (16), 8521-8531.
- 28071 346. Steinke, I.; Funk, R.; Busse, J.; Iturri, A.; Kirchen, S.; Leue, M.; Möhler, O.; Schwartz, T.;  
29072 Schnaiter, M.; Sierau, B.; Toprak, E.; Ullrich, R.; Ulrich, A.; Hoose, C.; Leisner, T., Ice nucleation  
30073 activity of agricultural soil dust aerosols from Mongolia, Argentina, and Germany. *J. Geophys. Res.*  
31074 **2016**, 121 (22), 13559-13576.
- 32075 347. O'Sullivan, D.; Murray, B. J.; Malkin, T. L.; Whale, T. F.; Umo, N. S.; Atkinson, J. D.; Price, H.  
33076 C.; Baustian, K. J.; Browne, J.; Webb, M. E., Ice nucleation by fertile soil dusts: relative importance of  
34077 mineral and biogenic components. *Atmos. Chem. Phys.* **2014**, 14 (4), 1853-1867.
- 35078 348. Hill, T. C. J.; DeMott, P. J.; Tobo, Y.; Fröhlich-Nowoisky, J.; Moffett, B. F.; Franc, G. D.;  
36079 Kreidenweis, S. M., Sources of organic ice nucleating particles in soils. *Atmos. Chem. Phys.* **2016**, 16  
37080 (11), 7195-7211.
- 38081 349. Fornea, A. P.; Brooks, S. D.; Dooley, J. B.; Saha, A., Heterogeneous freezing of ice on  
39082 atmospheric aerosols containing ash, soot, and soil. *J. Geophys. Res.* **2009**, 114, D13201.
- 40083 350. Schnell, R. C.; Vali, G., World-wide source of leaf derived freezing nuclei. *Nature* **1973**, 246  
41084 (5430), 212-213.
- 42085 351. Schnell, R. C.; Vali, G., Atmospheric ice nuclei from decomposing vegetation. *Nature* **1972**, 236  
43086 (5343), 163-165.
- 44087 352. Hiranuma, N.; Möhler, O.; Yamashita, K.; Tajiri, T.; Saito, A.; Kiselev, A.; Hoffmann, N.;  
45088 Hoose, C.; Jantsch, E.; Koop, T.; Murakami, M., Ice nucleation by cellulose and its potential  
46089 contribution to ice formation in clouds. *Nat. Geosci.* **2015**, 8 (4), 273-277.
- 47090 353. Du, R.; Ariya, P. A., The test freezing temperature of C(2)-C(6) dicarboxylic acid: The  
48091 important indicator for ice nucleation processes. *Chin. Sci. Bull.* **2008**, 53 (17), 2685-2691.
- 49092 354. Prenni, A. J.; DeMott, P. J.; Kreidenweis, S. M.; Sherman, D. E.; Russell, L. M.; Ming, Y., The  
50093 effects of low molecular weight dicarboxylic acids on cloud formation. *J. Phys. Chem. A* **2001**, 105  
51094 (50), 11240-11248.
- 52095 355. Koop, T.; Zobrist, B., Parameterizations for ice nucleation in biological and atmospheric  
53096 systems. *Phys. Chem. Chem. Phys.* **2009**, 11 (46), 10839-10850.

- 2097 356. Zobrist, B.; Marcolli, C.; Peter, T.; Koop, T., Heterogeneous ice nucleation in aqueous solutions:  
12098 the role of water activity. *J. Phys. Chem. A* **2008**, *112* (17), 3965-3975.  
2099 357. Kanji, Z. A.; Florea, O.; Abbatt, J. P. D., Ice formation via deposition nucleation on mineral dust  
42100 and organics: dependence of onset relative humidity on total particulate surface area. *Environ. Res. Lett.*  
52101 **2008**, *3*, 025004.  
62102 358. Wilson, T. W.; Murray, B. J.; Wagner, R.; Möhler, O.; Saathoff, H.; Schnaiter, M.; Skrotzki, J.;  
72103 Price, H. C.; Malkin, T. L.; Dobbie, S.; Al-Jumur, S. M. R. K., Glassy aerosols with a range of  
82104 compositions nucleate ice heterogeneously at cirrus temperatures. *Atmos. Chem. Phys.* **2012**, *12* (18),  
92105 8611-8632.  
102106 359. Schill, G. P.; Tolbert, M. A., Depositional Ice Nucleation on Monocarboxylic Acids: Effect of  
112107 the O:C Ratio. *J. Phys. Chem. A* **2012**, *116* (25), 6817-6822.  
12108 360. Rigg, Y. J.; Alpert, P. A.; Knopf, D. A., Immersion freezing of water and aqueous ammonium  
13109 sulfate droplets initiated by humic-like substances as a function of water activity. *Atmos. Chem. Phys.*  
14110 **2013**, *13* (13), 6603-6622.  
15111 361. Primm, K. M.; Schill, G. P.; Veghte, D. P.; Freedman, M. A.; Tolbert, M. A., Depositional ice  
16112 nucleation on NX illite and mixtures of NX illite with organic acids. *J. Atmos. Chem.* **2017**, *74* (1), 55-  
17113 69.  
18114 362. Murray, B. J., Inhibition of ice crystallisation in highly viscous aqueous organic acid droplets.  
19115 *Atmos. Chem. Phys.* **2008**, *8* (17), 5423-5433.  
20116 363. Zobrist, B.; Marcolli, C.; Koop, T.; Luo, B. P.; Murphy, D. M.; Lohmann, U.; Zardini, A. A.;  
21117 Krieger, U. K.; Corti, T.; Cziczo, D. J.; Fueglistaler, S.; Hudson, P. K.; Thomson, D. S.; Peter, T.,  
22118 Oxalic acid as a heterogeneous ice nucleus in the upper troposphere and its indirect aerosol effect.  
23119 *Atmos. Chem. Phys.* **2006**, *6*, 3115-3129.  
24120 364. DeMott, P. J.; Petters, M. D.; Prenni, A. J.; Carrico, C. M.; Kreidenweis, S. M.; Collett, J. L.;  
25121 Moosmuller, H., Ice nucleation behavior of biomass combustion particles at cirrus temperatures. *J. Geophys. Res.*  
26122 **2009**, *114*, D16205.  
27123 365. Petters, M. D.; Parsons, M. T.; Prenni, A. J.; DeMott, P. J.; Kreidenweis, S. M.; Carrico, C. M.;  
28124 Sullivan, A. P.; McMeeking, G. R.; Levin, E.; Wold, C. E.; Collett, J. L.; Moosmuller, H., Ice nuclei  
29125 emissions from biomass burning. *J. Geophys. Res.* **2009**, *114*, D07209.  
30126 366. Levin, E. J. T.; McMeeking, G. R.; DeMott, P. J.; McCluskey, C. S.; Carrico, C. M.; Nakao, S.;  
31127 Jayaraman, T.; Stone, E. A.; Stockwell, C. E.; Yokelson, R. J.; Kreidenweis, S. M., Ice-nucleating  
32128 particle emissions from biomass combustion and the potential importance of soot aerosol. *J. Geophys. Res.*  
33129 **2016**, *121* (10), 5888-5903.  
34130 367. Prenni, A. J.; Petters, M. D.; Faulhaber, A.; Carrico, C. M.; Zieman, P. J.; Kreidenweis, S. M.;  
35131 DeMott, P. J., Heterogeneous ice nucleation measurements of secondary organic aerosol generated from  
36132 ozonolysis of alkenes. *Geophys. Res. Lett.* **2009**, *36* (6), L06808.  
37133 368. Wagner, R.; Hohler, K.; Huang, W.; Kiselev, A.; Möhler, O.; Mohr, C.; Pajunoja, A.; Saathoff,  
38134 H.; Schiebel, T.; Shen, X. L.; Virtanen, A., Heterogeneous ice nucleation of  $\alpha$ -pinene SOA particles  
39135 before and after ice cloud processing. *J. Geophys. Res.-Atmos.* **2017**, *122* (9), 4924-4943.  
40136 369. Gao, S.; Ng, N. L.; Keywood, M.; Varutbangkul, V.; Bahreini, R.; Nenes, A.; He, J. W.; Yoo, K.  
41137 Y.; Beauchamp, J. L.; Hodyss, R. P.; Flagan, R. C.; Seinfeld, J. H., Particle phase acidity and oligomer  
42138 formation in secondary organic aerosol. *Environ. Sci. Technol.* **2004**, *38* (24), 6582-6589.  
43139 370. Tolocka, M. P.; Jang, M.; Ginter, J. M.; Cox, F. J.; Kamens, R. M.; Johnston, M. V., Formation  
44140 of oligomers in secondary organic aerosol. *Environ. Sci. Technol.* **2004**, *38* (5), 1428-1434.  
45141 371. Gruber, E. R.; Rudich, Y., Atmospheric HULIS: How humic-like are they? A comprehensive  
46142 and critical review. *Atmos. Chem. Phys.* **2006**, *6* (3), 729-753.  
47143 372. Kanji, Z. A.; Florea, O.; Abbatt, J. P. D., Ice formation via deposition nucleation on mineral dust  
48144 and organics: dependence of onset relative humidity on total particulate surface area. *Environ. Res. Lett.*  
49145 **2008**, *3* (2), 025004.  
50146 373. Knopf, D. A.; Alpert, P. A., Water Activity Based Model of Heterogeneous Ice Nucleation  
51147 Kinetics for Freezing of Water and Aqueous Solution Droplets. *Farad. Disc.* **2013**, *165*, 513-534.

- 2148 374. Rudich, Y.; Donahue, N. M.; Mentel, T. F., Aging of organic aerosol: Bridging the gap between  
2149 laboratory and field studies. *Annu. Rev. Phys. Chem.* **2007**, *58*, 321-352.  
2150 375. Rudich, Y., Laboratory perspectives on the chemical transformations of organic matter in  
2151 atmospheric particles. *Chem. Rev.* **2003**, *103* (12), 5097-5124.  
2152 376. Taraniuk, I.; Rudich, Y.; Gruber, E. R., Hydration-Influenced Sorption of Organic Compounds  
2153 by Model and Atmospheric Humic-Like Substances (HULIS). *Environ. Sci. Technol.* **2009**, *43* (6),  
2154 1811-1817.  
2155 377. Slade, J. H.; Shiraiwa, M.; Arangio, A.; Su, H.; Pöschl, U.; Wang, J.; Knopf, D. A., Cloud  
2156 droplet activation through oxidation of organic aerosol influenced by temperature and particle phase  
2157 state. *Geophys. Res. Lett.* **2017**, *44* (3), 1583-1591.  
2158 378. Augustin, S.; Wex, H.; Niedermeier, D.; Pummer, B.; Grothe, H.; Hartmann, S.; Tomsche, L.;  
2159 Clauss, T.; Voigtlaender, J.; Ignatius, K.; Stratmann, F., Immersion freezing of birch pollen washing  
2160 water. *Atmos. Chem. Phys.* **2013**, *13* (21), 10989-11003.  
2161 379. Fröhlich-Nowoisky, J.; Hill, T. C. J.; Pummer, B. G.; Yordanova, P.; Franc, G. D.; Pöschl, U.,  
2162 Ice nucleation activity in the widespread soil fungus Mortierella alpina. *Biogeosciences* **2015**, *12* (4),  
2163 1057-1071.  
2164 380. Pummer, B. G.; Bauer, H.; Bernardi, J.; Chazallon, B.; Facq, S.; Lendl, B.; Whitmore, K.;  
2165 Grothe, H., Chemistry and morphology of dried-up pollen suspension residues. *J. Raman Spectrosc.*  
2166 **2013**, *44* (12), 1654-1658.  
2167 381. Sicard, M.; Izquierdo, R.; Alarcon, M.; Belmonte, J.; Comeron, A.; Baldasano, J. M., Near-  
2168 surface and columnar measurements with a micro pulse lidar of atmospheric pollen in Barcelona, Spain.  
2169 *Atmos. Chem. Phys.* **2016**, *16* (11), 6805-6821.  
2170 382. Yttri, K. E.; Dye, C.; Kiss, G., Ambient aerosol concentrations of sugars and sugar-alcohols at  
2171 four different sites in Norway. *Atmos. Chem. Phys.* **2007**, *7* (16), 4267-4279.  
2172 383. Rathnayake, C. M.; Metwali, N.; Jayaratne, T.; Kettler, J.; Huang, Y. F.; Thorne, P. S.;  
2173 O'Shaughnessy, P. T.; Stone, E. A., Influence of rain on the abundance of bioaerosols in fine and coarse  
2174 particles. *Atmos. Chem. Phys.* **2017**, *17* (3), 2459-2475.  
2175 384. Hawkins, L. N.; Russell, L. M., Polysaccharides, Proteins, and Phytoplankton Fragments: Four  
2176 Chemically Distinct Types of Marine Primary Organic Aerosol Classified by Single Particle  
2177 Spectromicroscopy. *Adv. Meteo.* **2010**, 612132.  
2178 385. Burrows, S. M.; Hoose, C.; Pöschl, U.; Lawrence, M. G., Ice nuclei in marine air: biogenic  
2179 particles or dust? *Atmos. Chem. Phys.* **2013**, *13* (1), 245-267.  
2180 386. Yun, Y. X.; Penner, J. E., An evaluation of the potential radiative forcing and climatic impact of  
2181 marine organic aerosols as heterogeneous ice nuclei. *Geophys. Res. Lett.* **2013**, *40* (15), 4121-4126.  
2182 387. Alpert, P. A.; Aller, J. Y.; Knopf, D. A., Ice nucleation from aqueous NaCl droplets with and  
2183 without marine diatoms. *Atmos. Chem. Phys.* **2011**, *11* (12), 5539-5555.  
2184 388. Alpert, P. A.; Aller, J. Y.; Knopf, D. A., Initiation of the ice phase by marine biogenic surfaces  
2185 in supersaturated gas and supercooled aqueous phases. *Phys. Chem. Chem. Phys.* **2011**, *13* (44), 19882-  
2186 19894.  
2187 389. Knopf, D. A.; Alpert, P. A.; Wang, B.; Aller, J. Y., Stimulation of ice nucleation by marine  
2188 diatoms. *Nature Geosci.* **2011**, *4* (2), 88-90.  
2189 390. Ladino, L. A.; Yakobi-Hancock, J. D.; Kilthau, W. P.; Mason, R. H.; Si, M.; Li, J.; Miller, L. A.;  
2190 Schiller, C. L.; Huffman, J. A.; Aller, J. Y.; Knopf, D. A.; Bertram, A. K.; Abbatt, J. P. D., Addressing  
2191 the ice nucleating abilities of marine aerosol: A combination of deposition mode laboratory and field  
2192 measurements. *Atmos. Environ.* **2016**, *132*, 1-10.  
2193 391. Aller, J. Y.; Radway, J. C.; Kilthau, W. P.; Bothe, D. W.; Wilson, T. W.; Vaillancourt, R. D.;  
2194 Quinn, P. K.; Coffman, D. J.; Murray, B. J.; Knopf, D. A., Size-resolved characterization of the  
2195 polysaccharidic and proteinaceous components of sea spray aerosol. *Atmos. Environ.* **2017**, *154*, 331-  
2196 347.  
2197 392. McCluskey, C. S.; Hill, T. C. J.; Malfatti, F.; Sultana, C. M.; Lee, C.; Santander, M. V.; Beall, C.  
2198 M.; Moore, K. A.; Cornwell, G. C.; Collins, D. B.; Prather, K. A.; Jayaratne, T.; Stone, E. A.; Azam,  
59  
60

- 2199 F.; Kreidenweis, S. M.; DeMott, P. J., A Dynamic Link between Ice Nucleating Particles Released in  
12200 Nascent Sea Spray Aerosol and Oceanic Biological Activity during Two Mesocosm Experiments. *J.  
2201 Atmos. Sci.* **2016**, 74 (1), 151-166.
- 42202 393. Archuleta, C. M.; DeMott, P. J.; Kreidenweis, S. M., Ice nucleation by surrogates for  
52203 atmospheric mineral dust and mineral dust/sulfate particles at cirrus temperatures. *Atmos. Chem. Phys.*  
62204 **2005**, 5 (10), 2617-2634.
- 72205 394. Augustin-Bauditz, S.; Wex, H.; Kanter, S.; Ebert, M.; Niedermeier, D.; Stoltz, F.; Prager, A.;  
82206 Stratmann, F., The immersion mode ice nucleation behavior of mineral dusts: A comparison of different  
92207 pure and surface modified dusts. *Geophys. Res. Lett.* **2014**, 41 (20), 7375-7382.
- 12208 395. Kulkarni, G.; Sanders, C.; Zhang, K.; Liu, X.; Zhao, C., Ice nucleation of bare and sulfuric acid-  
12209 coated mineral dust particles and implication for cloud properties. *J. Geophys. Res.* **2014**, 119 (16),  
12210 9993-10011.
- 12211 396. Kulkarni, G.; Zhang, K.; Zhao, C.; Nandasiri, M.; Shutthanandan, V.; Liu, X.; Fast, J.; Berg, L.,  
12212 Ice formation on nitric acid-coated dust particles: Laboratory and modeling studies. *J. Geophys. Res.*  
12213 **2015**, 120 (15), 7682-7698.
- 12214 397. Reitz, P.; Spindler, C.; Mentel, T. F.; Poulain, L.; Wex, H.; Mildnerberger, K.; Niedermeier, D.;  
12215 Hartmann, S.; Clauss, T.; Stratmann, F.; Sullivan, R. C.; DeMott, P. J.; Petters, M. D.; Sierauf, B.;  
20216 Schneider, J., Surface modification of mineral dust particles by sulphuric acid processing: implications  
22217 for ice nucleation abilities. *Atmos. Chem. Phys.* **2011**, 11 (15), 7839-7858.
- 22218 398. Tobo, Y.; DeMott, P. J.; Raddatz, M.; Niedermeier, D.; Hartmann, S.; Kreidenweis, S. M.;  
22219 Stratmann, F.; Wex, H., Impacts of chemical reactivity on ice nucleation of kaolinite particles: A case  
24220 study of levoglucosan and sulfuric acid. *Geophys. Res. Lett.* **2012**, 39 (19), L19803.
- 22221 399. Wex, H.; DeMott, P. J.; Tobo, Y.; Hartmann, S.; Rösch, M.; Clauss, T.; Tomsche, L.;  
22222 Niedermeier, D.; Stratmann, F., Kaolinite particles as ice nuclei: learning from the use of different  
28223 kaolinite samples and different coatings. *Atmos. Chem. Phys.* **2014**, 14 (11), 5529-5546.
- 29224 400. Tang, M. J.; Cziczo, D. J.; Grassian, V. H., Interactions of Water with Mineral Dust Aerosol:  
30225 Water Adsorption, Hygroscopicity, Cloud Condensation, and Ice Nucleation. *Chem. Rev.* **2016**, 116 (7),  
31226 4205-4259.
- 32227 401. Eastwood, M. L.; Cremel, S.; Wheeler, M.; Murray, B. J.; Girard, E.; Bertram, A. K., Effects of  
33228 sulfuric acid and ammonium sulfate coatings on the ice nucleation properties of kaolinite particles.  
34229 *Geophys. Res. Lett.* **2009**, 36, L02811.
- 35230 402. Chernoff, D. I.; Bertram, A. K., Effects of sulfate coatings on the ice nucleation properties of a  
36231 biological ice nucleus and several types of minerals. *J. Geophys. Res.* **2010**, 115, D20205.
- 38232 403. Bond, T. C.; Doherty, S. J.; Fahey, D. W.; Forster, P. M.; Berntsen, T.; DeAngelo, B. J.; Flanner,  
39233 M. G.; Ghan, S.; Kärcher, B.; Koch, D.; Kinne, S.; Kondo, Y.; Quinn, P. K.; Sarofim, M. C.; Schultz,  
40234 M. G.; Schulz, M.; Venkataraman, C.; Zhang, H.; Zhang, S.; Bellouin, N.; Guttikunda, S. K.; Hopke, P.  
41235 K.; Jacobson, M. Z.; Kaiser, J. W.; Klimont, Z.; Lohmann, U.; Schwarz, J. P.; Shindell, D.; Storelvmo,  
42236 T.; Warren, S. G.; Zender, C. S., Bounding the role of black carbon in the climate system: A scientific  
43237 assessment. *J. Geophys. Res.* **2013**, 118 (11), 5380-5552.
- 44238 404. China, S.; Scarnato, B.; Owen, R. C.; Zhang, B.; Ampadu, M. T.; Kumar, S.; Dzepina, K.;  
45239 Dziobak, M. P.; Fialho, P.; Perlinger, J. A.; Hueber, J.; Helmig, D.; Mazzoleni, L. R.; Mazzoleni, C.,  
46240 Morphology and mixing state of aged soot particles at a remote marine free troposphere site:  
47241 Implications for optical properties. *Geophys. Res. Lett.* **2015**, 42 (4), 1243-1250.
- 48242 405. China, S.; Mazzoleni, C.; Gorkowski, K.; Aiken, A. C.; Dubey, M. K., Morphology and mixing  
49243 state of individual freshly emitted wildfire carbonaceous particles. *Nat. Commun.* **2013**, 4, 2122.
- 50244 406. Dzepina, K.; Mazzoleni, C.; Fialho, P.; China, S.; Zhang, B.; Owen, R. C.; Helmig, D.; Hueber,  
51245 J.; Kumar, S.; Perlinger, J. A.; Kramer, L. J.; Dziobak, M. P.; Ampadu, M. T.; Olsen, S.; Wuebbles, D.  
52246 J.; Mazzoleni, L. R., Molecular characterization of free tropospheric aerosol collected at the Pico  
53247 Mountain Observatory: a case study with a long-range transported biomass burning plume. *Atmos.  
54248 Chem. Phys.* **2015**, 15 (9), 5047-5068.

- 2249 407. China, S.; Kulkarni, G.; Scarnato, B. V.; Sharma, N.; Pekour, M.; Shilling, J. E.; Wilson, J.;  
12250 Zelenyuk, A.; Chand, D.; Liu, S.; Aiken, A. C.; Dubey, M.; Laskin, A.; Zaveri, R. A.; Mazzoleni, C.,  
2251 Morphology of diesel soot residuals from supercooled water droplets and ice crystals: implications for  
4252 optical properties. *Environ. Res. Lett.* **2015**, *10* (11), 114010.
- 52253 408. Ullrich, R.; Hoose, C.; Möhler, O.; Niemand, M.; Wagner, R.; Hohler, K.; Hiranuma, N.;  
62254 Saathoff, H.; Leisner, T., A New Ice Nucleation Active Site Parameterization for Desert Dust and Soot.  
72255 *J. Atmos. Sci.* **2017**, *74* (3), 699-717.
- 82256 409. Friedman, B.; Kulkarni, G.; Beranek, J.; Zelenyuk, A.; Thornton, J. A.; Cziczo, D. J., Ice  
92257 nucleation and droplet formation by bare and coated soot particles. *J. Geophys. Res.* **2011**, *116*, D17203
- 102258 410. Chou, C.; Kanji, Z. A.; Stetzer, O.; Tritscher, T.; Chirico, R.; Heringa, M. F.; Weingartner, E.;  
112259 Prévôt, A. S. H.; Baltensperger, U.; Lohmann, U., Effect of photochemical ageing on the ice nucleation  
12260 properties of diesel and wood burning particles. *Atmos. Chem. Phys.* **2013**, *13* (2), 761-772.
- 13261 411. Kulkarni, G.; China, S.; Liu, S.; Nandasiri, M.; Sharma, N.; Wilson, J.; Aiken, A. C.; Chand, D.;  
14262 Laskin, A.; Mazzoleni, C.; Pekour, M.; Shilling, J.; Shutthanandan, V.; Zelenyuk, A.; Zaveri, R. A., Ice  
15263 nucleation activity of diesel soot particles at cirrus relevant temperature conditions: Effects of hydration,  
16264 secondary organics coating, soot morphology, and coagulation. *Geophys. Res. Lett.* **2016**, *43* (7), 3580-  
17265 3588.
- 18266 412. Schill, G. P.; Jathar, S. H.; Kodros, J. K.; Levin, E. J. T.; Galang, A. M.; Friedman, B.; Link, M.  
19267 F.; Farmer, D. K.; Pierce, J. R.; Kreidenweis, S. M.; DeMott, P. J., Ice-nucleating particle emissions  
20268 from photochemically aged diesel and biodiesel exhaust. *Geophys. Res. Lett.* **2016**, *43* (10), 5524-5531.
- 21269 413. Liu, P. F.; Li, Y. J.; Wang, Y.; Gilles, M. K.; Zaveri, R. A.; Bertram, A. K.; Martin, S. T.,  
22270 Lability of secondary organic particulate matter. *Proc. Natl. Acad. Sci. U. S. A.* **2016**, *113* (45), 12643-  
23271 12648.
- 24272 414. Yli-Juuti, T.; Pajunoja, A.; Tikkanen, O. P.; Buchholz, A.; Faiola, C.; Vaisanen, O.; Hao, L. Q.;  
25273 Kari, E.; Perakyla, O.; Garmash, O.; Shiraiwa, M.; Ehn, M.; Lehtinen, K.; Virtanen, A., Factors  
26274 controlling the evaporation of secondary organic aerosol from alpha-pinene ozonolysis. *Geophys. Res.*  
27275 **2017**, *44* (5), 2562-2570.
- 28276 415. Saha, P. K.; Khlystov, A.; Yahya, K.; Zhang, Y.; Xu, L.; Ng, N. L.; Grieshop, A. P., Quantifying  
29277 the volatility of organic aerosol in the southeastern US. *Atmos. Chem. Phys.* **2017**, *17* (1), 501-520.
- 30278 416. Giorio, C.; Monod, A.; Bregonzio-Rozier, L.; DeWitt, H. L.; Cazaunau, M.; Temime-Roussel,  
31279 B.; Gratien, A.; Michoud, V.; Pangui, E.; Ravier, S.; Zielinski, A. T.; Tapparo, A.; Vermeylen, R.;  
32280 Claeys, M.; Voisin, D.; Kalberer, M.; Doussin, J. F., Cloud Processing of Secondary Organic Aerosol  
33281 from Isoprene and Methacrolein Photooxidation. *J. Phys. Chem. A* **2017**, *121* (40), 7641-7654.
- 34282 417. Boyd, C. M.; Nah, T.; Xu, L.; Berkemeier, T.; Ng, N. L., Secondary Organic Aerosol (SOA)  
35283 from Nitrate Radical Oxidation of Monoterpenes: Effects of Temperature, Dilution, and Humidity on  
36284 Aerosol Formation, Mixing, and Evaporation. *Environ. Sci. Technol.* **2017**, *51* (14), 7831-7841.
- 37285 418. Wilson, J.; Imre, D.; Beranek, J.; Shrivastava, M.; Zelenyuk, A., Evaporation Kinetics of  
38286 Laboratory-Generated Secondary Organic Aerosols at Elevated Relative Humidity. *Environ. Sci.*  
39287 *Technol.* **2015**, *49* (1), 243-249.
- 40288 419. Moise, T.; Flores, J. M.; Rudich, Y., Optical properties of secondary organic aerosols and their  
41289 changes by chemical processes. *Chem. Rev.* **2015**, *115* (10), 4400-4439.
- 42290 420. Pöschl, U.; Shiraiwa, M., Multiphase Chemistry at the Atmosphere-Biosphere Interface  
43291 Influencing Climate and Public Health in the Anthropocene. *Chem. Rev.* **2015**, *115* (10), 4440-4475.
- 44292 421. Pöschl, U., Atmospheric aerosols: Composition, transformation, climate and health effects.  
45293 *Angew. Chem.-Int. Edit.* **2005**, *44* (46), 7520-7540.
- 46294 422. Slade, J. H.; Knopf, D. A., Heterogeneous OH oxidation of biomass burning organic aerosol  
47295 surrogate compounds: assessment of volatilisation products and the role of OH concentration on the  
48296 reactive uptake kinetics. *Phys. Chem. Chem. Phys.* **2013**, *15* (16), 5898-5915.
- 49297 423. Shiraiwa, M.; Pöschl, U.; Knopf, D. A., Multiphase Chemical Kinetics of NO<sub>3</sub> Radicals  
50298 Reacting with Organic Aerosol Components from Biomass Burning. *Environ. Sci. Technol.* **2012**, *46* (12),  
51299 6630-6636.

- 2300 424. Knopf, D. A.; Forrester, S. M.; Slade, J. H., Heterogeneous oxidation kinetics of organic  
1 2301 biomass burning aerosol surrogates by O<sub>3</sub>, NO<sub>2</sub>, N<sub>2</sub>O<sub>5</sub>, and NO<sub>3</sub>. *Phys. Chem. Chem. Phys.* **2011**, *13*  
2 2302 (47), 21050-21062.  
3 2303 425. Brooks, S. D.; Suter, K.; Olivarez, L., Effects of Chemical Aging on the Ice Nucleation Activity  
4 2304 of Soot and Polycyclic Aromatic Hydrocarbon Aerosols. *J. Phys. Chem. A* **2014**, *118* (43), 10036-  
5 2305 10047.  
6 2306 426. Renbaum, L. H.; Smith, G. D., The importance of phase in the radical-initiated oxidation of  
7 2307 model organic aerosols: reactions of solid and liquid brassidic acid particles. *Phys. Chem. Chem. Phys.*  
8 2308 **2009**, *11* (14), 2441-2451.  
9 2309 427. Shiraiwa, M.; Ammann, M.; Koop, T.; Pöschl, U., Gas uptake and chemical aging of semisolid  
10 2310 organic aerosol particles. *P. Natl. Acad. Sci. USA* **2011**, *108* (27), 11003-11008.  
11 2311 428. Arangio, A. M.; Slade, J. H.; Berkemeier, T.; Pöschl, U.; Knopf, D. A.; Shiraiwa, M.,  
12 2312 Multiphase Chemical Kinetics of OH Radical Uptake by Molecular Organic Markers of Biomass  
13 2313 Burning Aerosols: Humidity and Temperature Dependence, Surface Reaction, and Bulk Diffusion. *J.*  
14 2314 *Phys. Chem. A* **2015**, *119* (19), 4533-4544.  
15 2315 429. Slade, J. H.; Knopf, D. A., Multiphase OH oxidation kinetics of organic aerosol: The role of  
16 2316 particle phase state and relative humidity. *Geophys. Res. Lett.* **2014**, *41* (14), 5297-5306.  
17 2317 430. Kroll, J. H.; Lim, C. Y.; Kessler, S. H.; Wilson, K. R., Heterogeneous Oxidation of Atmospheric  
18 2318 Organic Aerosol: Kinetics of Changes to the Amount and Oxidation State of Particle-Phase Organic  
19 2319 Carbon. *J. Phys. Chem. A* **2015**, *119* (44), 10767-10783.  
20 2320 431. Kessler, S. H.; Nah, T.; Daumit, K. E.; Smith, J. D.; Leone, S. R.; Kolb, C. E.; Worsnop, D. R.;  
21 2321 Wilson, K. R.; Kroll, J. H., OH-Initiated Heterogeneous Aging of Highly Oxidized Organic Aerosol. *J.*  
22 2322 *Phys. Chem. A* **2012**, *116* (24), 6358-6365.  
23 2323 432. Mikhailov, E.; Vlasenko, S.; Rose, D.; Pöschl, U., Mass-based hygroscopicity parameter  
24 2324 interaction model and measurement of atmospheric aerosol water uptake. *Atmos. Chem. Phys.* **2013**, *13*  
25 2325 (2), 717-740.  
26 2326 433. Ruehl, C. R.; Davies, J. F.; Wilson, K. R., An interfacial mechanism for cloud droplet formation  
27 2327 on organic aerosols. *Science* **2016**, *351* (6280), 1447-1450.  
28 2328 434. Pathak, R. K.; Stanier, C. O.; Donahue, N. M.; Pandis, S. N., Ozonolysis of  $\alpha$ -pinene at  
29 2329 atmospherically relevant concentrations: Temperature dependence of aerosol mass fractions (yields). *J.*  
30 2330 *Geophys. Res.* **2007**, *112* (D3), D03201.  
31 2331 435. Warren, B.; Austin, R. L.; Cocker, D. R., Temperature dependence of secondary organic aerosol.  
32 2332 *Atmos. Environ.* **2009**, *43* (22-23), 3548-3555.  
33 2333 436. Saathoff, H.; Naumann, K. H.; Möhler, O.; Jonsson, A. M.; Hallquist, M.; Kiendler-Scharr, A.;  
34 2334 Mentel, T. F.; Tillmann, R.; Schurath, U., Temperature dependence of yields of secondary organic  
35 2335 aerosols from the ozonolysis of alpha-pinene and limonene. *Atmos. Chem. Phys.* **2009**, *9* (5), 1551-  
36 2336 1577.  
37 2337 437. Kristensen, K.; Jensen, L. N.; Glasius, M.; Bilde, M., The effect of sub-zero temperature on the  
38 2338 formation and composition of secondary organic aerosol from ozonolysis of  $\alpha$ -pinene. *Environ. Sci.:*  
39 2339 *Processes Impacts* **2017**, *19*, 1220-1234.  
40 2340 438. Hallquist, M.; Wenger, J. C.; Baltensperger, U.; Rudich, Y.; Simpson, D.; Claeys, M.; Dommen,  
41 2341 J.; Donahue, N. M.; George, C.; Goldstein, A. H.; Hamilton, J. F.; Herrmann, H.; Hoffmann, T.; Iinuma,  
42 2342 Y.; Jang, M.; Jenkin, M. E.; Jimenez, J. L.; Kiendler-Scharr, A.; Maenhaut, W.; McFiggans, G.; Mentel,  
43 2343 T. F.; Monod, A.; Prevot, A. S. H.; Seinfeld, J. H.; Surratt, J. D.; Szmigielski, R.; Wildt, J., The  
44 2344 formation, properties and impact of secondary organic aerosol: current and emerging issues. *Atmos.*  
45 2345 *Chem. Phys.* **2009**, *9* (14), 5155-5236.  
46 2346 439. Massoli, P.; Lambe, A. T.; Ahern, A. T.; Williams, L. R.; Ehn, M.; Mikkila, J.; Canagaratna, M.  
47 2347 R.; Brune, W. H.; Onasch, T. B.; Jayne, J. T.; Petaja, T.; Kulmala, M.; Laaksonen, A.; Kolb, C. E.;  
48 2348 Davidovits, P.; Worsnop, D. R., Relationship between aerosol oxidation level and hygroscopic  
49 2349 properties of laboratory generated secondary organic aerosol (SOA) particles. *Geophys. Res. Lett.* **2010**,  
50 2350 *37*, L24801.

- 2351 440. Pajunoja, A.; Lambe, A. T.; Hakala, J.; Rastak, N.; Cummings, M. J.; Brogan, J. F.; Hao, L. Q.;  
2352 Paramonov, M.; Hong, J.; Prisle, N. L.; Malila, J.; Romakkaniemi, S.; Lehtinen, K. E. J.; Laaksonen, A.;  
2353 Kulmala, M.; Massoli, P.; Onasch, T. B.; Donahue, N. M.; Riipinen, I.; Davidovits, P.; Worsnop, D. R.;  
2354 Petaja, T.; Virtanen, A., Adsorptive uptake of water by semisolid secondary organic aerosols. *Geophys. Res. Lett.* **2015**, *42* (8), 3063-3068.  
2355  
62356 441. Ickes, L.; Welti, A.; Lohmann, U., Classical nucleation theory of immersion freezing: sensitivity  
72357 of contact angle schemes to thermodynamic and kinetic parameters. *Atmos. Chem. Phys.* **2017**, *17* (3),  
82358 1713-1739.  
92359 442. Beydoun, H.; Polen, M.; Sullivan, R. C., Effect of particle surface area on ice active site  
102360 densities retrieved from droplet freezing spectra. *Atmos. Chem. Phys.* **2016**, *16* (20), 13359-13378.  
112361 443. Wheeler, M. J.; Bertram, A. K., Deposition nucleation on mineral dust particles: a case against  
122362 classical nucleation theory with the assumption of a single contact angle. *Atmos. Chem. Phys.* **2012**, *12*  
132363 (2), 1189-1201.  
142364 444. Niedermeier, D.; Shaw, R. A.; Hartmann, S.; Wex, H.; Clauss, T.; Voigtlaender, J.; Stratmann,  
152365 F., Heterogeneous ice nucleation: exploring the transition from stochastic to singular freezing behavior.  
162366 *Atmos. Chem. Phys.* **2011**, *11* (16), 8767-8775.  
172367 445. Murray, B. J.; Broadley, S. L.; Wilson, T. W.; Atkinson, J. D.; Wills, R. H., Heterogeneous  
202368 freezing of water droplets containing kaolinite particles. *Atmos. Chem. Phys.* **2011**, *11* (9), 4191-4207.  
212369 446. Vali, G.; Snider, J. R., Time-dependent freezing rate parcel model. *Atmos. Chem. Phys.* **2015**, *15*  
222370 (4), 2071-2079.  
232371 447. Marcolli, C.; Gedamke, S.; Peter, T.; Zobrist, B., Efficiency of immersion mode ice nucleation  
242372 on surrogates of mineral dust. *Atmos. Chem. Phys.* **2007**, *7* (19), 5081-5091.  
252373 448. Lüönd, F.; Stetzer, O.; Welti, A.; Lohmann, U., Experimental study on the ice nucleation ability  
262374 of size-selected kaolinite particles in the immersion mode. *J. Geophys. Res.* **2010**, *115*, D14201.  
272375 449. Vali, G., Quantitative evaluation of experimental results on heterogeneous freezing nucleation of  
282376 supercooled liquids. *J. Atmos. Sci.* **1971**, *28* (3), 402-409.  
292377 450. Connolly, P. J.; Möhler, O.; Field, P. R.; Saathoff, H.; Burgess, R.; Choularton, T.; Gallagher,  
302378 M., Studies of heterogeneous freezing by three different desert dust samples. *Atmos. Chem. Phys.* **2009**,  
312379 9 (8), 2805-2824.  
322380 451. Vali, G., Repeatability and randomness in heterogeneous freezing nucleation. *Atmos. Chem.*  
332381 *Phys.* **2008**, *8* (16), 5017-5031.  
342382 452. Ervens, B.; Feingold, G., Sensitivities of immersion freezing: Reconciling classical nucleation  
352383 theory and deterministic expressions. *Geophys. Res. Lett.* **2013**, *40* (12), 3320-3324.  
362384 453. Ervens, B.; Feingold, G., On the representation of immersion and condensation freezing in cloud  
372385 models using different nucleation schemes. *Atmos. Chem. Phys.* **2012**, *12* (13), 5807-5826.  
382386 454. Westbrook, C. D.; Illingworth, A. J., The formation of ice in a long-lived supercooled layer  
392387 cloud. *Q. J. Roy. Meteor. Soc.* **2013**, *139* (677), 2209-2221.  
402388 455. Wang, Y.; Liu, X.; Hoose, C.; Wang, B., Different contact angle distributions for heterogeneous  
412389 ice nucleation in the Community Atmospheric Model version 5. *Atmos. Chem. Phys.* **2014**, *14* (19),  
422390 10411-10430.  
432391 456. English, J. M.; Kay, J. E.; Gettelman, A.; Liu, X. H.; Wang, Y.; Zhang, Y. Y.; Chepfer, H.,  
442392 Contributions of Clouds, Surface Albedos, and Mixed-Phase Ice Nucleation Schemes to Arctic  
452393 Radiation Biases in CAM5. *J. Clim.* **2014**, *27* (13), 5174-5197.  
462394 457. Spichtinger, P.; Cziczo, D. J., Aerosol-cloud interactions - a challenge for measurements and  
472395 modeling at the cutting edge of cloud-climate interactions. *Environ. Res. Lett.* **2008**, *3* (2), 025002.  
482396 458. Peter, T.; Marcolli, C.; Spichtinger, P.; Corti, T.; Baker, M. B.; Koop, T., When dry air is too  
492397 humid. *Science* **2006**, *314* (5804), 1399-1402.  
502398 459. Bergeron, T., On the physics of cloud and precipitation. *Proc. 5th Assembly U.G.G.I. Lisbon*  
512399 **1935**, *2*, 156.  
522400 460. Findeisen, W., Die kolloidmeteorologischen Vorgänge bei der Niederschlagsbildung (Colloidal  
532401 meteorological processes in the formation of precipitation). *Met. Z.* **1938**, *55*, 121.

- 2402 461. Wegener, A., *Thermodynamik der Atmosphäre*. Barth: Leipzig, 1911.  
12403 462. Broadley, S. L.; Murray, B. J.; Herbert, R. J.; Atkinson, J. D.; Dobbie, S.; Malkin, T. L.;  
22404 Condiffe, E.; Neve, L., Immersion mode heterogeneous ice nucleation by an illite rich powder  
42405 representative of atmospheric mineral dust. *Atmos. Chem. Phys.* **2012**, *12* (1), 287-307.  
52406 463. Avramov, A.; Ackerman, A. S.; Fridlind, A. M.; van Diedenhoven, B.; Botta, G.; Aydin, K.;  
62407 Verlinde, J.; Korolev, A. V.; Strapp, J. W.; McFarquhar, G. M.; Jackson, R.; Brooks, S. D.; Glen, A.;  
72408 Wolde, M., Toward ice formation closure in Arctic mixed-phase boundary layer clouds during ISDAC.  
82409 *J. Geophys. Res.* **2011**, *116*, D00T08.  
92410 464. Ovchinnikov, M.; Ackerman, A. S.; Avramov, A.; Cheng, A. N.; Fan, J. W.; Fridlind, A. M.;  
102411 Ghan, S.; Harrington, J.; Hoose, C.; Korolev, A.; McFarquhar, G. M.; Morrison, H.; Paukert, M.; Savre,  
112412 J.; Shipway, B. J.; Shupe, M. D.; Solomon, A.; Sulia, K., Intercomparison of large-eddy simulations of  
122413 Arctic mixed-phase clouds: Importance of ice size distribution assumptions. *J. Adv. Model. Earth Syst.*  
132414 **2014**, *6* (1), 223-248.  
142415 465. Morrison, H.; Pinto, J. O.; Curry, J. A.; McFarquhar, G. M., Sensitivity of modeled arctic mixed-  
152416 phase stratocumulus to cloud condensation and ice nuclei over regionally varying surface conditions. *J.*  
162417 *Geophys. Res.* **2008**, *113* (D5), D05203.  
172418 466. Niemand, M.; Möhler, O.; Vogel, B.; Vogel, H.; Hoose, C.; Connolly, P.; Klein, H.; Bingemer,  
182419 H.; DeMott, P.; Skrotzki, J.; Leisner, T., A Particle-Surface-Area-Based Parameterization of Immersion  
212420 Freezing on Desert Dust Particles. *J. Atmos. Sci.* **2012**, *69* (10), 3077-3092.  
222421 467. Boose, Y.; Kanji, Z. A.; Kohn, M.; Sierau, B.; Zipori, A.; Crawford, I.; Lloyd, G.; Bukowiecki,  
232422 N.; Herrmann, E.; Kupiszewski, P.; Steinbacher, M.; Lohmann, U., Ice Nucleating Particle  
242423 Measurements at 241 K during Winter Months at 3580m MSL in the Swiss Alps. *J. Atmos. Sci.* **2016**,  
252424 *73* (5), 2203-2228.

272425  
28

29  
30  
312426

32  
33  
342427

35  
36

372428

382429

392430

402431

412432

422433

432434

442435

452436

462437

472438

482439

492440

502441

512442

522443

532444

542445

552446

562447

572448

582449

592450

602451

2447

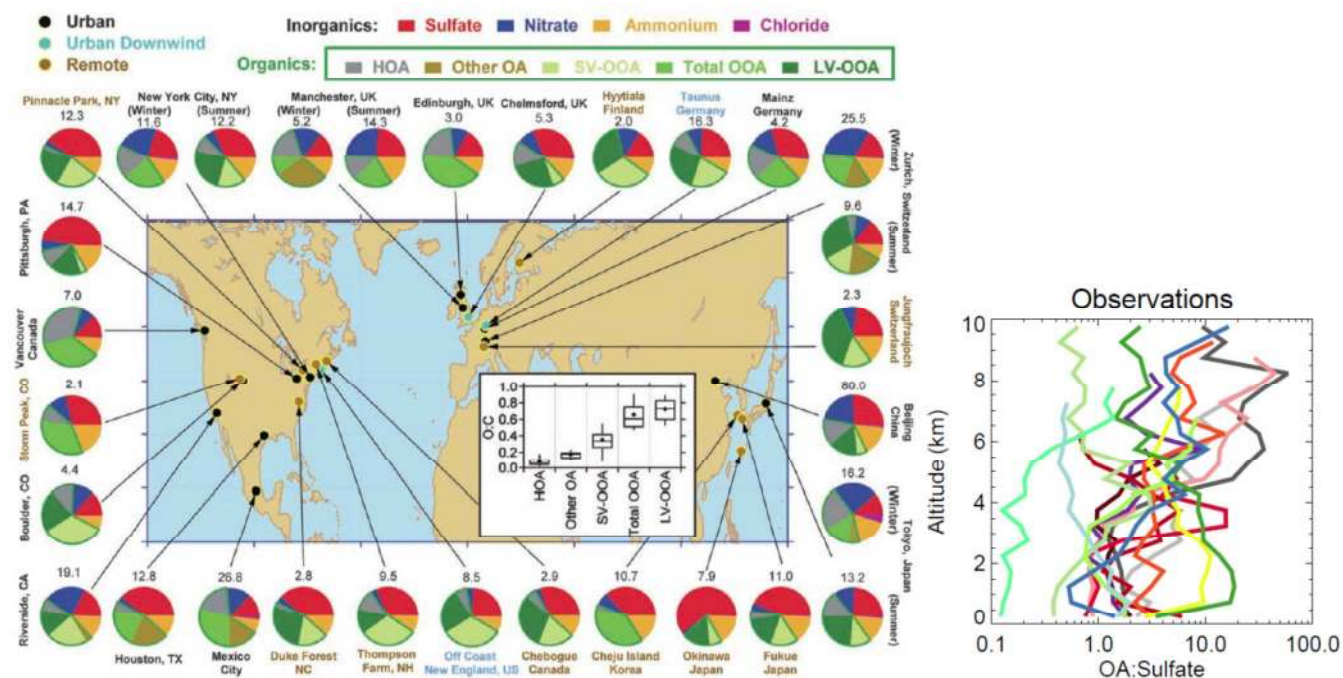
**Fig. 1**

Fig. 1. L.H.S. Total mass concentration (in  $\mu\text{g m}^{-3}$ ) and mass fractions of non-refractory inorganic species and organic components in submicrometer aerosols and oxidation level expressed as oxygen to carbon ratio (O:C) measured with the aerosol mass spectrometer at multiple surface locations in the Northern Hemisphere. Reprinted from Jimenez et al. (2009)<sup>29</sup>. R.H.S. Organic aerosol (OA) to sulfate ratio (OA:sulfate) as a function of altitude derived from 17 field campaigns. Reprinted from Heald et al. (2011)<sup>59</sup>.

34448

35

36449

37

38

39

40

41

42

43

44

45

46

47

48

49

50

51

52

53

54

55

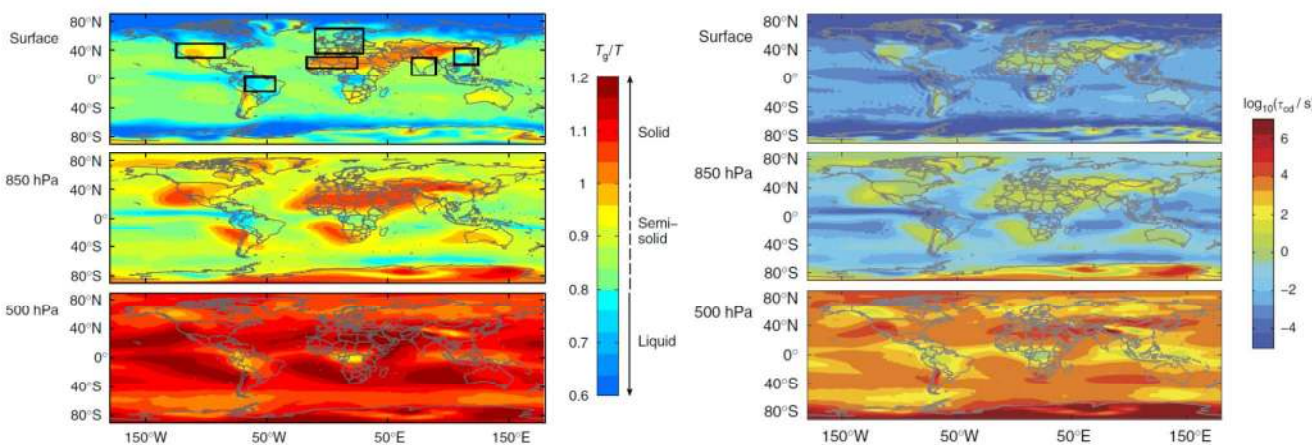
56

57

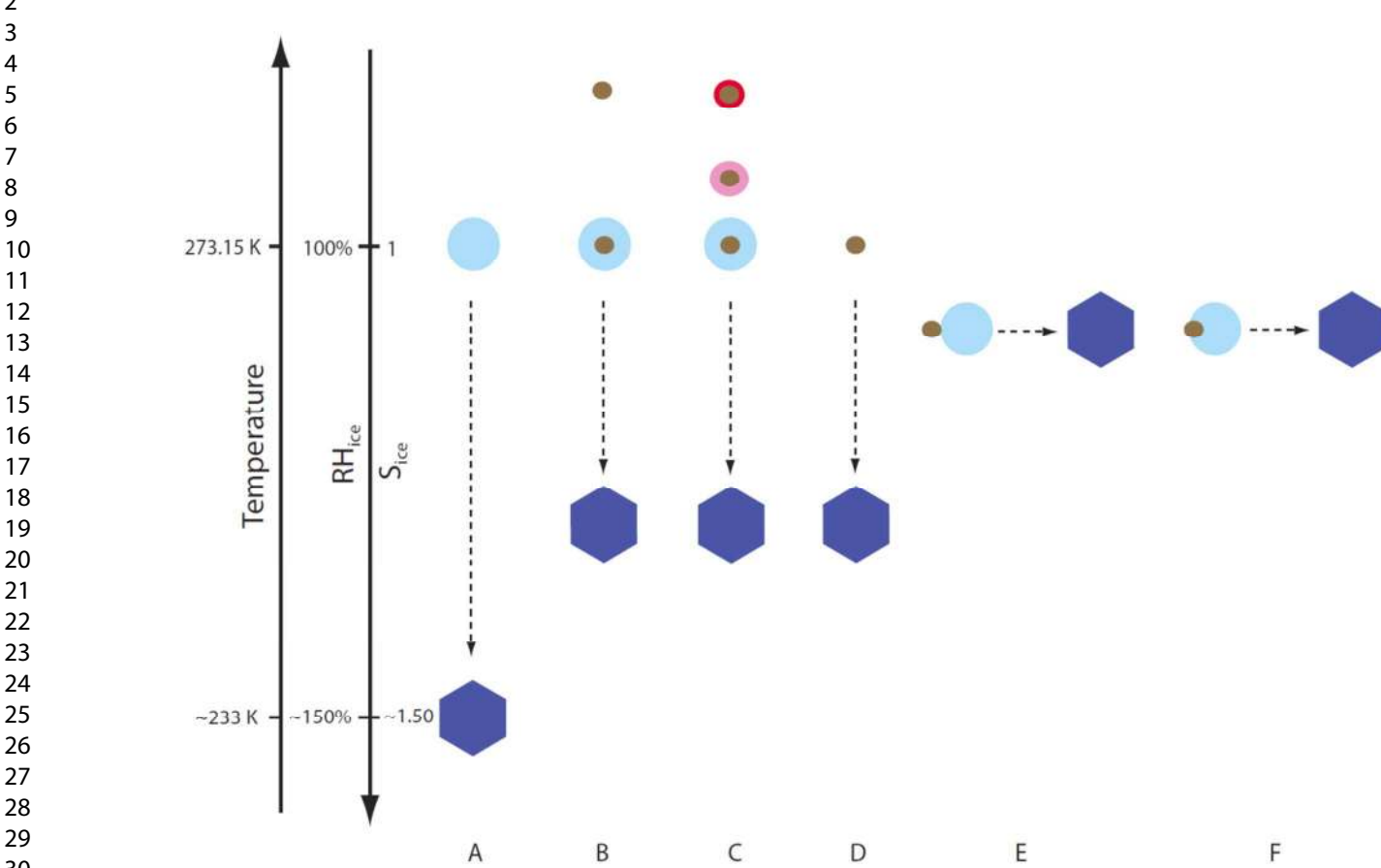
58

59

60

2450 **Fig. 2**

17  
18 Fig. 2. Modelled SOA phase state in the global atmosphere (a) and characteristic mixing timescales of  
19 water (b) in SOA particles at the surface, 850 hPa, and 500 hPa. Reprinted and adapted from Shiraiwa et  
20 al. (2017)<sup>122</sup>.

2453  
1  
2  
3**Fig. 3**4  
5  
6  
7  
8

31 Fig. 3. Schematic overview of different ice nucleation pathways, exemplary given as a function of  
32 temperature, relative humidity and supersaturation with respect to ice ( $RH_{ice}$  and  $S_{ice}$ , respectively).  
33 A: homogeneous ice nucleation. B: immersion freezing. C: deliquescence and water uptake followed  
34 by immersion freezing. D: deposition ice nucleation. E: contact ice nucleation. F: Inside-out freez-  
35 ing. Symbol forms and sizes not to scale.  
36  
37  
38  
39  
40  
41  
42  
43  
44  
45  
46  
47  
48  
49  
50  
51  
52  
53  
54  
55  
56  
57  
58  
59  
60

2461 Fig. 4

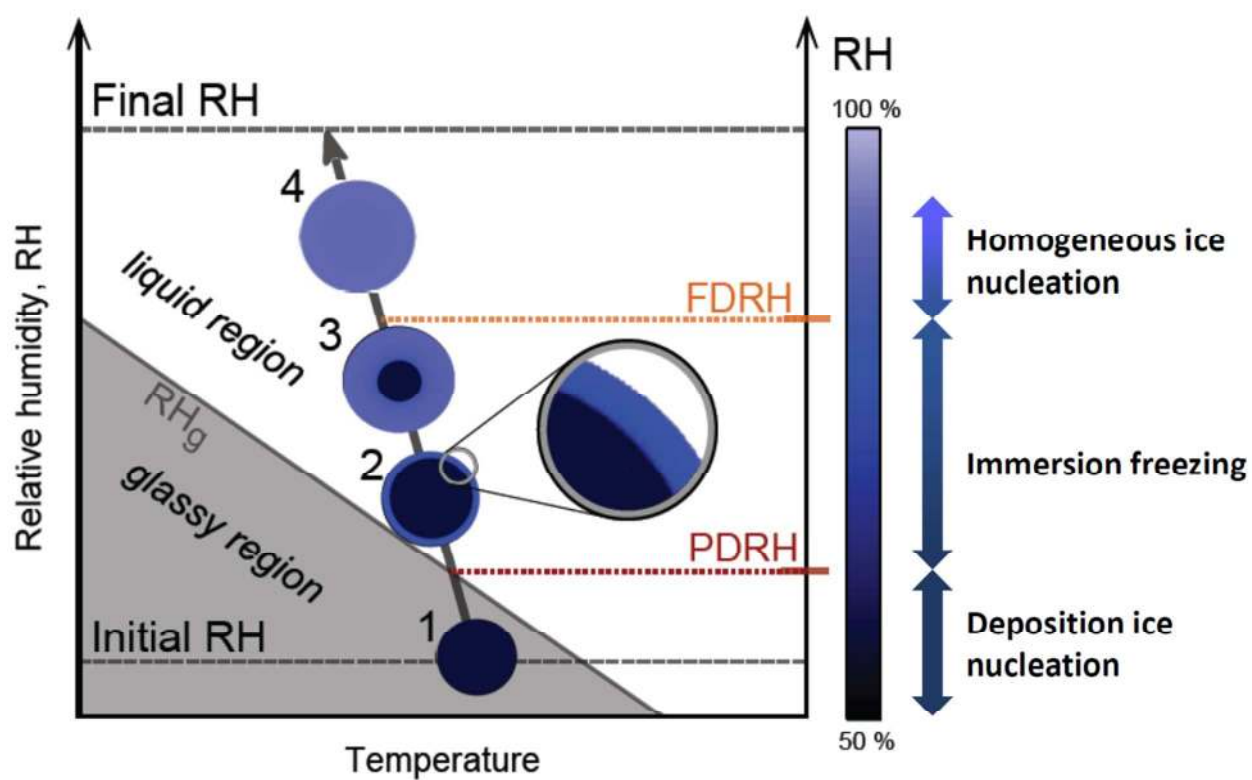


Fig. 4. The transition of the amorphous organic phase upon increase in RH from a solid (glassy) state via partial deliquescence relative humidity (PDRH) to a liquid state at full deliquescence relative humidity (FDRH). Potential ice nucleation pathways are indicated. Adapted and reprinted from Berkemeier et al. (2014)<sup>119</sup>.

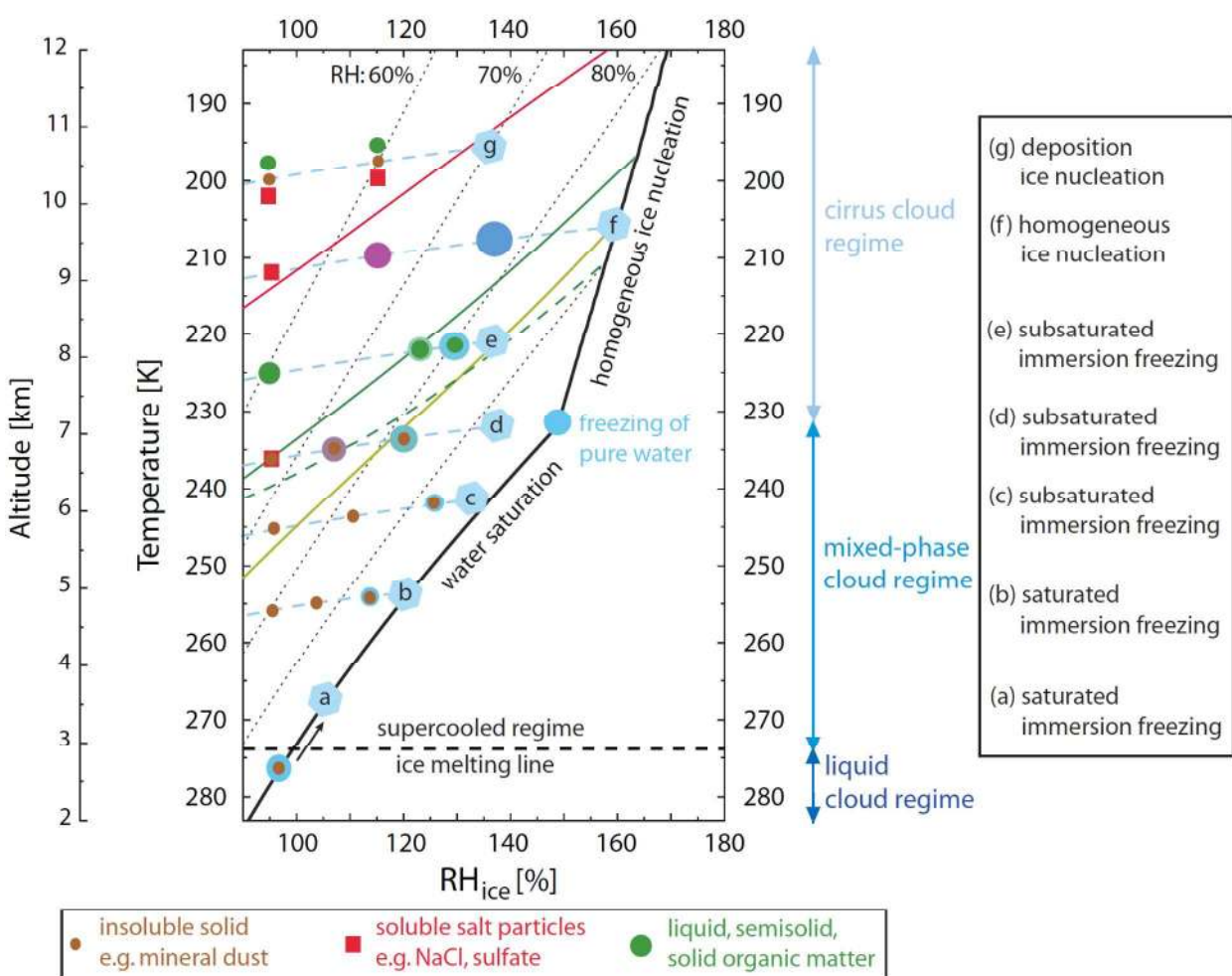
2470  
1  
2  
3  
4  
5  
6  
7  
8  
9  
10  
11  
12  
13  
14  
15  
16  
17  
18  
19  
20  
21  
22  
23  
24  
25  
26  
27  
28  
29  
30  
31  
32  
33  
34  
35  
36  
37  
38  
39  
40  
41  
42  
43  
44  
45  
46  
47  
48  
49  
50  
51  
52  
53  
54  
55  
56  
57  
58  
59  
60**Fig. 5**

Fig. 5. Potential immersion freezing and deposition ice nucleation under atmospheric thermodynamic conditions for particles of different chemical compositions. Dotted lines give conditions of constant relative humidity with respect to water. Altitude is given as an estimate using a dry adiabatic lapse rate of  $10 \text{ K km}^{-1}$ . Particle trajectories are given as blue dashed lines. Red, green, and golden solid lines represent the glass transition temperature for  $\alpha$ -pinene SOA with and without the presence of sulfates (Charnawskas et al., 2017<sup>112</sup>) and naphthalene SOA (Wang et al., 2012<sup>105</sup>), respectively. Green dashed line represents the full deliquescence relative humidity of  $\alpha$ -pinene SOA (Charnawskas et al., 2017<sup>112</sup>). The symbol forms and sizes do not reflect actual particle size and morphology changes but rather indicate the particles' phase states. Trajectories d and f involve deliquescence of the inorganic material followed by water uptake.

2471

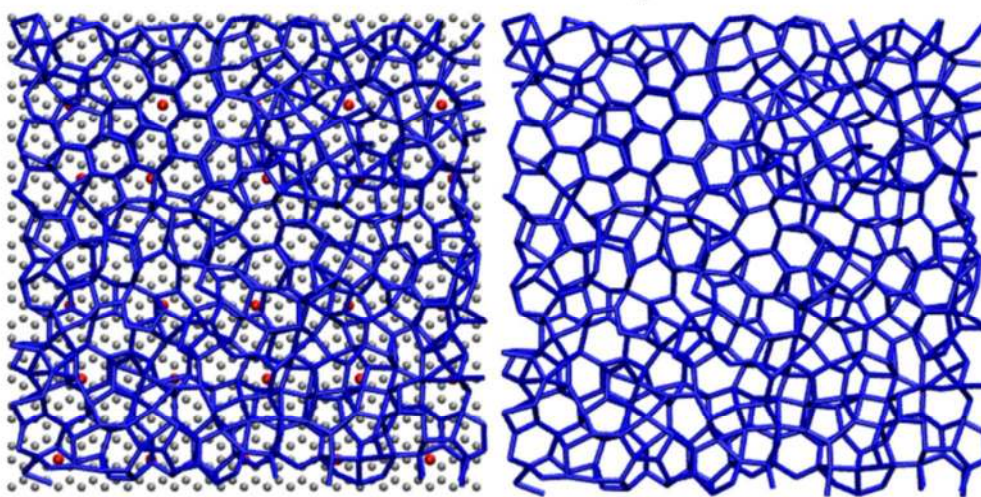
**Fig. 6****1<sup>st</sup> and 2<sup>nd</sup> Layers**

Fig. 6. Structure of interfacial water in contact with a modified graphitic surface with OH placed in 1 nm distances. Carbon atoms of the surface are shown with gray spheres, OH-like groups with red spheres, and water as blue sticks that connect neighbors within 0.35 nm. Both first and second layers are shown to highlight the presence of bilayer hexagonal patches (showing the surface in the left panel, and hiding it for clarity in the right panel). There is no apparent alignment between the water molecules and the surface atoms, indicating that the surface does not template the formation of ice. Reprinted from Lupi et al. (2014)<sup>257</sup>.

2473

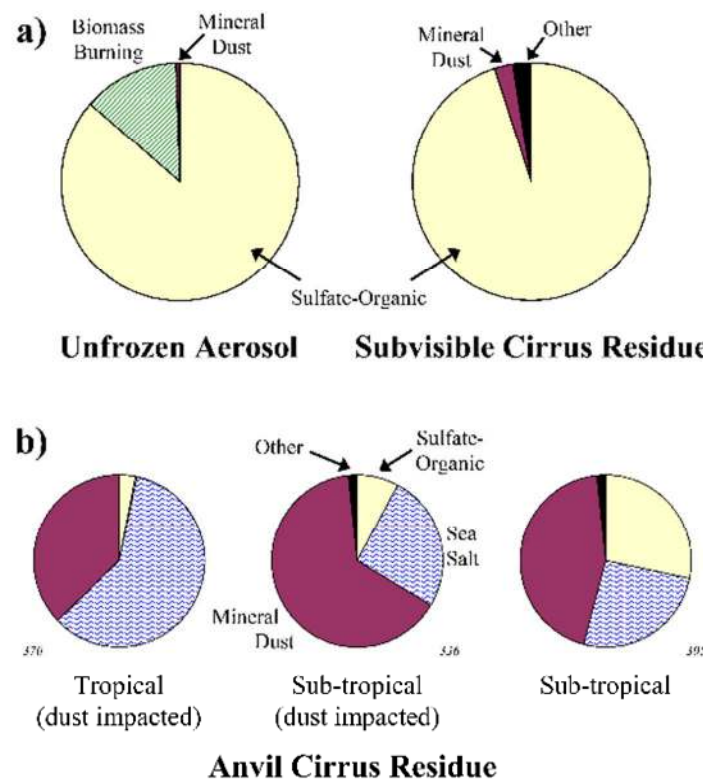
**Fig. 7**

Fig. 7. Particle types in the tropical tropopause region. (a) Subvisible cirrus residues at 16.0–17.4 km are compared to unfrozen aerosols. (b) Residues from several anvil cirrus encounters at lower altitudes, 12–14 km. Reprinted from Froyd et al. (2010)<sup>290</sup>.

2475 Fig. 8

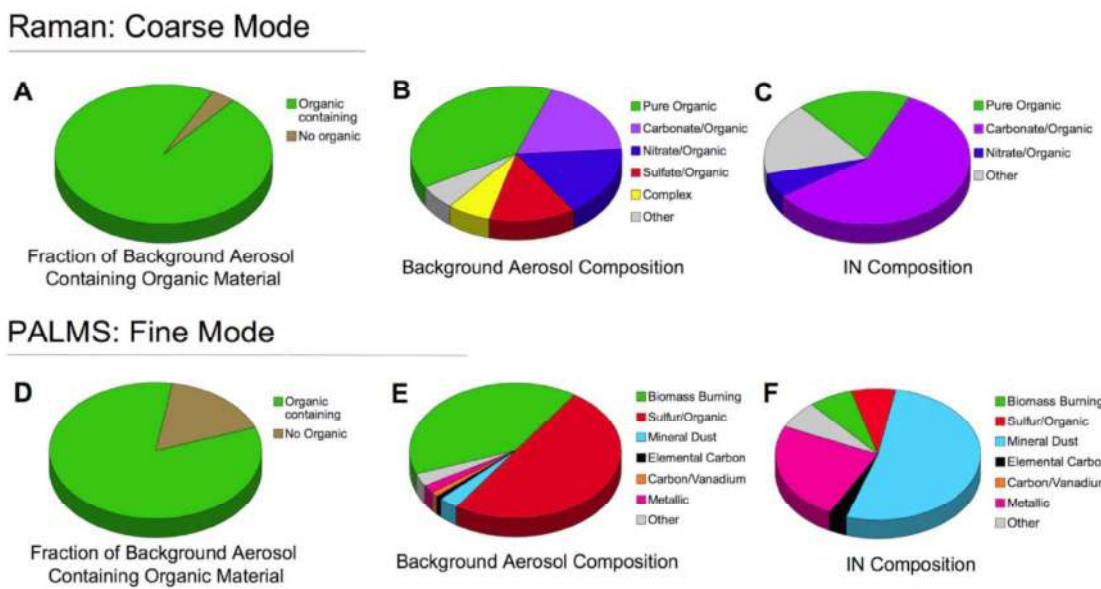


Fig. 8. Compositional summary of coarse ( $> 2 \mu\text{m}$ ) and fine ( $< 2 \mu\text{m}$ ) mode background aerosol particles and INPs, collected at Storm Peak Laboratory using both particle analysis by laser mass spectrometry (PALMS) and Raman analyses. Reprinted from Baustian et al. (2012)<sup>287</sup>.

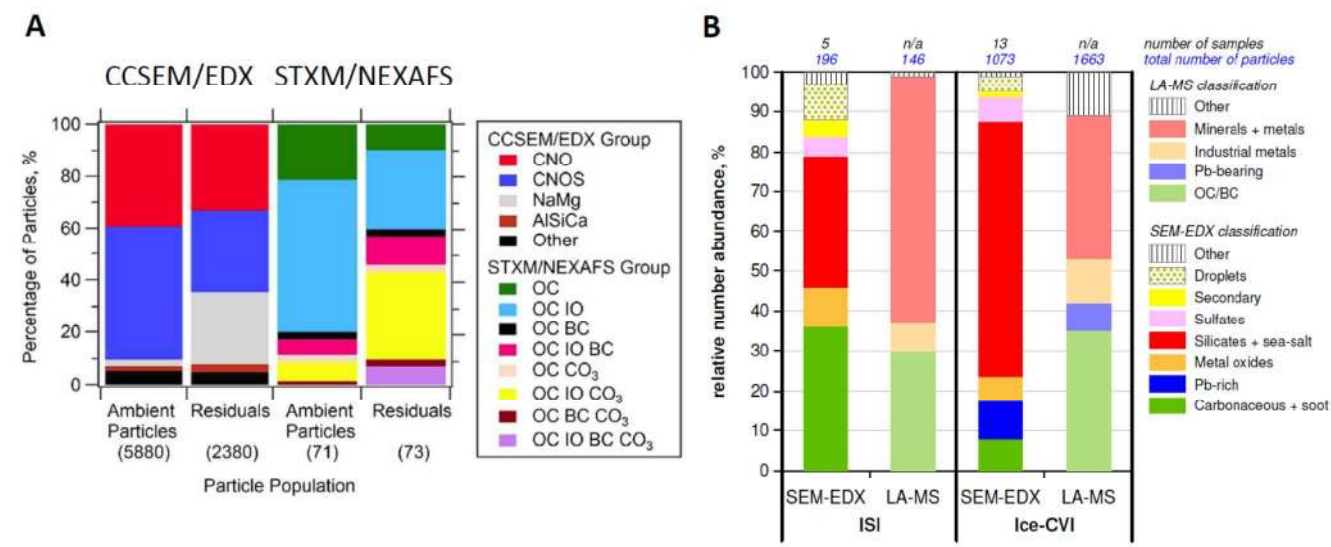
2477  
1  
2  
3**Fig. 9**

Fig. 9. (A) ISDAC field campaign: Particle groups of ambient particles and in-cloud residual particles. CCSEM/EDX groups particles according to major elemental composition. For STXM/NEXAFS analyses, the colors indicate particle classes distinguished by different combinations of organic carbon (OC) and internally mixed with other components: inorganics (IO), black carbon (BC), and carbonates (CO<sub>3</sub>). The numbers in parenthesis represent the total number of particles analyzed. Adapted from Hiranuma et al. (2013)<sup>288</sup>. (B) High Alpine Research Station Jungfraujoch: Relative number abundance of particle groups determined by SEM/EDX and laser ablation mass spectrometry (LA-MS) for IRs sampled by ice selective inlet (ISI) and ice counterflow-virtual-impactor (Ice-CVI). Reprinted from Worringen et al. (2015)<sup>301</sup>.

2478  
33  
34  
35  
36  
37  
38  
39  
40  
41  
42  
43  
44  
45  
46  
47  
48  
49  
50  
51  
52  
53  
54  
55  
56  
57  
58  
59  
60

2479

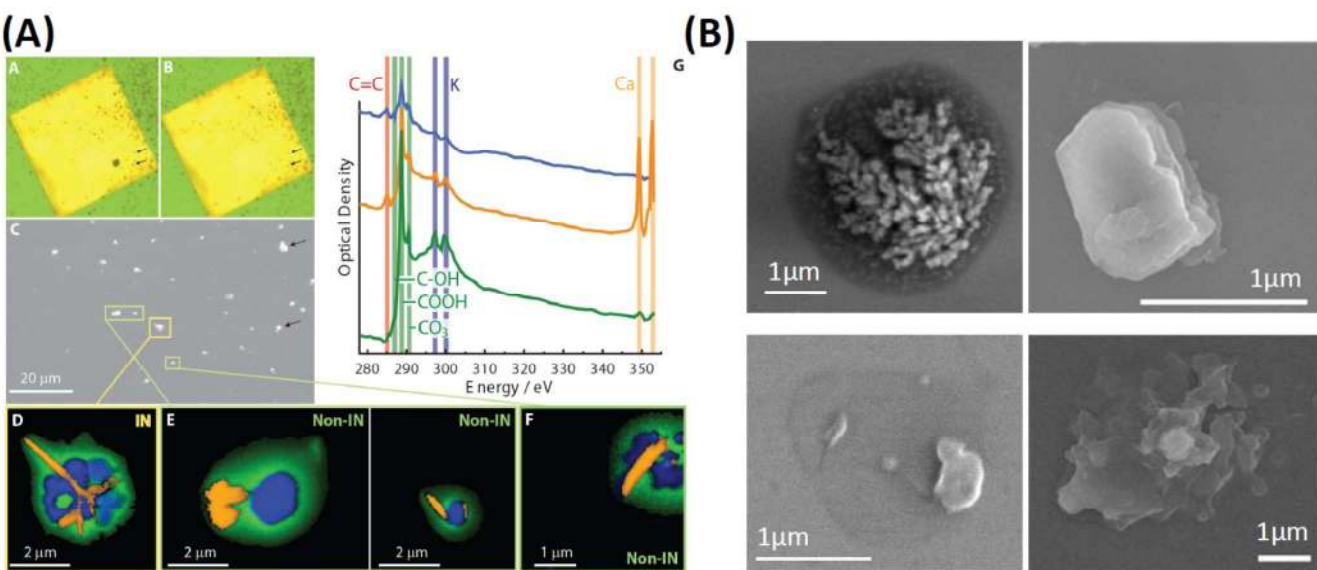
**Fig. 10**

Fig. 10. A: INP identification and STXM/NEXAFS chemical imaging of INP and non-INPs. (a and b) The ice formation and ice sublimation event observed in the experiment, respectively. (c) SEM image of the same sample area at higher magnification. (d) Identified INP and panels E and F show non-INPs component images emphasizing the contrast between non-carbonaceous inorganic species (blue), organic carbon (green), and calcium (orange). (g) NEXAFS spectra of the particles with the major functionalities highlighted. Reprinted from Knopf et al. (2014)<sup>96</sup>. B: The two SEM images on each the left and right hand side represent identified INPs with organic coatings. Reprinted and adapted from Knopf et al. (2014)<sup>96</sup> and China et al. (2017)<sup>102</sup>, respectively.

2481

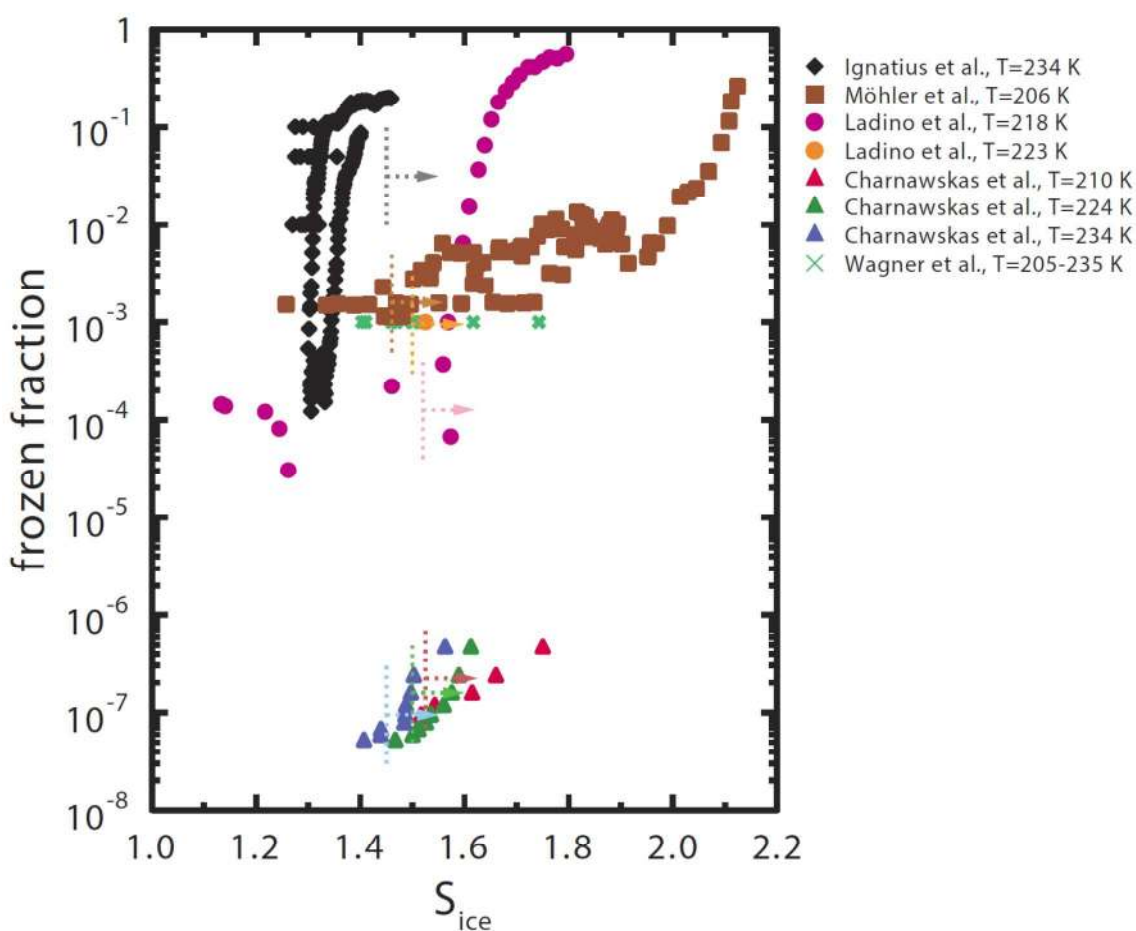
**Fig. 11**

Fig. 11. Compilation of frozen particle fractions as function of ice supersaturation,  $S_{\text{ice}}$ , for laboratory generated  $\alpha$ -pinene SOA particles generated from  $\alpha$ -pinene reaction with  $\text{O}_3$  and OH in the presence of UV light (black, Ignatius et al., 2016<sup>327</sup>),  $\alpha$ -pinene reaction with  $\text{O}_3$  (brown, Möhler et al., 2008<sup>321</sup>, light green, Wagner et al., 2017<sup>368</sup> and purple and orange, Ladino et al., 2014<sup>326</sup>) and  $\alpha$ -pinene reaction with OH (red, green, and blue Charnawskas et al., 2017<sup>110</sup>). Vertical dotted lines indicate the homogeneous freezing limit for particle sizes used in each study (Koop et al., 2000<sup>197</sup>). Lighter colored arrows for all data sets point toward conditions in which homogeneous freezing becomes drastically more favorable. Arrows for Wagner et al. (2017<sup>368</sup>) are omitted for clarity.

42

43

44

45

46

47

48

49

50

484

51

52

485

53

54

55

56

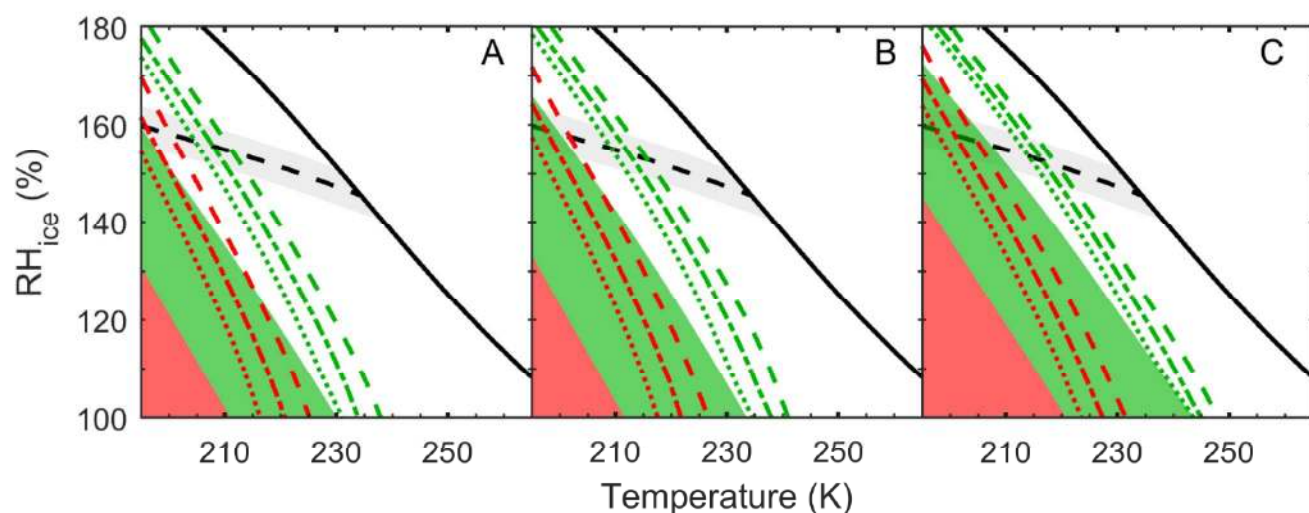
57

58

59

60

2486 Fig. 12



20  
21  
22  
23  
24  
25 Fig. 12. Simulated  $T_g$  (solid lines) for isoprene (A),  $\alpha$ -pinene (B), and naphthalene (C) SOA with (red)  
26  
27 and without sulfate (green) and corresponding FDRH for different updraft velocities of 0.03, 0.28, and  
28  
29 2.8  $m\ s^{-1}$  as dotted, dash-dotted, and dashed lines, respectively. Black solid and dashed lines represent  
30  
31 water saturation and homogeneous freezing limit<sup>195</sup>, respectively. Reprinted from Charnawskas et al.  
32  
33 (2017)<sup>112</sup>.  
34  
35  
36  
37  
38  
39  
40  
41  
42  
43  
44  
45  
46  
47  
48  
49  
50  
51  
52  
53  
54  
55  
56  
57  
58  
59  
60

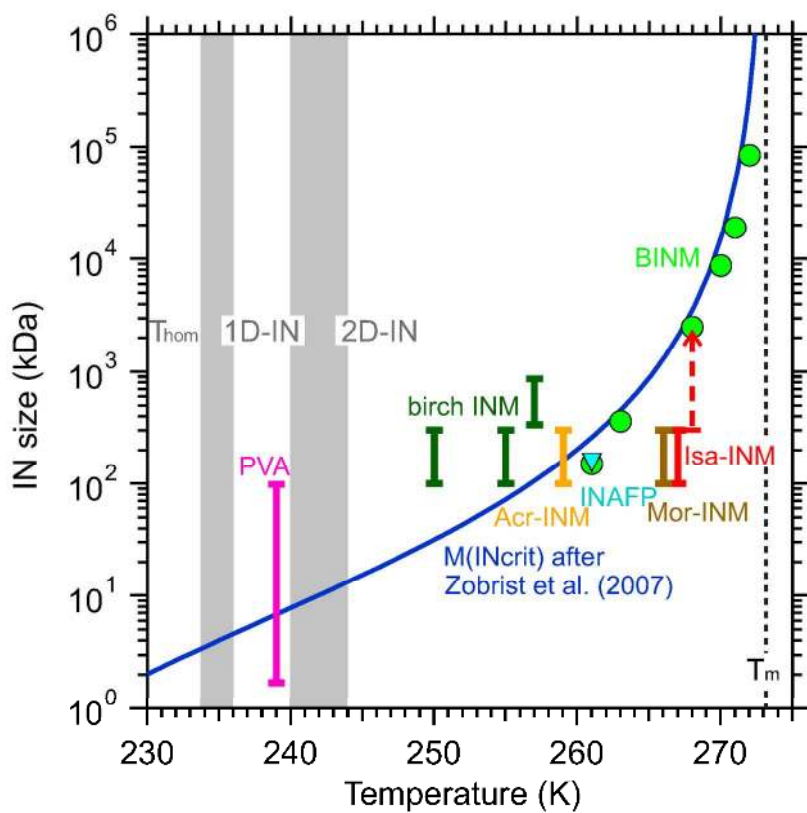
2488  
1**Fig. 13**

Fig. 13. Size of ice nucleating macromolecules (INM) derived from polyvinyl alcohol (PVA, magenta), birch INM (green), bacterial INM (BINM, lime) bacterial ice nucleating/anti-freeze proteins (INAfp, cyan), and fungal spores from *Acremonium implicatum* (Acr-INM, orange), *Isaria farinose* (Isa-INM, red) and *Mortierella alpine* (Mor-INM, brown) as a function on observed median ice nucleation temperature. The blue line is the size of the critical ice nucleus from classical nucleation theory<sup>108</sup>. Assumed regions in one and two dimensions of water molecular templating to form ice (1D-IN and 2D-IN, respectively) are shown. Melting and homogeneous freezing temperature of pure water,  $T_m$  and  $T_{\text{hom}}$ , respectively, are given. Reprinted from Pummer et al. (2015)<sup>104</sup>.

4889  
49490  
44491  
45492  
46493  
47494  
48495  
49496  
50497  
51498  
52499  
53500  
54501  
55502  
56503  
57504  
58505  
59506  
60

2495

**Fig. 14**

1

2

3

4

5

6

7

8

9

10

11

12

13

14

15

16

17

18

19

20

21

22

23

24

25

26

27

28

29

30

497

31

32

3498

34

35

36

37

38

39

40

41

42

43

44

45

46

47

48

49

50

51

52

53

54

55

56

57

58

59

60

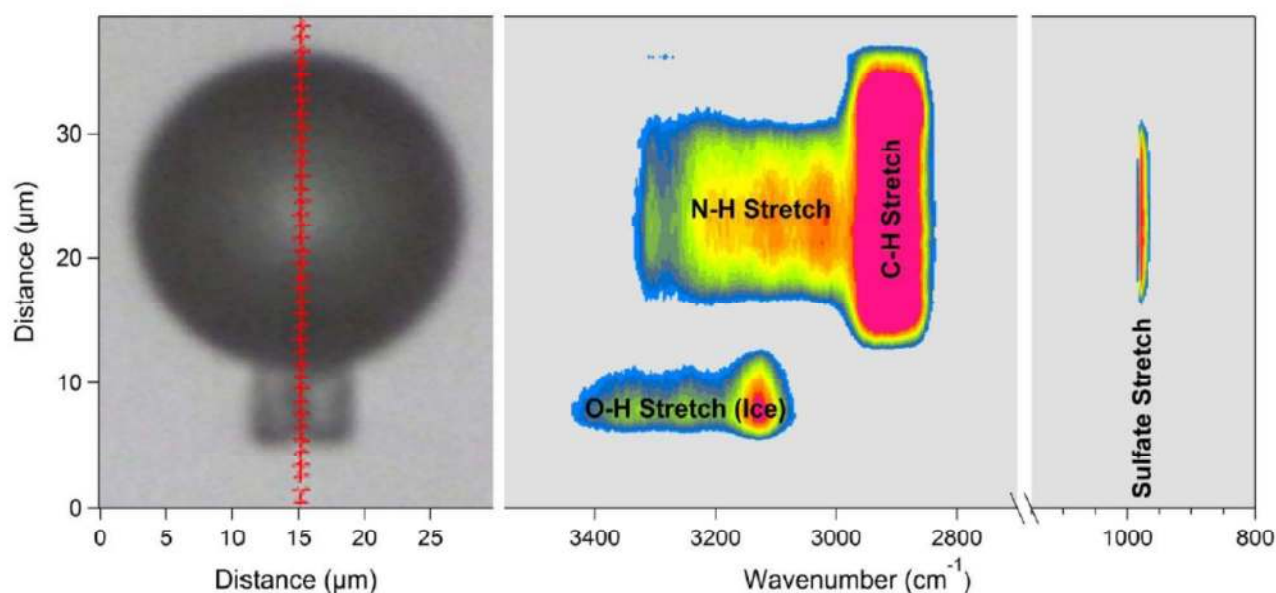


Fig. 14. Optical microscope images and Raman spectroscopy line scans (red hashed line) of a glassy organic particle with an ammonium sulfate core nucleating ice at 215 K. Reprinted from Schill and Tolbert (2013)<sup>324</sup>.

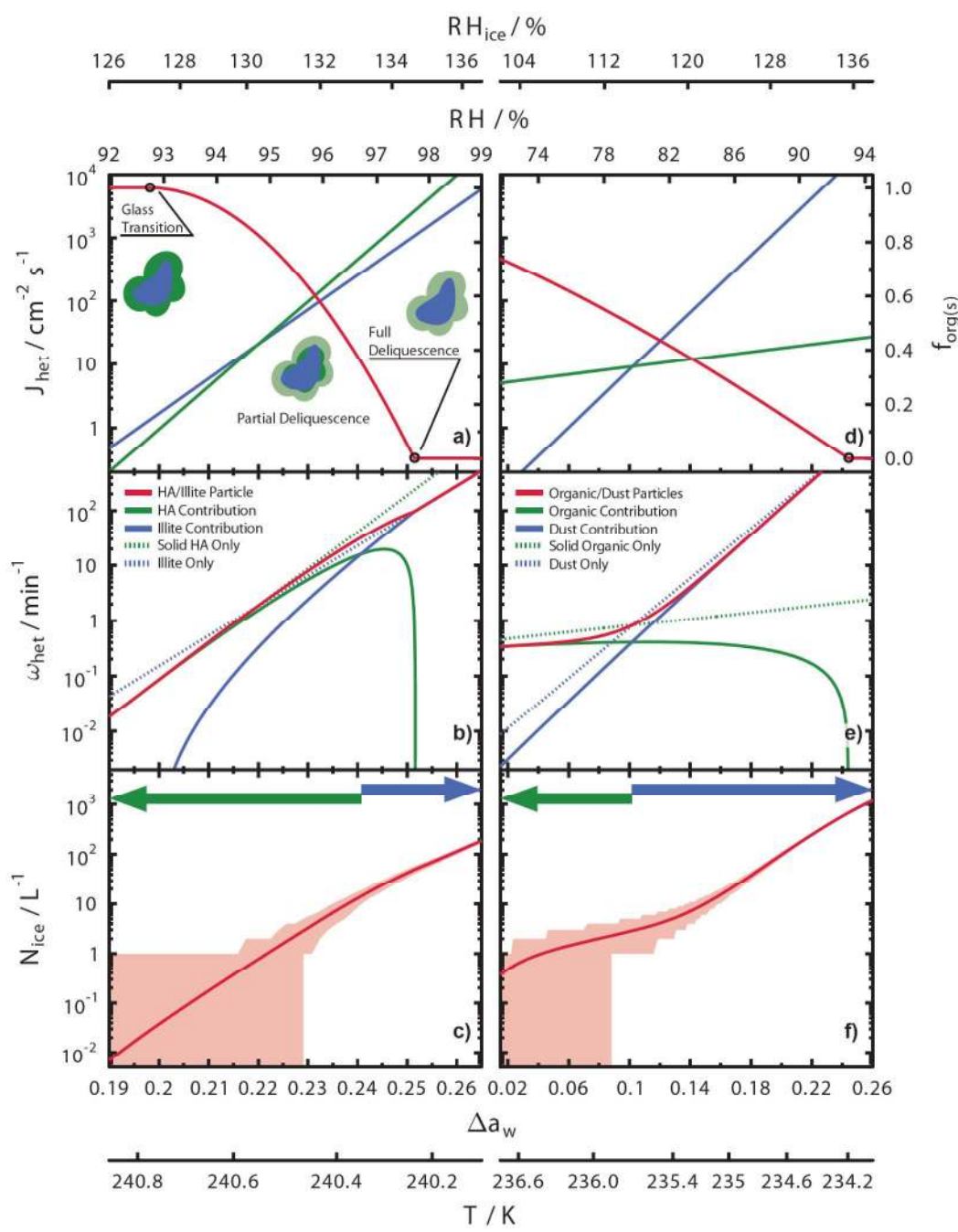
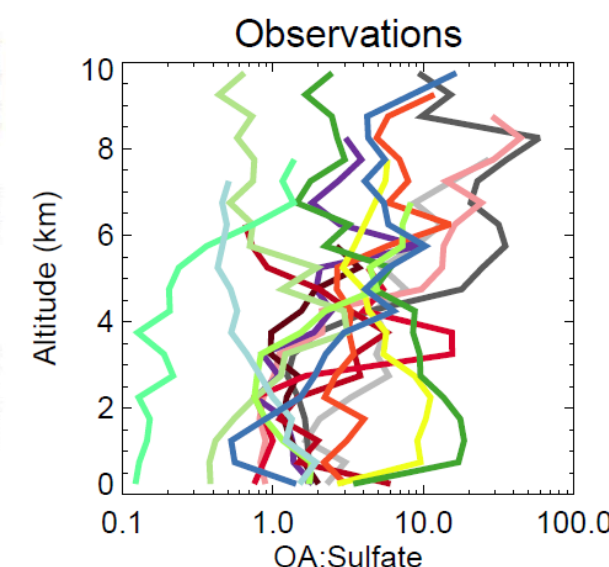
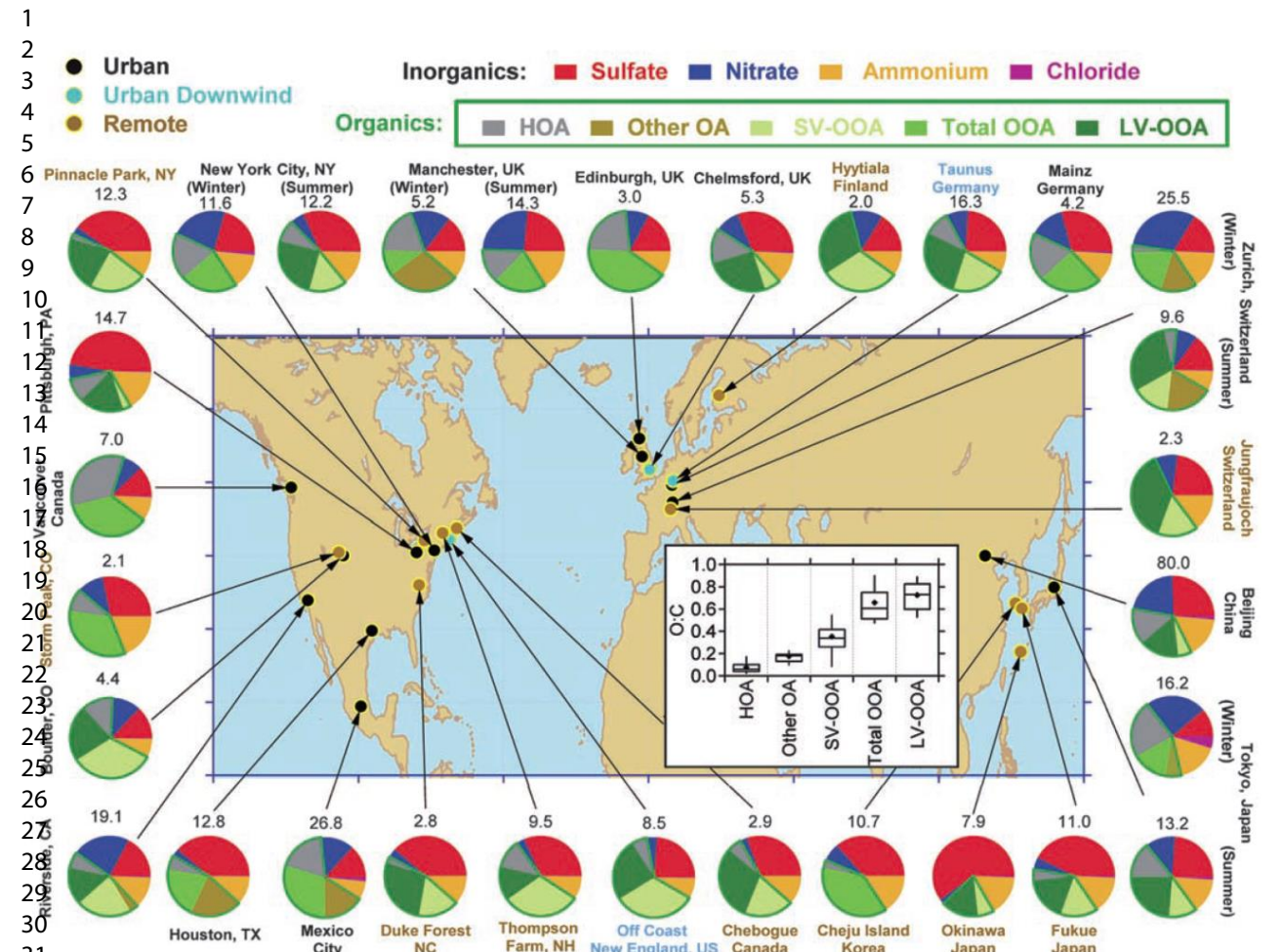
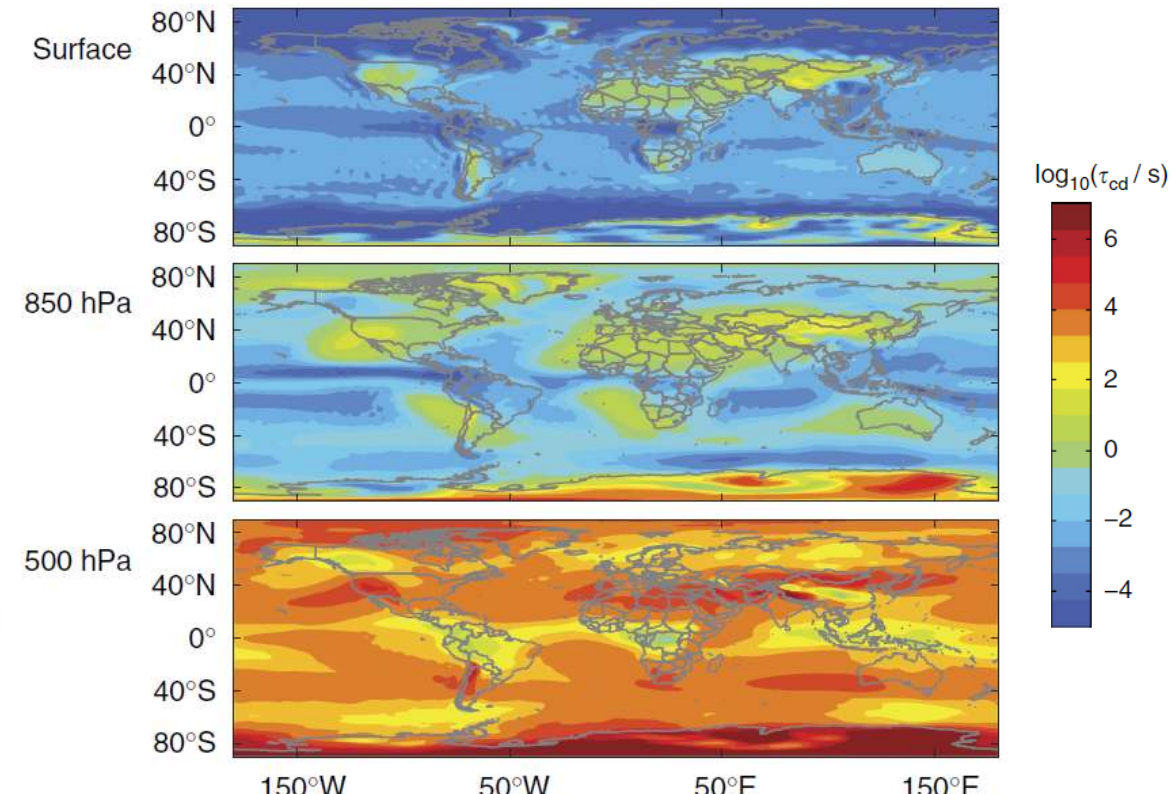
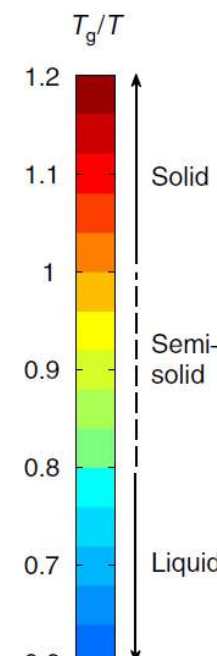
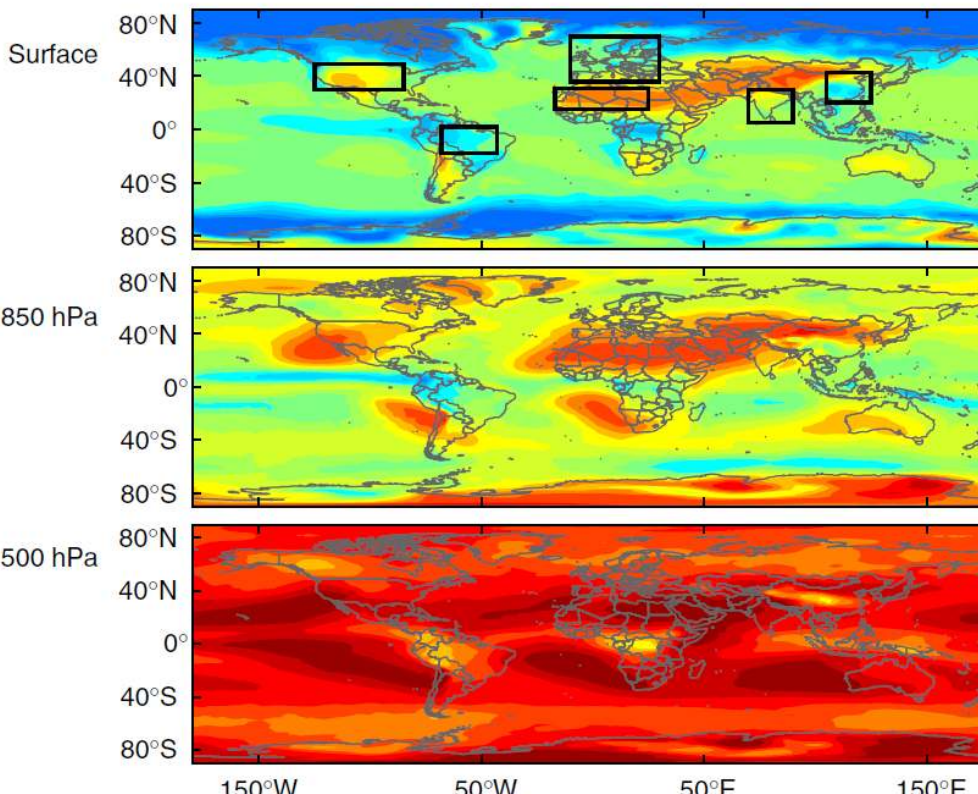
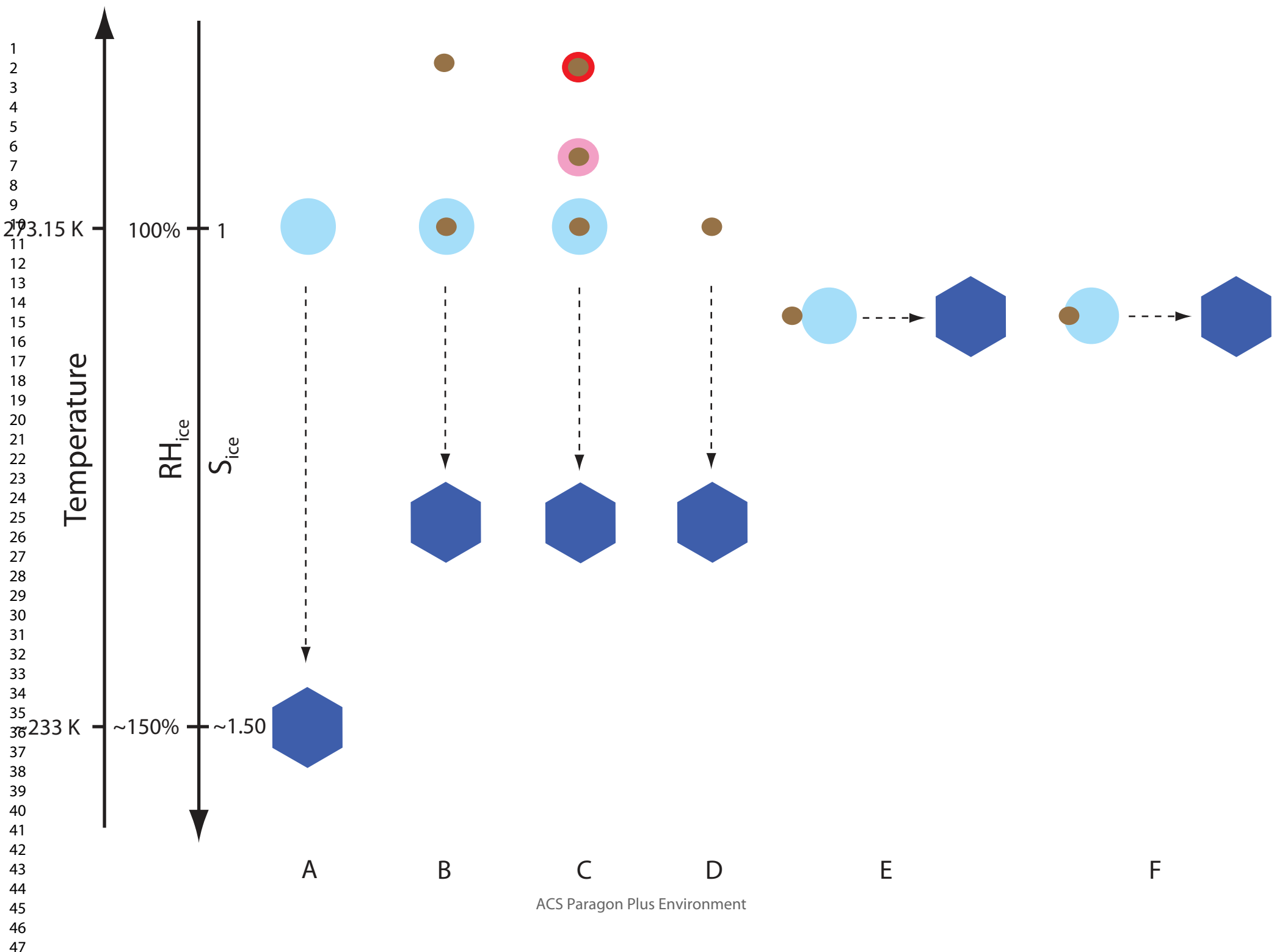
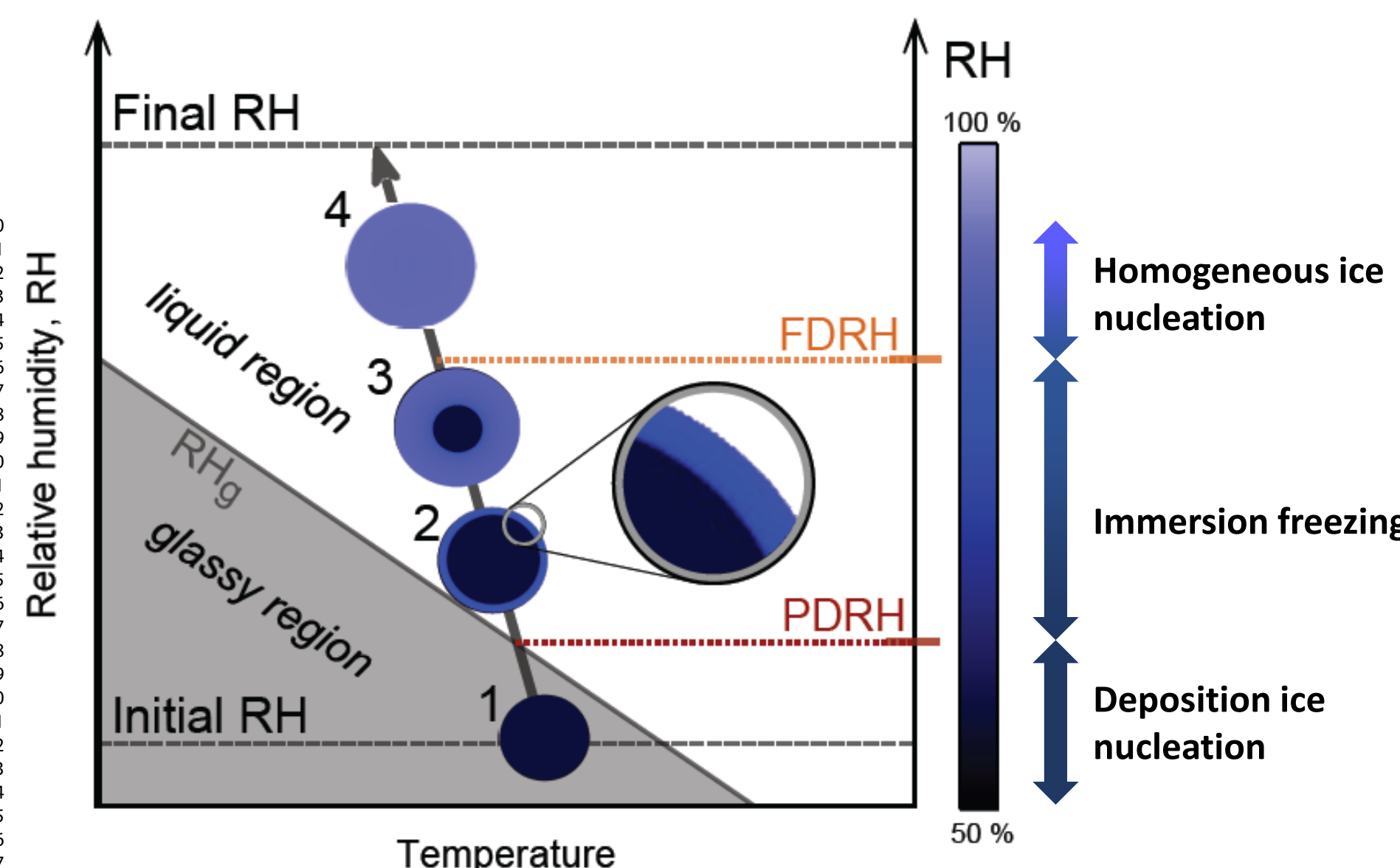
2499  
1**Fig. 15**

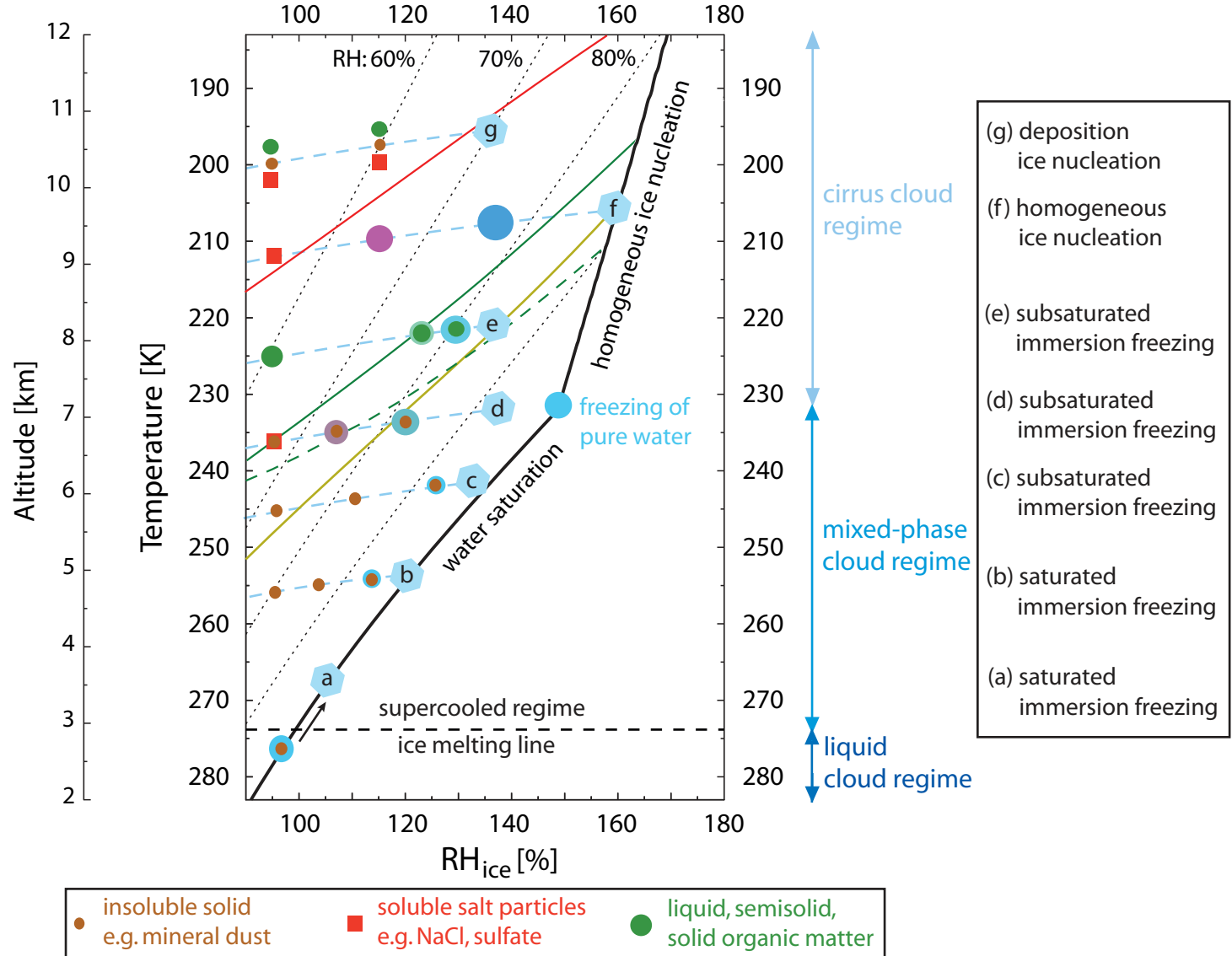
Fig. 15. Representation of immersion freezing from illite dust particles coated by humic acid (HA) (a-c) and mixed ambient OM containing particles and natural mineral dust (d-f). (a) and (d): The fraction that solid OM coats the mineral dust,  $f_{org(s)}$ , is shown as red lines. A visual representation is illustrated under glass-like and partial and fully deliquesced conditions where blue is the mineral, dark green is the solid OM and light green is the deliquesced OM. Heterogeneous ice nucleation rate coefficients,  $J_{het}$ , as a function  $\Delta a_w$  for the solid OM and mineral dust are shown as green and blue lines, respectively. (b) and (e): Calculated heterogeneous ice nucleation rates,  $\omega_{het}$ , for mixed organic/dust particles (red) and the contribution from either OM (green) and mineral dust (blue).  $\omega_{het}$  calculated from only OM or mineral dust particles are shown as dotted green and blue lines, respectively. (c) and (f): Simulated ice concentration,  $N_{ice}$ , per liter of air. The shaded area represents the combined random error from stochastic freezing and random sampling of particle size. Green and blue arrows indicate the range at which ice nucleation rates are dominated by solid OM or mineral dust, respectively.



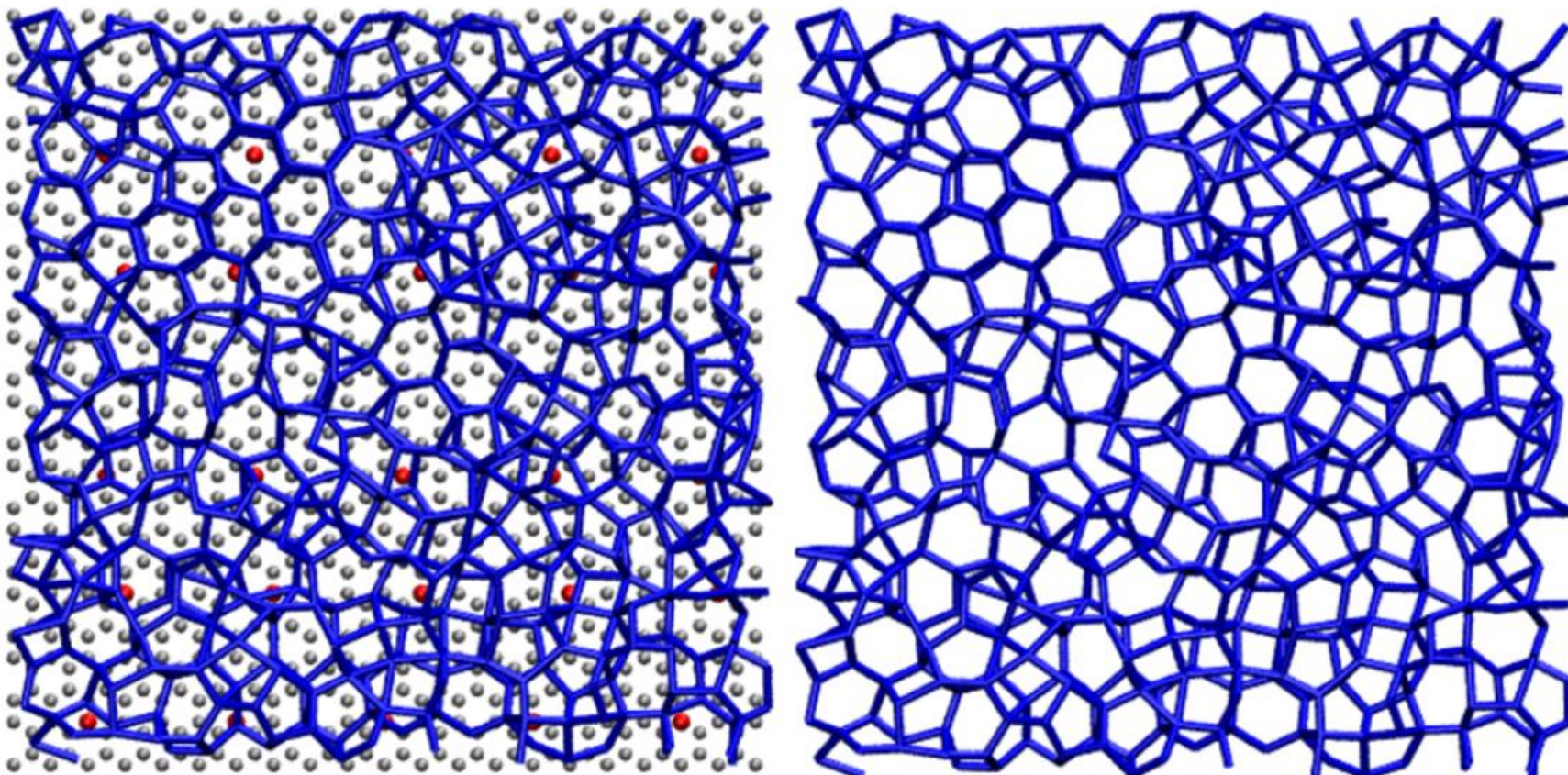


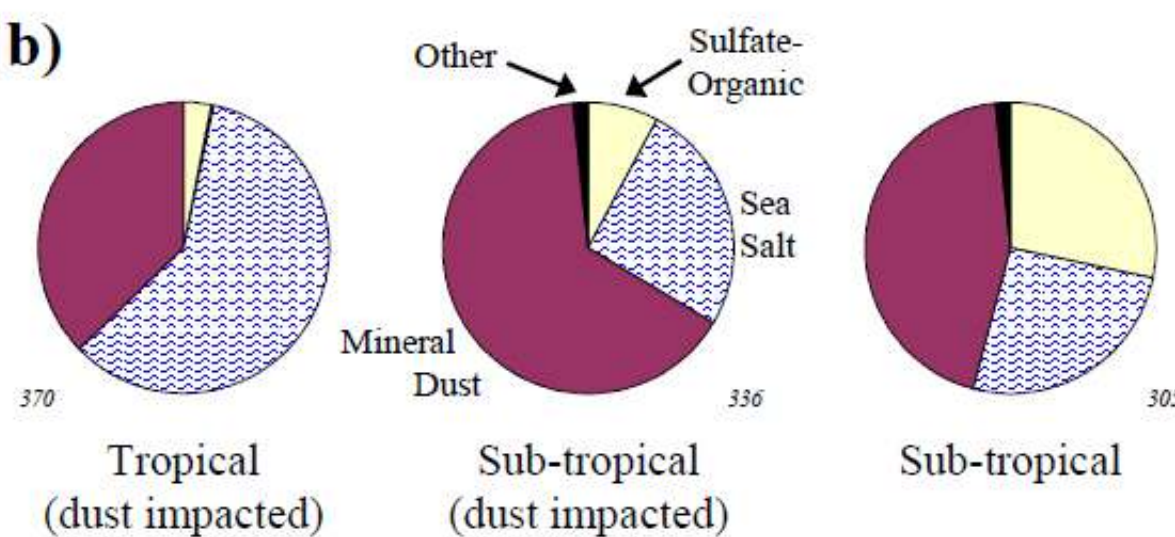
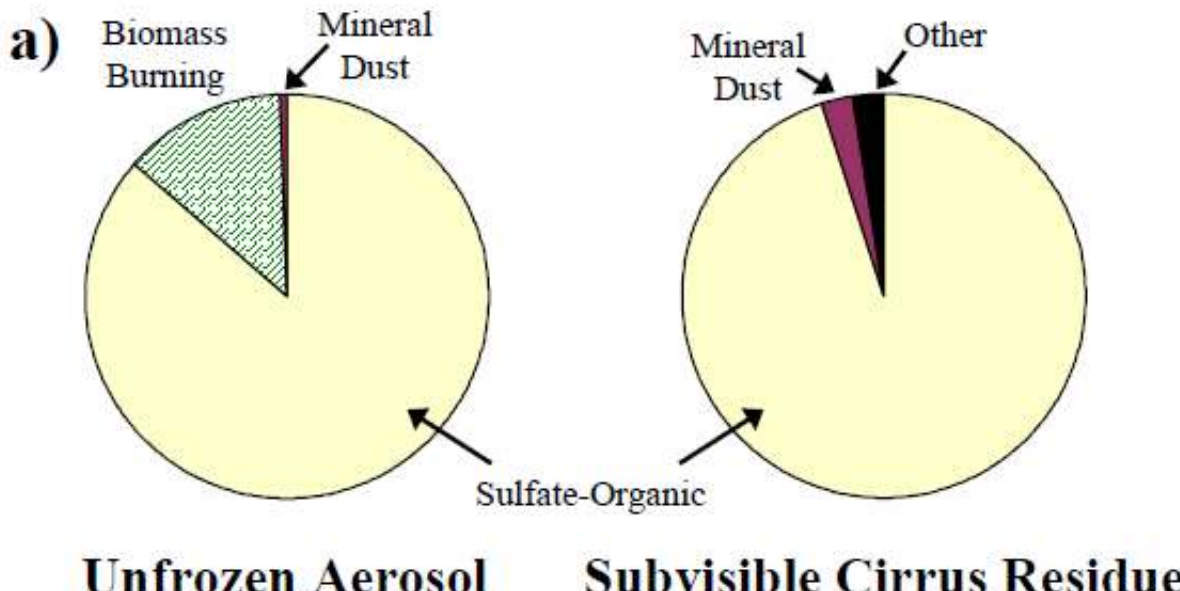






# 1<sup>st</sup> and 2<sup>nd</sup> Layers

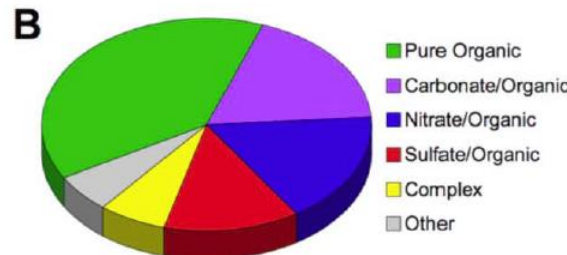




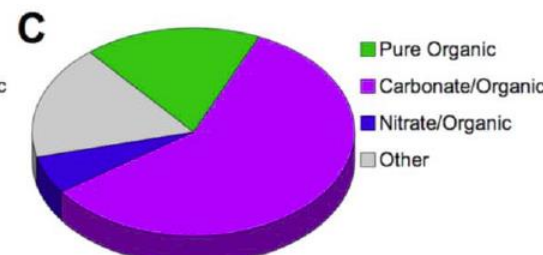
## Raman: Coarse Mode



Fraction of Background Aerosol Containing Organic Material

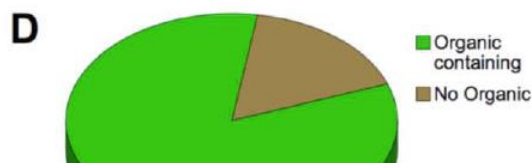


Background Aerosol Composition

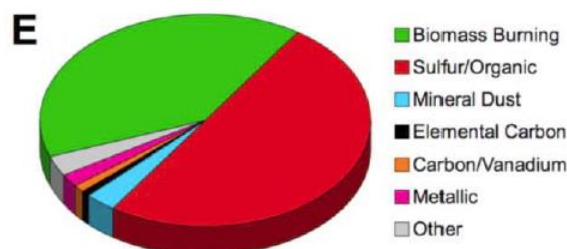


IN Composition

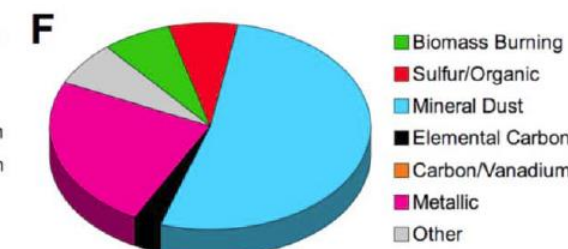
## PALMS: Fine Mode



Fraction of Background Aerosol Containing Organic Material



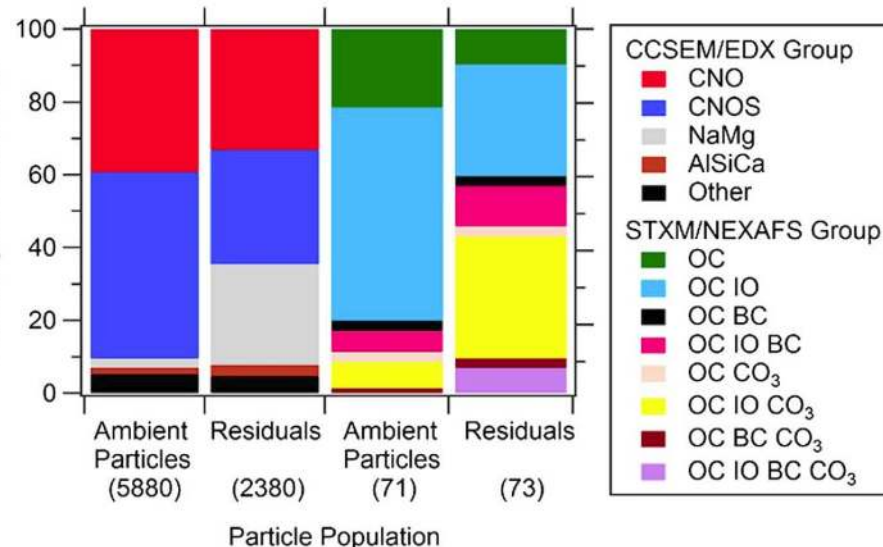
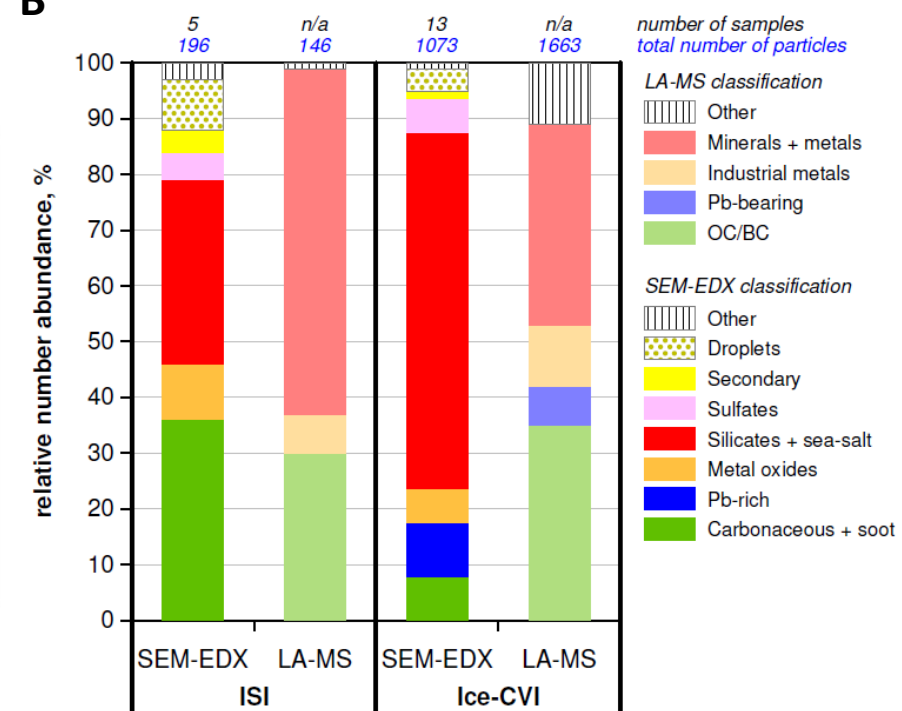
Background Aerosol Composition



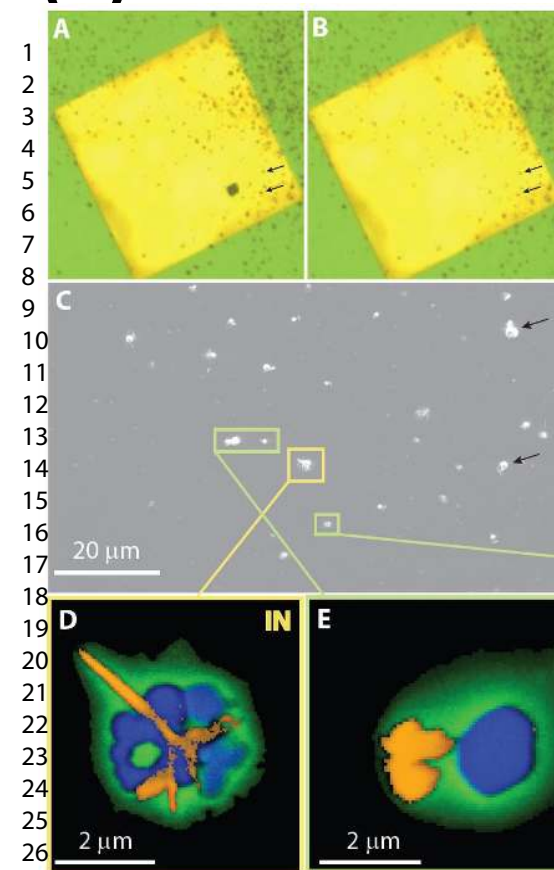
IN Composition

1  
2  
3  
4**A**

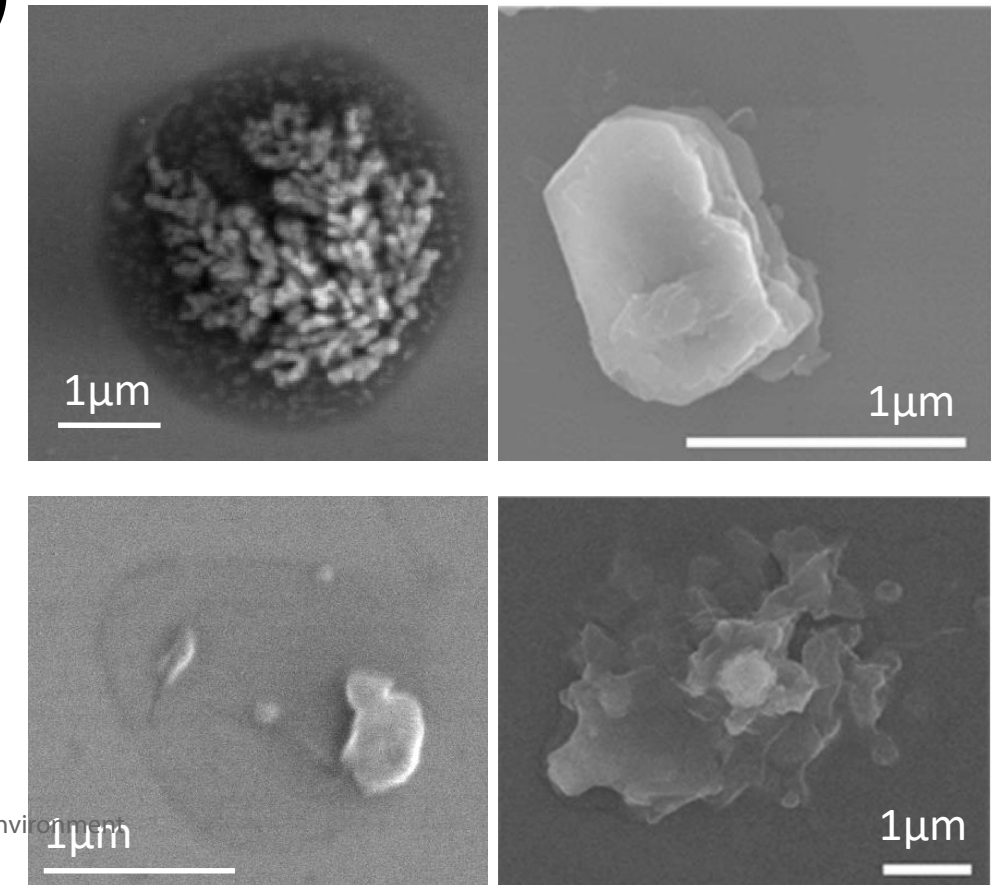
## CCSEM/EDX STXM/NEXAFS

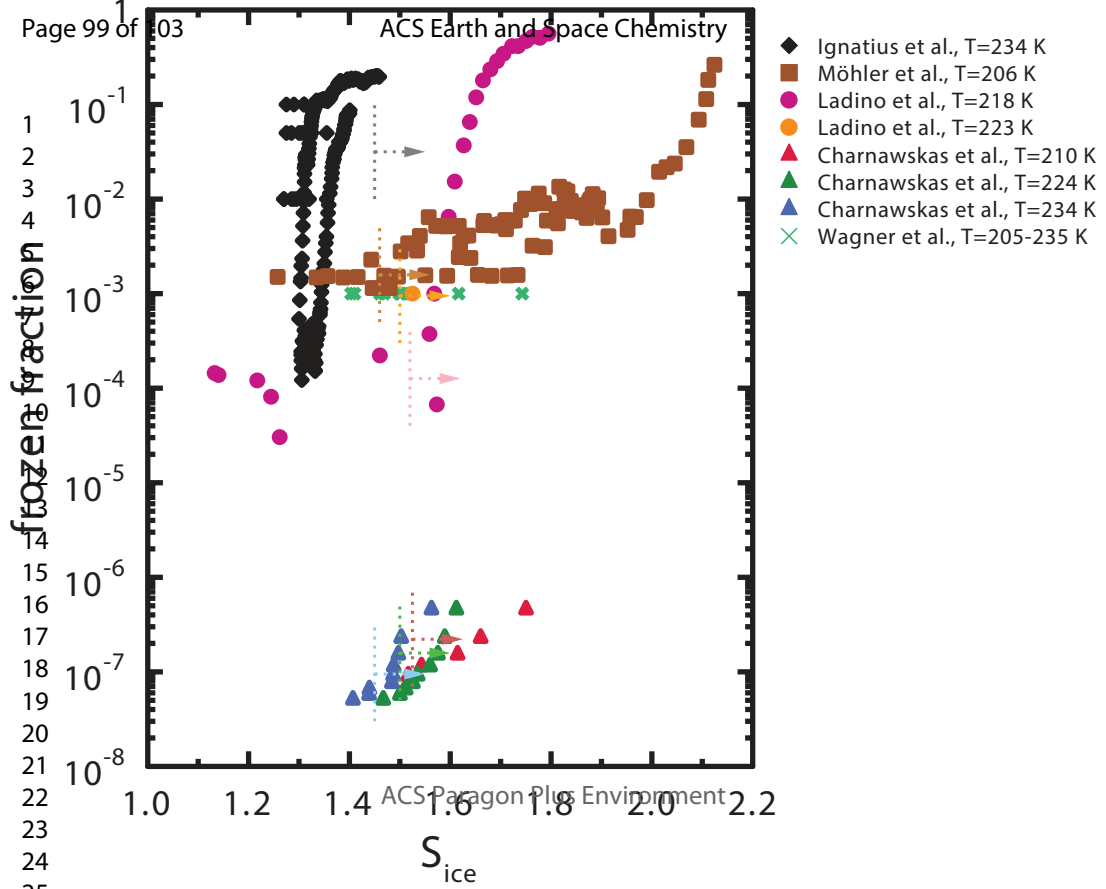
**B**

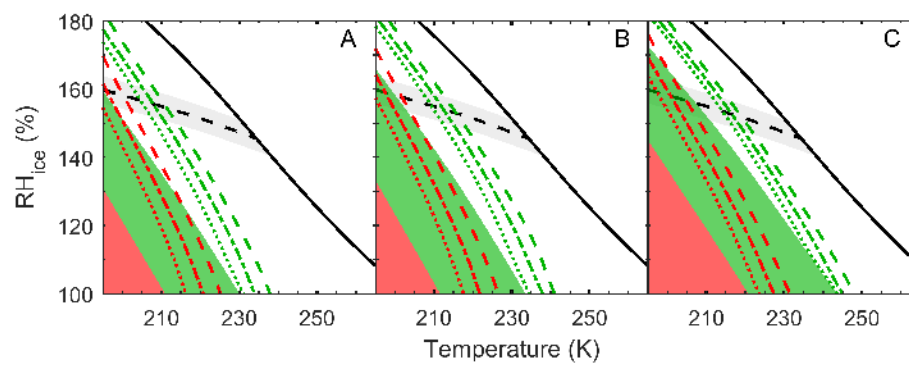
(A)

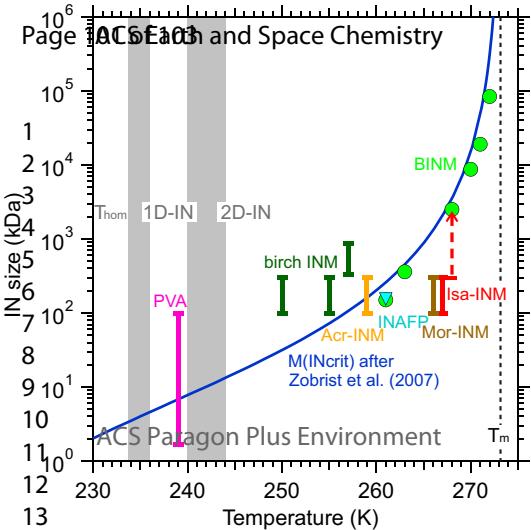


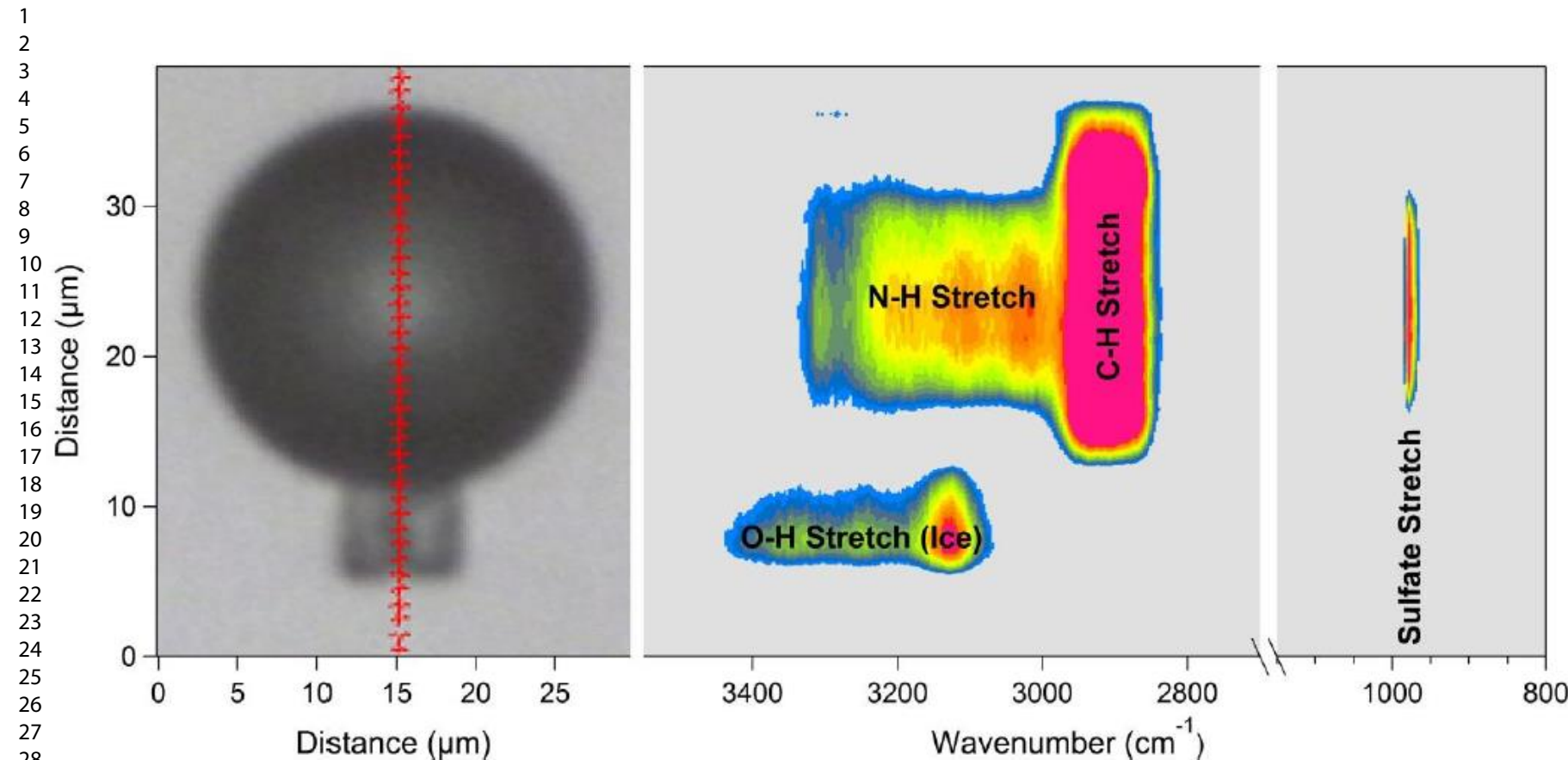
(B)













R H / %

